OKLAHOMA TRANSPORTATION CENTER

ECONOMIC ENHANCEMENT THROUGH INFRASTRUCTURE STEWARDSHIP

LABORATORY MODELING OF ENERGY DISSIPATION IN BROKEN-BACK CULVERTS-PHASE II

AVDHESH TYAGI, PH.D, P.E.
JOHN VEENSTRA, PH.D, P.E.
JAMES BROWN
ABDELFATAH ALI
NICHOLAS JOHNSON

OTCREOS10.1-47-F

Oklahoma Transportation Center
2601 Liberty Parkway, Suite 110
Midwest City, Oklahoma 73110

Phone: 405.732.6580
Fax: 405.732.6586
www.oktc.org

DISCLAIMER

The contents of this report reflect the views of the authors, who are responsible for the facts and accuracy of the information presented herein. This document is disseminated under the sponsorship of the Department of Transportation University Transportation Centers Program, in the interest of information exchange. The U.S. Government assumes no liability for the contents or use thereof.

TECHNICAL REPORT DOCUMENTATION PAGE

1. REPORT NO. OTCREOS10.1-47-F	2. GOVERNMENT ACCESSION NO.	3. RECIPIENTS CATALOG NO.
4. TITLE AND SUBTITLE Laboratory Modeling of Energy Dissipation in Broken-back Culverts – Phase II		5. REPORT DATE May 2011 6. PERFORMING ORGANIZATION CODE
7. AUTHOR(S) Avdhesh Tyagi, Ph.D., P.E., John N. Veenstra, Ph.D., P.E., James Brown, Abdelfatah Ali, and Nicholas Johnson		8. PERFORMING ORGANIZATION REPORT
9. PERFORMING ORGANIZATION NAME AND ADDRESS Oklahoma Infrastructure Consortium School of Civil & Environmental Engineering Oklahoma State University 207 Engineering South Stillwater, OK 74078		10. WORK UNIT NO. 11. CONTRACT OR GRANT NO. DTRT06-G-0016
12. SPONSORING AGENCY NAME AND ADDRESS Oklahoma Transportation Center (Fiscal) 201 ATRC Stillwater, OK 74078 (Technical) 2601 Liberty Parkway, Suite 110 Midwest City, OK 73110		13. TYPE OF REPORT AND PERIOD COVERED Final July 2009 – May 2011 14. SPONSORING AGENCY CODE
15. SUPPLEMENTARY NOTES University Transportation Center		

16. ABSTRACT

This report represents Phase II of broken-back culverts with a drop of 6 feet. The first phase of this research was performed for a drop of 24 feet. This research investigates the reduction in scour downstream of a broken-back culvert by forming a hydraulic jump inside the culvert. A broken-back culvert is used in areas of high relief and steep topography as it has one or more breaks in profile slope. A broken-back culvert in the laboratory represents a 1 (vertical) to 2 (horizontal) slope after the upstream inlet and then continuing 138 feet at a 1 percent slope in the flat part of the culvert to the downstream outlet. The prototypes for these experiments were either a two barrel 10-foot by 10-foot, or a two barrel 10-foot by 20-foot reinforced concrete. The drop between inlet and outlet is selected as 6 feet. Three flow conditions were simulated, consisting of 0.8, 1.0 and 1.2 times the culvert depth. The Froude number of the hydraulic jump created in the flat part of the culvert ranges between 1.8 and 2.3. This Fr classifies the jump as a weak jump. The jump in experiments began nearly at the toe by placing sills in the flat part. The optimal location was determined at a distance of 42 feet from the outlet face of the culvert in pressure flow conditions. The sills contain two small orifices at the bottom to allow the culvert to completely drain. The impact of friction blocks was found to be minimal. No friction blocks were used to further dissipate the energy. The length of the culvert cannot be reduced as the pressure flow fills up the culvert barrels completely.

For new culvert construction, the best option to maximize energy dissipation under open channel flow conditions is to use one sill located 69 feet from the outlet. Again, frictional blocks had minimum effect in further reduction of energy. The maximum length of the culvert can be reduced by 42 feet to 56 feet. Such a scenario is important where right-of-way problems exist for culvert construction.

17. KEY WORDS Hydraulic jump, broken-back culvert, energy dissipation, pressure flow, open-channel flow	18. DISTRIBUTION STATEMENT No restriction. This publication is available at www.oktc.org		
19. SECURITY CLASSIF. (OF THIS REPORT) unclassified	20. SECURITY CLASSIF. (OF THIS PAGE) unclassified	21. NO. OF PAGES 94 + Covers	22. PRICE

SI (METRIC) CONVERSION FACTORS

Approximate Conversions to SI Units

Symbol	When you know	Multiply by	To Find	Symbol
	LENGTH			
in	inches	25.40	millimeters	mm
ft	feet	0.3048	meters	m
yd	yards	0.9144	meters	m
mi	miles	1.609	kilometers	km
	AREA			
in^2	square inches	645.2	square millimeters	mm
ft^2	square feet	0.0929	square meters	m^2
yd^2	square yards	0.8361	square meters	m^2
ac	acres	0.4047	hectares	ha
mi^2	square miles	2.590	square kilometers	km^2
	VOLUME			
fl oz	fluid ounces	29.57	milliliters	mL
gal	gallons	3.785	liters	L
ft^3	cubic feet	0.0283	cubic meters	m^3
yd^3	cubic yards	0.7645	cubic meters	m^3
	MASS			
oz	ounces	28.35	grams	g
lb	pounds	0.4536	kilograms	kg
T	short tons (2000 lb)	0.907	megagrams	Mg
	TEMPERATURE (exact)			
°F	degrees Fahrenheit	(°F-32)/1.8	degrees Celsius	°C
	FORCE and PRESSURE or STRESS			
lbf	poundforce	4.448	Newtons	N
lbf/in^2	poundforce per square inch	6.895	kilopascals	kPa

Approximate Conversions from SI Units

Symbol	When you know	Multiply by	To Find	Symbol
	LENGTH			
mm	millimeters	0.0394	inches	in
m	meters	3.281	feet	ft
m	meters	1.094	yards	yd
km	kilometers	0.6214	miles	mi
	AREA			
mm^2	square millimeters	0.00155	square inches	in^2
m^2	square meters	10.764	square feet	ft^2
m^2	square meters	1.196	square yards	yd^2
ha	hectares	2.471	acres	ac
km^2	square kilometers	0.3861	square miles	mi^2
	VOLUME			
mL	milliliters	0.0338	fluid ounces	fl oz
L	liters	0.2642	gallons	gal
m^3	cubic meters	35.315	cubic feet	ft^3
m^3	cubic meters	1.308	cubic yards	yd^3
	MASS			
g	grams	0.0353	ounces	oz
kg	kilograms	2.205	pounds	lb
Mg	megagrams	1.1023	short tons (2000 lb)	T
	TEMPERATURE (exact)			
°C	degrees Celsius	9/5+32	degrees Fahrenheit	°F
	FORCE and PRESSURE or STRESS			
N	Newtons	0.2248	poundforce	lbf
kPa	kilopascals	0.1450	poundforce per square inch	lbf/in^2

ACKNOWLEDGMENTS

This project was funded by the Oklahoma Transportation Center jointly with the Oklahoma Department of Transportation. We would like to thank Mr. Bob Rusch, P.E., Bridge Division Engineer, Oklahoma Department of Transportation for his active participation in incorporating ideas to make this research more practical to field conditions.

In addition, Dr. Greg Hanson, P.E., Dr. Sherry Hunt, Raymond Cox and Kem Kadavy, P.E., Hydraulic Engineers of the U.S. Department of Agriculture, Agricultural Research Service each contributed their ideas in the early stages of this project regarding ways to improve physical construction of the model.

LABORATORY MODELING OF ENERGY DISSIPATION IN BROKEN-BACK CULVERTS – PHASE II

Final Report

June 2011

Avdhesh K. Tyagi, Ph.D., P.E.
Principal Investigator
John N. Veenstra, Ph.D., P.E.
Co-Principal Investigator
Abdelfatah Ali
Nicholas Johnson
James Brown
Graduate Research Associates

Oklahoma Infrastructure Consortium
School of Civil and Environmental Engineering
Oklahoma State University
Stillwater, OK 74078

TABLE OF CONTENTS

LIST OF FIGURES

LIST OF TABLES

EXECUTIVE SUMMARY

This research investigates the reduction in scour downstream of a broken-back culvert by forming a hydraulic jump inside the culvert. A broken-back culvert is used in areas of high relief and steep topography as it has one or more breaks in profile slope. A broken-back culvert in the laboratory represents a 1 (vertical) to 2 (horizontal) slope after the upstream inlet and then continues 138 feet at a 1 percent slope in the flat part of the culvert to the downstream outlet. The prototype for these experiments was either a two barrel 10-foot by 10-foot, or a two barrel 10-foot by 20-foot reinforced concrete culvert. The drop between inlet and outlet was selected as 6 feet. Three flow conditions were simulated, consisting of 0.8, 1.0 and 1.2 times the culvert depth.

The Froude number of the hydraulic jump created in the flat part of the culvert ranges between 1.8 and 2.3. This Froude number classifies the jump as a weak jump. The jump in experiments began nearly at the toe by placing sills in the flat part. The optimal location was determined at a distance of 42 feet under pressure flow condition from the outlet face of the culvert under pressure flow conditions. The sills contain two small orifices at the bottom to allow the culvert to completely drain.

Friction blocks had minimal impact on energy dissipation in the broken-back culvert. No friction blocks were used to further energy dissipation. The length of the culvert cannot be reduced as the pressure flow fills up the culvert barrels completely.

For new culvert construction, the best option to maximize energy dissipation under open channel flow condition is to use one 3.0 ft. high sill located 69 feet from the outlet. The maximum length of the culvert can then be reduced between 42 to 56 feet. Such a scenario is important where right-of-way problems exist for culvert construction.

This Page Is Intentionally Blank

INTRODUCTION

A recent research study conducted by the Oklahoma Transportation Center at Oklahoma State University indicated that there are 121 scour-critical culverts on the Interstate System (ISTAT), the National Highway System (NHS), and the State Transportation Program (STP) in Oklahoma (Tyagi, 2002). The average replacement cost of these culverts is about $121M. A survey of culverts in Oklahoma indicates that the drop in flowline between upstream and downstream ends ranges between 6 and 24 feet. In this research, a drop of 6 feet was used in the laboratory model because it is the lower limit. Results of this research could maximize the energy loss within the culvert, thus minimizing the scour around the culvert and decreasing the degradation downstream in the channel. This reduces the construction and rehabilitation costs of culverts in Oklahoma. The project is supported by the Bridge Division, Oklahoma Department of Transportation (ODOT).

The purpose of this project is to develop a methodology to analyze broken-back culverts in Oklahoma such that the energy is mostly dissipated within the culverts to minimize the degradation downstream. A broken-back culvert is used in areas of high relief and steep topography as it has one or more breaks in profile slope. The purpose of a culvert is to safely pass water underneath the roadways constructed in hilly topography or on the side of a relatively steep hill. The project investigates culverts with a vertical drop of 6 feet that may result in effective energy dissipation inside the culvert and consequently minimize the scour downstream of broken-back culverts. Culvert dimensions and hydraulic parameters for the scale model were provided by the Bridge Division, ODOT (personal communication with B. Rusch, 2007).

The research investigation includes the following tasks: 1) to obtain and review existing research currently available for characterizing the hydraulic jump in culverts; 2) to build a scale model to represent a prototype of a broken-back culvert 150 feet long, with two barrels of 10 X 10 feet, and a vertical drop of 6 feet; 3) to simulate different flow conditions for 0.8, 1.0 and 1.2 times the culvert depth (d) in the scale model constructed in Task 2; 4) to evaluate the energy dissipation between upstream and downstream ends of the broken-back culvert with and without friction blocks of different shapes; 5) to

observe in physical experiments the efficiency of the hydraulic jump with and without friction blocks between upstream and downstream ends of the culvert and the location of the hydraulic jump from the toe of the drop in the culvert; and 6) to prepare a final report incorporating analysis of the hydraulic jump and devices to create the jump and energy loss. These tasks are presented in the following sections.

LITERATURE REVIEW

The literature search was performed for hydraulic jump and Acoustic Doppler Velocimeter and the results are discussed in the following sections.

HYDRAULIC JUMP

The hydraulic jump is a natural phenomenon of a sudden rise in water level due to change from supercritical flow to subcritical flow, i.e., when there is a sudden decrease in velocity of the flow. This sudden change in the velocity causes the considerable turbulence and loss of energy. Consequently, the hydraulic jump has been recognized as an effective method for energy dissipation for many years. There have been many studies carried out to explain the characteristics of the hydraulic jump. Some of these studies are summarized in the following paragraphs.

Varol et al. (2009) carried out many experiments to determine the effect of a water jet device at varying upstream Froude numbers and flow rates on hydraulic jump characteristics. They analyzed hydraulic jump experiments by high speed (SVHS camera) image processing techniques. Flow structure, roller lengths, water surface profiles, and energy losses were studied experimentally for both free jump and jump modified by water jet. It was observed that the roller of the hydraulic jump moved upstream as the water jet flow increased. Moreover, it was noted that the downstream water depth (y_2) and roller length increased with increased water jets discharge. Furthermore, they found that forced hydraulic jumps initiated by water jet had higher energy losses than free jumps.

Ohtsu et al. (1996) evaluated incipient hydraulic jump conditions on flows over vertical sills. They identified two methods of obtaining an incipient jump: (1) increasing the sill height, or (2) increasing the tailwater depth until a surface roller forms upstream of the sill. For wide channels, predicted and experimental data were in agreement, but in the case of narrow channels, incipient jump was affected by channel width.

Mignot and Cienfuegos (2010) focused on an experimental investigation of energy dissipation and turbulence production in weak hydraulic jumps. Froude numbers ranged from 1.34 to 1.99. They observed two peak turbulence production regions for the partially developed inflow jump, one in the upper shear layer and the other in the near-

wall region. The energy dissipation distribution in the jumps was measured and revealed a similar longitudinal decay of energy dissipation, which was integrated over the flow sections and maximum turbulence production values from the intermediate jump region towards its downstream section. It was found that the energy dissipation and the turbulence production were strongly affected by the inflow development. Turbulent production showed a common behavior for all measured jumps. It appeared that the elevation of maximum Turbulent Kinetic Energy (TKE) and turbulence production in the shear layer were similar.

Alikhani et al. (2010) conducted many experiments to evaluate effects of a continuous vertical end sill in a stilling basin. They measured the effects of sill position on the depth and length of a hydraulic jump without considering the tailwater depth. In the experiments, they used five different sill heights placed at three separate longitudinal distances in their 1:30 scaled model. The characteristics of the hydraulic jump were measured and compared with the classical hydraulic jump under varied discharges. They proposed a new relationship between sill height and position, and sequent depth to basin length ratio. The study concluded that a 30% reduction in basin length could be accomplished by efficiently controlling the hydraulic jump length through sill height.

Finnemore, et al. (2002) state that the characteristics of the hydraulic jump depend on Froude number (Fr). The Froude number is the ratio between inertia force and gravity force. They added that in order for the hydraulic jump to occur, the flow must be supercritical, i.e. a jump can occur only when the Froude number is greater than 1.0. The hydraulic jump is classified according to its Froude number. When Fr is between 1.7 and 2.5, the flow is classified as a weak jump and will have a smooth rise in the water surface with less energy dissipation. A Fr between 2.5 and 4.5 results in an oscillating jump with 15-45% energy dissipation. A steady jump will occur when Fr ranges from 4.5 to 9.0. and results in energy dissipation from 45% to 70%. When Fr is above 9.0, a strong jump will occur with energy losses ranging from 70% to 85%.

Ohtsu, et al (2001) investigated undular hydraulic jump conditions in a smooth rectangular horizontal channel. They found that the formation of an undular jump depends only on the inflow Froude number and the boundary-layer development at the

toe of the jump. At these Froude number ranges, they found that the effects of the aspect ratio and the Reynolds number on the flow characteristics were negligible. Under experimental investigation, it was found that the upper limits of the Froude numbers range between 1.3 and 2.3 at the inflow. Furthermore, a Froude number of 1.7 was found to be the critical velocity point in which inflow was fully developed. They obtained the ratio thickness of the boundary layer to the depth of the toe of the jump to be 0.45 to 1.0, which agreed with predicted values from experimental results.

Bhutto et al. (1989) provided analytical solutions for computing sequent depth and relative energy loss for a free hydraulic jump in horizontal and sloping rectangular channels from their experimental studies. They used the ratio of jump length to jump depth and the Froude number to compute the length of the free jump on a horizontal bed. Jump factor and shape factor were evaluated experimentally for the free jump on a sloping bed. To check the efficiency of the jump, they made comparisons with previous solutions by other researchers and found that the equations they derived could be used instead of equations by Ludin, Bakhmateff, Silvester and Chertoussove.

Gharanglk and Chaudhry (1991) present three models for the numerical simulation of hydraulic jumps in a rectangular channel while factoring in the considerable effect of nonhydrostatic pressure distribution. The one-dimensional Boussinesq equations are solved in time subject to appropriate boundary conditions which numerically simulate the hydraulic jump. The results were compared to experimental data which indicate that four-order models with or without Boussinesq terms give similar results for all Froude numbers tested. The Froude numbers ranged from 2.3 to 7.0. The MacCormack scheme and a dissipative two-four scheme were used to solve the governing equations subject to specified end conditions until a steady state was achieved.

A broken-back culvert is used in areas of high relief and steep topography as it has one or more breaks in profile slope. The purpose of a culvert is to safely pass water underneath the roadways constructed in hilly topography or on the side of a relatively steep hill. Hotchkiss and Donahoo (2001) report that the Broken-back Culvert Analysis Program (BCAP) is a simple but powerful analysis tool for the analysis of broken-back culverts and hydraulic jumps. This program is easy to understand, explain, and

document, and is based on the energy equation and momentum equation for classical jumps. It is able to plot rating curves for the headwater, outlet depth and outlet velocity. They described a computer code capable of analyzing hydraulic jumps in the broken-back culvert.

Hotchkiss et al (2003) describe the available predictive tools for hydraulic jumps, the performance of the Broken-back Culvert Analysis Program (BCAP) in analyzing the hydraulics of a broken-back culvert, and the current applications and distribution of BCAP. They conducted tests on the broken-back culvert made of Plexiglas® to assess the performance of BCAP in predicting headwater rating curves, the locations of hydraulic jumps, and the lengths of hydraulic jumps. They conclude that accounting for the losses within the jump because of the friction in corrugated metal pipes and more accurate predicting of the locations of hydraulic jumps may be improved by predictions of flow hydraulics within the culvert barrel.

The Utah Department of Transportation (UDOT) addresses aspects of broken-back culverts and hydraulic jumps in the state's Manual of Instruction – Roadway Drainage (US Customary units), Culverts (2004). This manual illustrates steps for the design of broken-back culverts which include: 1) Establish a flow-line profile, 2) sizing the culvert, 3) beginning to calculate a supercritical profile, 4) completing profile calculations, and 5) considering hydraulic jump cautions. In Section F of Appendix 9 of the manual, covers aspects of hydraulic jumps in culverts, including cause and effect, momentum friction, comparison of momentum and specific energy curves, and the potential occurrence of hydraulic jumps. The manual also takes into account the sequent depth of jump for rectangular conduits, circular conduits, and conduits of other shapes.

Larson, E. (2004), in her Master's thesis entitled Energy Dissipation in Culverts by Forcing a Hydraulic Jump at the Outlet, suggests forcing hydraulic jumps to reduce the outlet energy. She considered two design examples to create a hydraulic jump within a culvert barrel: (1) a rectangular weir placed on a flat apron and (2) a vertical drop along with a rectangular weir. These two designs were used to study the energy reduction in the energy of the flow at the outlet. From these experiments she found that

both designs were effective in reduction of outlet velocity, momentum, and energy. These reductions would decrease the need for downstream scour mitigation.

Hotchkiss et al. (2005) proposed that by controlling the water at the outlet of a culvert, water scour around the culvert can be reduced. The effectiveness of a simple weir near the culvert outlet is compared to that of a culvert having a weir with a drop upstream in the culvert barrel. These two designs are intended to reduce the specific energy of the water at the outlet by inducing a hydraulic jump within the culvert barrel, without the aid of tailwater. The design procedure was proposed after studying the geometry and effectiveness of each jump type in energy reduction. In this research, they found the Froude number ranged from 2.6 to 6.0. It was determined that both forms of outlets are effective in reducing the velocity of water and hence the energy and momentum will decrease the need for downstream scour mitigation.

The Hydraulic Design of Energy Dissipators for Culverts and Channels (July, 2006), from the Federal Highway Administration, provides design information for analyzing and mitigating problems associated with the energy dissipation at culvert outlets and in open channels. It recommends the use of the broken-back culvert design as an internal energy dissipator. The proposed design for a broken-back culvert is limited to the following conditions: 1) the slope of the steep section must be less than or equal to 1.4:1 (V: H) and 2) the hydraulic jump must be completed within the culvert barrel.

According to this report, for situations where the runout section is too short and/or there is insufficient tailwater for a jump to be completed within the barrel, modifications may be made to the outlet that will induce a jump. The design procedure for stilling basins, streambed level dissipaters, riprap basins and aprons, drop structures and stilling wells is also discussed.

Pagliara et. al. (2008) analyzed the hydraulic jump that occurs in homogeneous and nonhomogeneous rough bed channels. They investigated the sequent flow depth and the length of the jump which are the influence parameters of the hydraulic jump. In this research, they drew on the general jump equation to analyze the jump phenomenon. In analyzing the rough bed data, they were able to formulate a

representative equation to explain the phenomenon. The equations found in their study may be used to design stilling basins downstream of hydraulic structures.

Hotchkiss et al. (2008) analyzed the accuracy of the following seven programs on culvert hydraulics: HY-8, FishXing, Broken-back Culvert Analysis Program (BCAP), Hydraflow Express, CulvertMaster, Culvert, and Hydrologic Engineering Center River Analysis System (HEC-RAS). The software was tested on the accuracy of three calculations: headwater depths, flow control, and outlet velocities. The software comparison was made between software output values and hand calculations, not from laboratory experimental data. The hand calculations used were derived from laboratory experiments done by the National Bureau of Standards (NBS). Hotchkiss et al. concluded HEC-RAS is the most comprehensive program for both accuracy and features for culverts affected by upstream structures.

Tyagi et al. (2009) investigated hydraulic jump under pressure and open channel flow conditions in a broken-back culvert with a 24 foot drop. It was found that for pressure flow a two sill solution induced the most desirable jump, and for open channel a single sill close to the middle of the culvert was most desirable. The investigation was funded by the Oklahoma Transportation Center, Research and Innovative Technology Administration, Federal Highway Administration, and Oklahoma Department of Transportation.

Tyagi et al. (2010a) performed many experiments for open channel culvert conditions. Optimum energy dissipation was achieved by placing one sill at 40 feet from the outlet. Friction blocks and other modifications to the sill arrangement were not as effective.

Tyagi et al. (2010b) carried out many experiments to optimize flow condition and energy dissipation in a broken-back culvert under pressure flow. It was found that two sills, the first 5 ft high and 25 feet from the outlet and the second 3.34 ft high and 45 feet from the outlet, gave the best results. The culvert could not be shortened since it was full under the tested conditions.

ACOUSTIC DOPPLER VELOCIMETER

Acoustic Doppler Velocimeter (ADV) is a sonar device which tracks suspended solids (particles) in a fluid medium to determine an instantaneous velocity of the particles in a sampling volume. In general, ADV devices have one transmitter head and two to four receiver heads. Since their introduction in 1993, ADV have quickly become valuable tools for laboratory and field investigations of flow in rivers, canals, reservoirs, the oceans, around hydraulic structures and in laboratory scale models (Sontek, 2001).

Wahl (2000) discusses methods for filtering raw ADV data using a software application called WinADV. Wahl suggests that ADV data present unique requirements compared to traditional current-metering equipment, due to the types of data obtained, the analyses that are possible, and the need to filter the data to ensure that any technical limitations of ADV do not adversely affect the quality of the results. According to Wahl, the WinADV program is a valuable tool for filtering, analyzing, and processing data collected from ADV. Further, this program can be used to analyze ADV files recorded using the real time data acquisition programs provided by ADV manufacturers.

Goring and Nikora (2002) formulated a new post processing method for despiking raw ADV data. The method combines three concepts, including:

1. That differentiation of the data enhances the high frequency portion of a signal which is desirable in sonar measurements.
2. That the expected maximum of a random series is given by the Universal threshold function.
3. That good data clusters are a dense cloud in phase space maps

These concepts are used to construct an ellipsoid in three-dimensional phase space, while points lying outside the ellipsoid are designated as spikes (bad data). The new method has superior performance over various other methods with the added advantage of requiring no parameters. Several methods for replacing sequences of spurious data are presented. A polynomial fitted to good data on either side of the spike event, then interpolated across the event, is preferred by Goring and Nikora.

Mori et al. (2007) investigates measuring velocities in aerated flows using ADV techniques. ADV measurements are useful and powerful for measurements of mean

and turbulent components of fluids in both hydraulic experimental facilities and fields. However, it is difficult to use the ADV in bubbly flows because air bubbles generate spike noise in the ADV velocity data. This study describes the validity of the ADV measurements in bubbly flows. The true three-dimensional phase space method is significantly useful to eliminating the spike noise of ADV recorded data in bubbly flow as compared to the classical low correlation method (Goring and Nikora, 2002). The results of the data analysis suggest that:

1. There is no clear relationship between velocity and ADV's correlation/signal-to-noise ratio in bubbly flow;
2. Spike noise filtering methods based on low correlation and signal-to-noise ratio are not adequate for bubbly flow; and
3. The true 3D phase space method significantly removes spike noise of ADV velocity in comparison with the original 3D phase space method.

In addition the study found that ADV velocity measurements can be valid for 1% to 3% air void flows. The limitations of the ADV velocity measurements for high void fractions were not studied.

Chanson et al. (2008) investigated the use of ADVs to determine the velocity in turbulent open channel flow conditions in both laboratory and field experiments. They demonstrated that the ADV is a competent set of devices for steady and unsteady turbulent open channel flows. However, in order to accurately measure velocity, the ADV raw data must be processed and the unit must be calibrated to the suspended sediment concentrations. Accurately processing your ADV data requires practical knowledge and experience with the device's capabilities and limitations. Chanson concluded that turbulence properties should not be derived from unprocessed ADV signals and some despiking methods were not directly applicable to many field and laboratory applications.

HYDRAULIC SIMILITUDE THEORY

Similarity between a hydraulic model and a prototype may be achieved in three basic forms: a) geometric similarity, b) kinematic similarity, and c) dynamic similarity (Chow, 1959).

BROKEN-BACK CULVERT SIMILARITIES

a. Geometric similarity implies similarity of physical form. The model is a geometric reduction of the prototype and is accomplished by maintaining a fixed ratio for all homologous lengths between the physical quantities involved in geometric similarity: length (L), area (A), and volume (Vol). To keep the homologous lengths in the prototype (p) and the model (m) at a constant ratio (r), they may be expressed as:

$$\frac{L_p}{L_m} = L_r \tag{1}$$

An area (A), is the product of two homologous lengths; hence, the ratio of the homologous area is also a constant given as:

$$\frac{A_p}{A_m} = \frac{L_p^2}{L_m^2} = L_r^2 \tag{2}$$

A volume (Vol.) is the product of three homologous lengths; the ratio of the homologous volume can be represented as:

$$\frac{Vol_p}{Vol_m} = \frac{L_p^3}{L_m^3} = L_r^3 \tag{3}$$

b. Kinematic similarity implies similarity of motion. Kinematic similarity between the model and the prototype is attained if the homologous moving particles have the same velocity ratio along geometrically similar paths. This similarity involves the scale of time and length. The ratio of times required for homologous particles to travel homologous distances in a model and prototype is given by:

$$\frac{T_p}{T_m} = T_r \tag{4}$$

The velocity (V) is defined as distance per unit time; thus, the ratio of velocities may be expressed as:

$$\frac{V_p}{V_m} = \frac{\left(L_p / T_p\right)}{\left(L_m / T_m\right)} = \frac{L_r}{T_r} \tag{5}$$

The flow (Q) is expressed as volume per unit time and may be given by:

$$\frac{Q_p}{Q_m} = \frac{\left(L_p^3 / T_p\right)}{\left(L_m^3 / T_m\right)} = \frac{L_r^3}{T_r} \tag{6}$$

c. Dynamic similarity implies similarity in forces involved in motion. In broken-back culverts, inertial force and gravitational (g) force are considered dominant forces in fluid motion. The Froude number is defined as:

$$F_r = \frac{\left[V_p / \left(g_p L_p\right)^{1/2}\right]}{\left[V_m / \left(g_m L_m\right)^{1/2}\right]} = 1 \tag{7}$$

As g_p and g_m are the same in a model and the prototype, these cancel in Equation 7, yielding:

$$\frac{V_r}{\left(L_r\right)^{1/2}} = 1 \tag{8}$$

$$V_r = \frac{V_p}{V_m} = \left(L_r\right)^{1/2} \tag{9}$$

$$V_p = V_m \left(L_r\right)^{1/2} \tag{10}$$

Using the three similarities, a variable of interest can be extrapolated from the model to the prototype broken-back culvert.

LABORATORY MODEL

During the initial period of discussion regarding the construction of a scale model representing a 150 feet long broken-back culvert with two barrels of 10 x 10 feet each and a vertical drop of 6 feet, the research group visited the USDA Agricultural Research Service Hydraulic Engineering Research Laboratory in Stillwater, Oklahoma. This was the facility at which testing was done. The group visited with facility personnel and inspected the equipment that would be used to conduct tests. Physical dimensions of the flume that would be used were noted, as well as the flow capacity of the system.

Two scales were considered for the model. A scale of either 1:10 or 1:20 would allow for geometric similitude in a model that could easily be produced. The 1 to 20 scale was adopted due to space limitations at the testing facility, and in consideration of the potential need to expand the model depending on where the hydraulic jump occurred. If the hydraulic jump did not form within the model, the smaller scale would leave room to double the length of the culvert. In addition, a lower flow rate would be required during testing if a smaller scale were used.

Other considerations included what materials to use in building the model, and what construction methods would be best. The materials considered were wood and Plexiglas®. Plexiglas® was found preferable because it offered visibility as well as durability, and a surface which would more closely simulate the surface being modeled (Figures 1 through 3, 6 and 7). The Manning's roughness value for Plexiglas® is 0.010 which is very close to the roughness of finished concrete at 0.012. The thickness of the Plexiglas® was decided based on weight, rigidity, workability, and the ease with which the material would fit into scale. Half-inch Plexiglas® proved to be sturdy and was thick enough to allow connection hardware to be installed in the edges of the plates. This material also fit well into the proposed scale of 1 to 20 which equated one-half inch in the model to one foot in the prototype. The construction methods included constructing the model completely at the Oklahoma State University campus and moving it to the test facility, creating sections of the model at the university and assembling them at the test facility, or contracting with the testing facility to construct the model. It was decided that the model would be constructed at the test facility. During the course of the test

runs, it became apparent that a flow straightener would have to be installed inside the reservoir in order to calm the inlet flow. A sealed plywood divider was constructed with a series of openings covered with coarse mesh (Figure 12). Also, a divider wall was placed between the two inlet sections in the reservoir to better ensure equal flow into both channels in the culvert barrel.

In addition to the Plexiglas® model of the culvert, a reservoir was constructed upstream of the model to collect and calm the fluid entering the model. The reservoir was constructed with plywood because it was not necessary to observe the behavior of the fluid at that stage (Figure 6). Within the reservoir, wing walls at an angle of 60 degrees were constructed to channel flow into the model opening. The base of the wing walls was constructed with plywood and the exposed wing wall models were formed with Plexiglas®. The same design was used for the outlet structure of the culvert.

The objective of the test was to determine the effect of sill and friction blocks on the hydraulic jump within the prototype, therefore the model was constructed so that different arrangements of friction blocks could be placed and observed within the model. Friction blocks were mounted in different arrangements on a sheet of Plexiglas® the same width as the barrels, and placed in the barrel (Figure 8). Three friction block shapes were selected: a regular flat faced, a semi-circular faced, and a c-shaped face blocks (Figure 9). Sills were located only on the horizontal portion of the model.

Two sections were constructed and added to the model for several experiments. These sections served two purposes. During initial experimentation, it was observed that the original design was under pressure and that a theoretical hydraulic jump would occur above the confines of the existing culvert ceiling. The additional sections were inverted and mounted to the top of the original model making a culvert with 2 barrels 6 inches wide by 12 inches high and the original length of 82.8 inches (Figure 10). Figure 11 shows the downstream channel after wingwall made from plywood. Access holes were cut into the bottom of these sections to allow for placement of a velocity meter when used as a cover for the expanded height.

Figure and table variables key:

H. J. = Hydraulic jump

H = Head upstream of culvert, inches

Q = Flow rate, cfs

Y_s = Water depth at inclined channel, inch

Y_{toe} = Water depth at toe of culvert, inch

Y_1 = Water depth before hydraulic jump in supercritical flow, inch

Y_2 = Water depth after hydraulic jump in subcritical flow, inch

$Y_{d/s}$ = Water depth at downstream of culvert, inch

Fr_1 = Froude Number in supercritical flow

$V_{u/s}$ = Velocity at upstream of culvert, fps

V_1 = Velocity before hydraulic jump in supercritical flow, fps

V_2 = Velocity after hydraulic jump in subcritical flow, fps

$V_{d/s}$ = Velocity downstream of culvert, fps

X = Location of toe of the hydraulic jump to the beginning of the sill, inches

L = Length of hydraulic jump, inch

ΔE = Energy loss due to hydraulic jump, inches

THL = Total head loss for entire culvert, inches

E_2/E_1 = Efficiency of hydraulic jump

U.P. = Under Pressure

N = No hydraulic jump occurred

Y = Hydraulic jump occurred

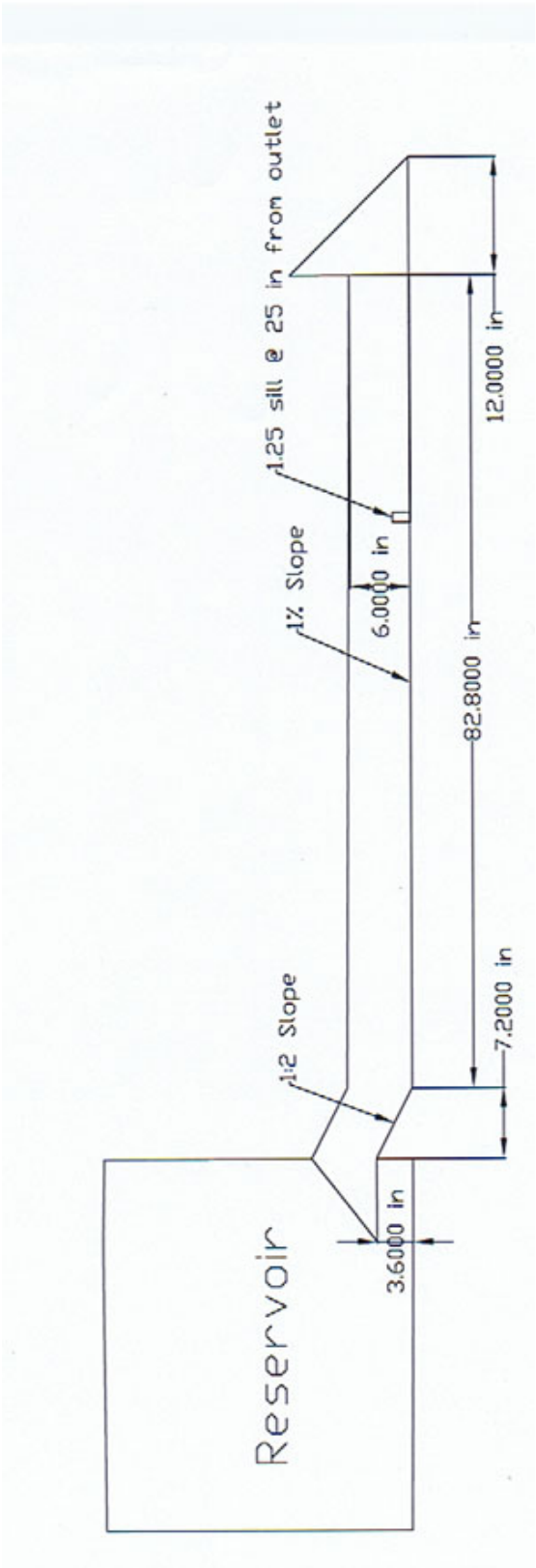

Figure 1. Profile view of model using 1:20 scale.

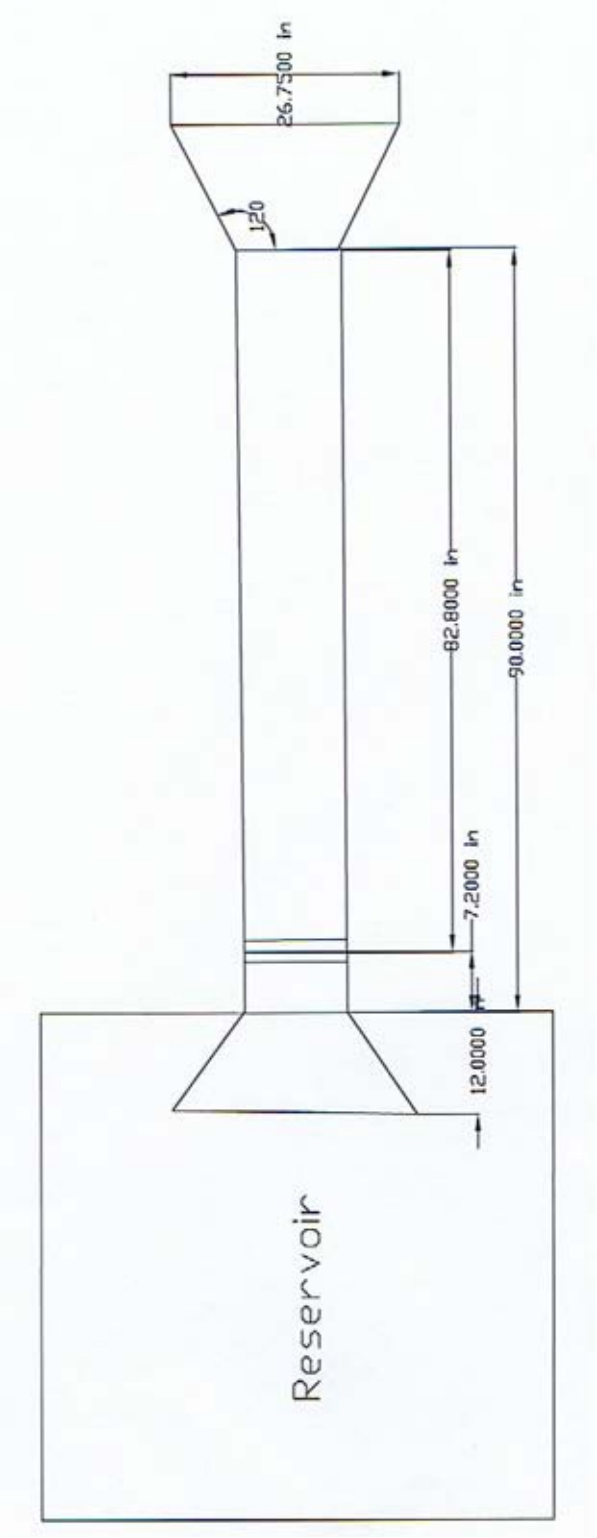

Figure 2. Plan view of model using 1:20 scale.

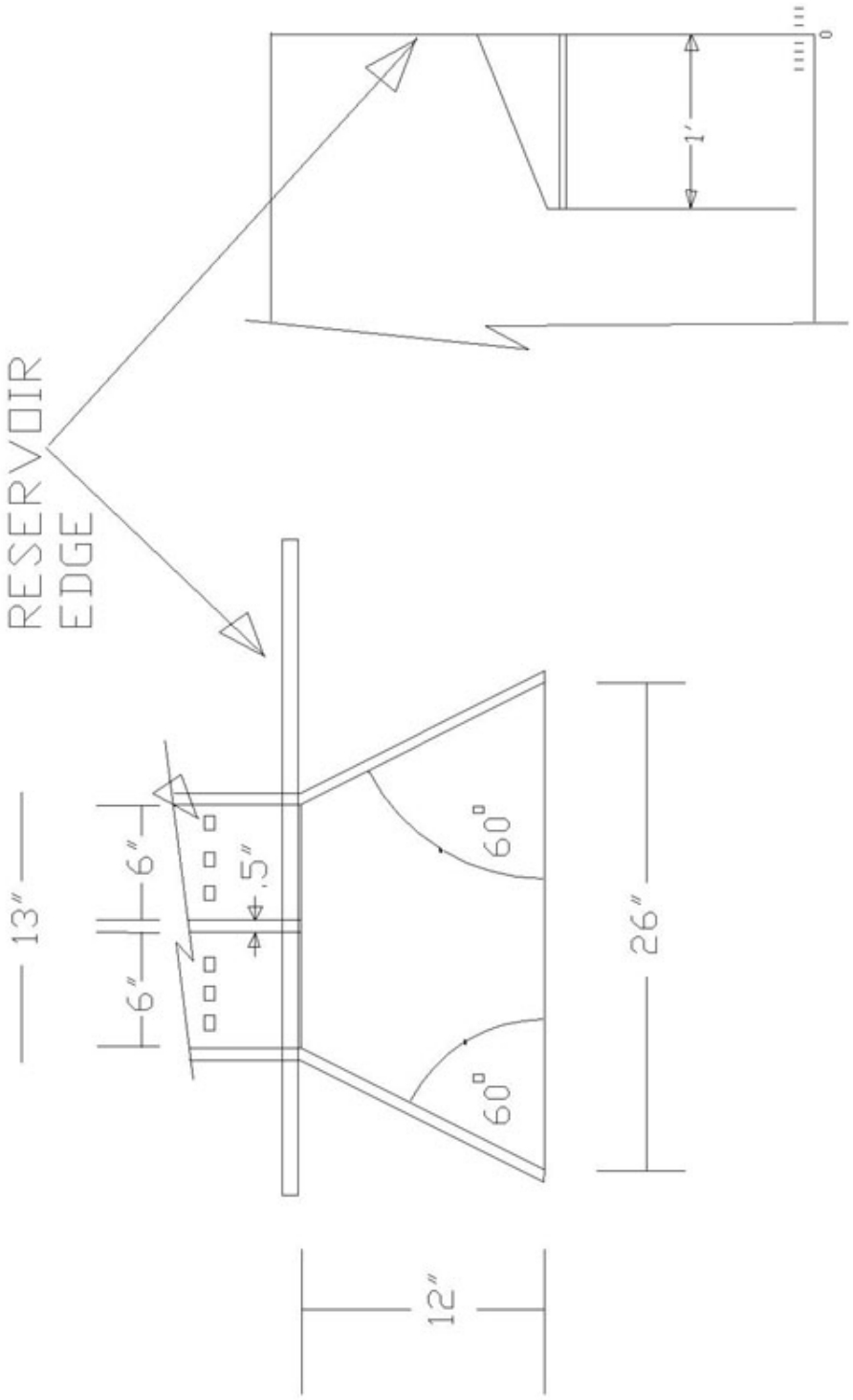

Figure 3. Inlet and outlet details.

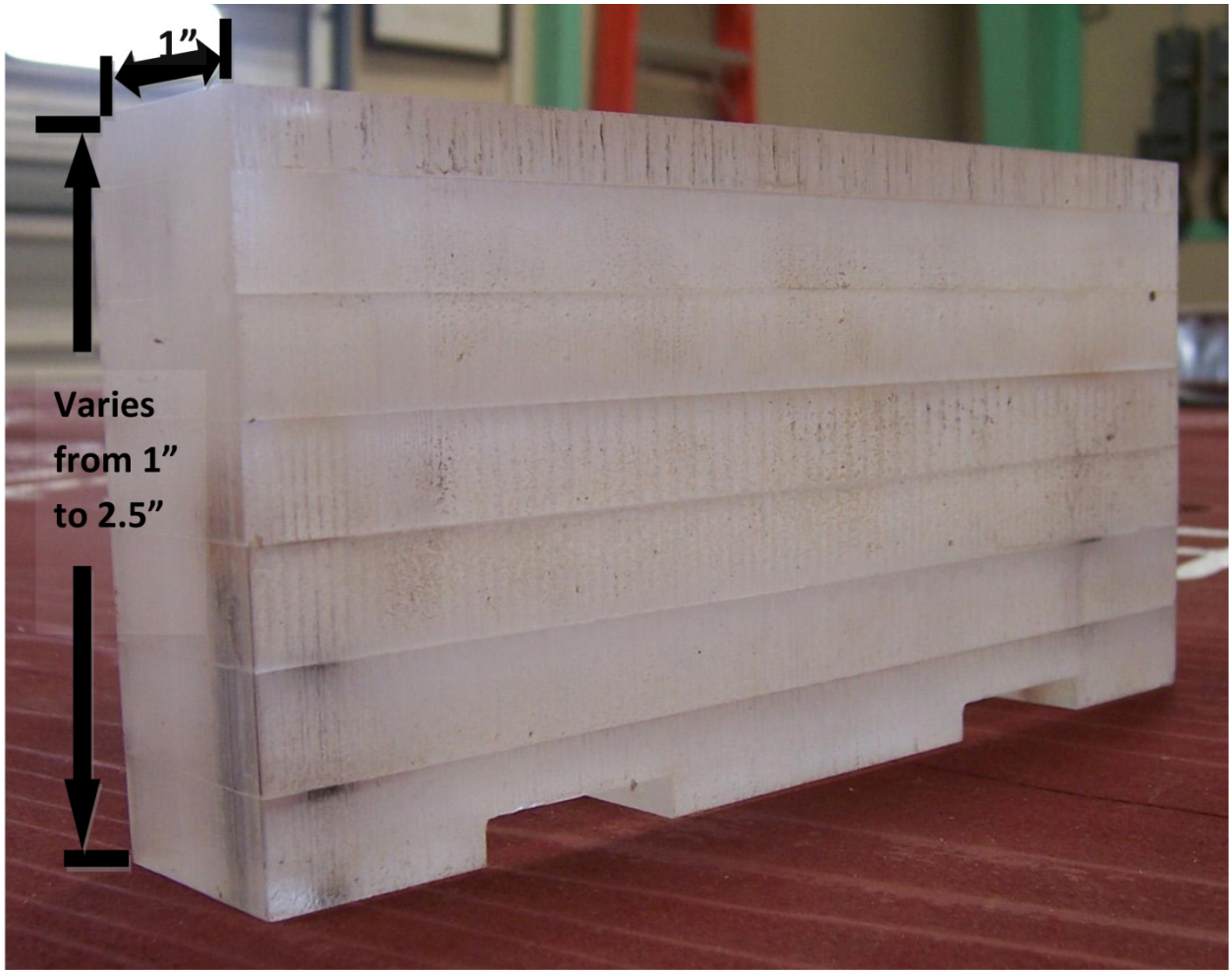

Figure 4. Typical sill dimensions.

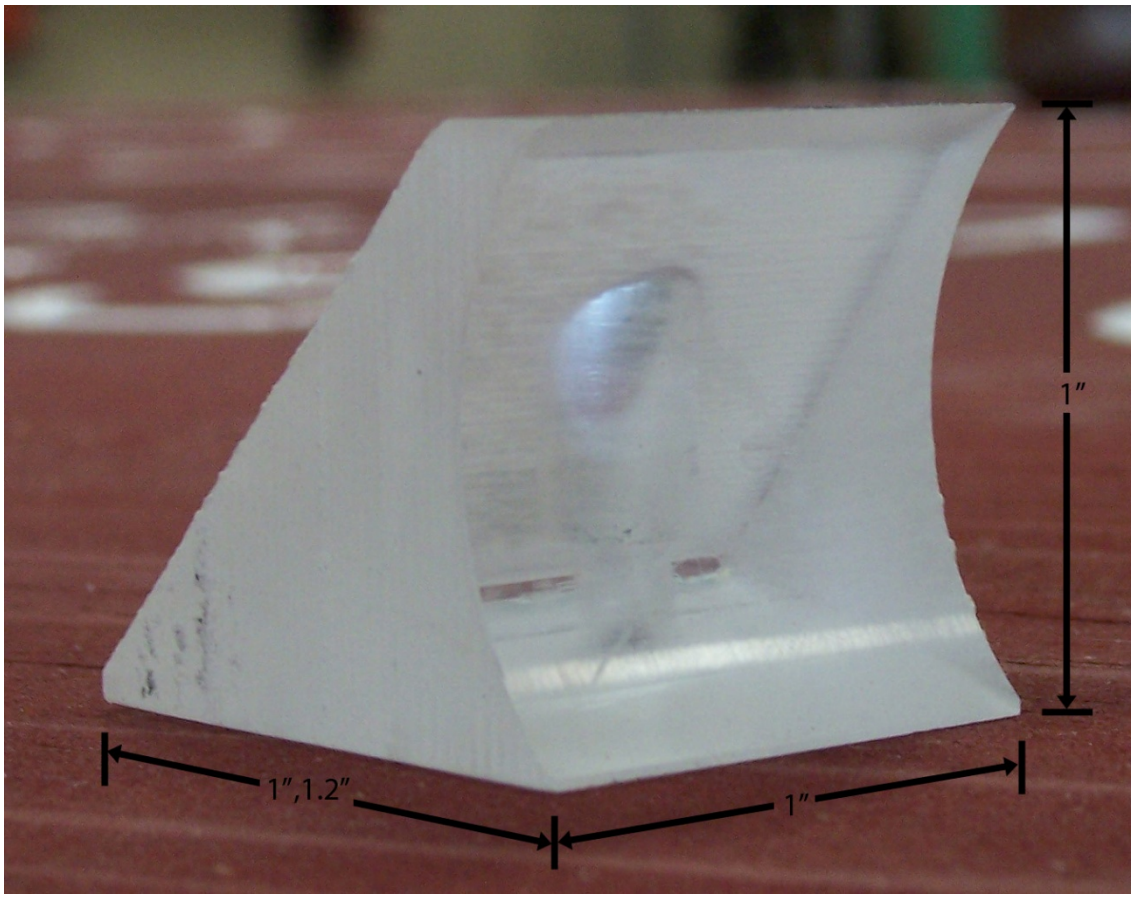

Figure 5. Example of friction block.

Figure 6. Front view of laboratory model.

Figure 7. Side view of laboratory model.

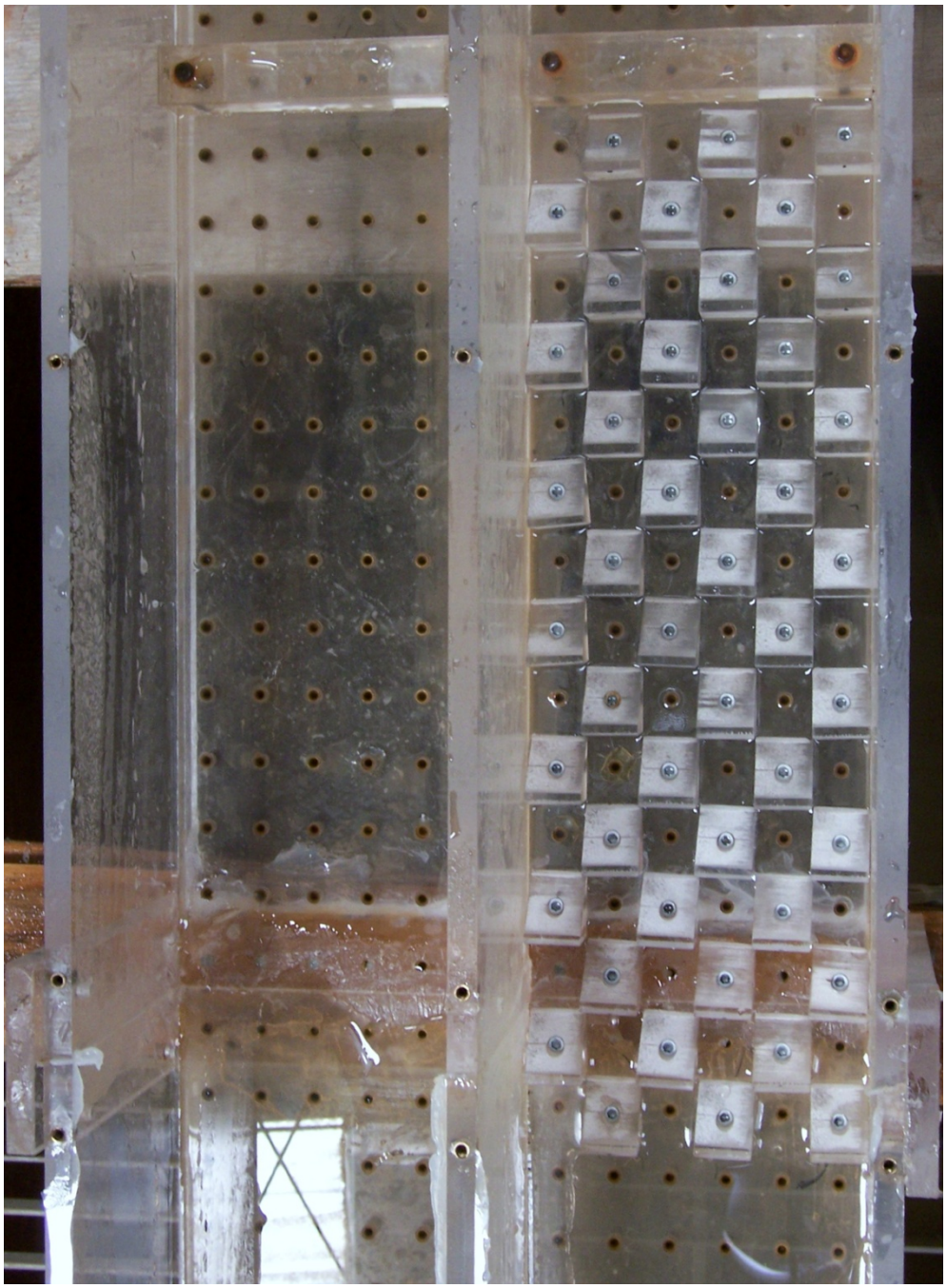

Figure 8. Example of flat faced friction blocks arranged on model bottom.

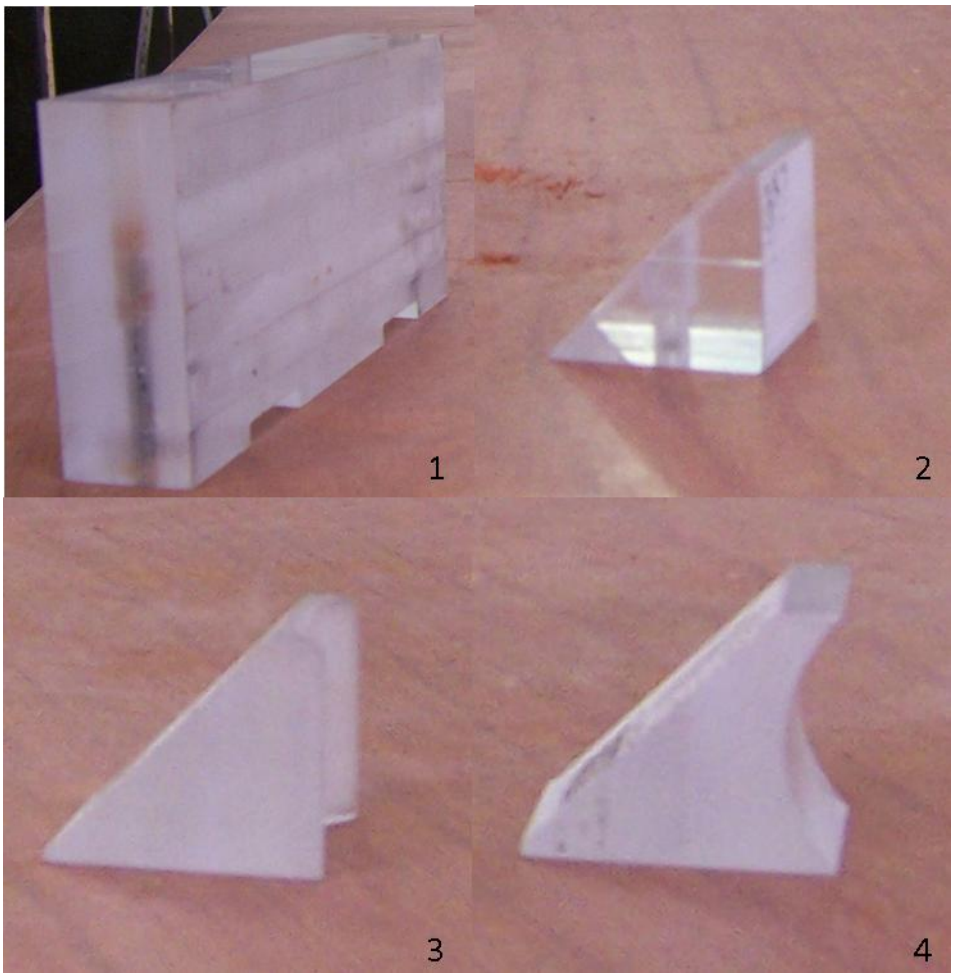

Figure 9. Example of friction block shapes and sill. (1. 3” Sill, 2. Regular flat-faced friction block, 3. Semi-circular friction block, 4. C-shaped friction block)

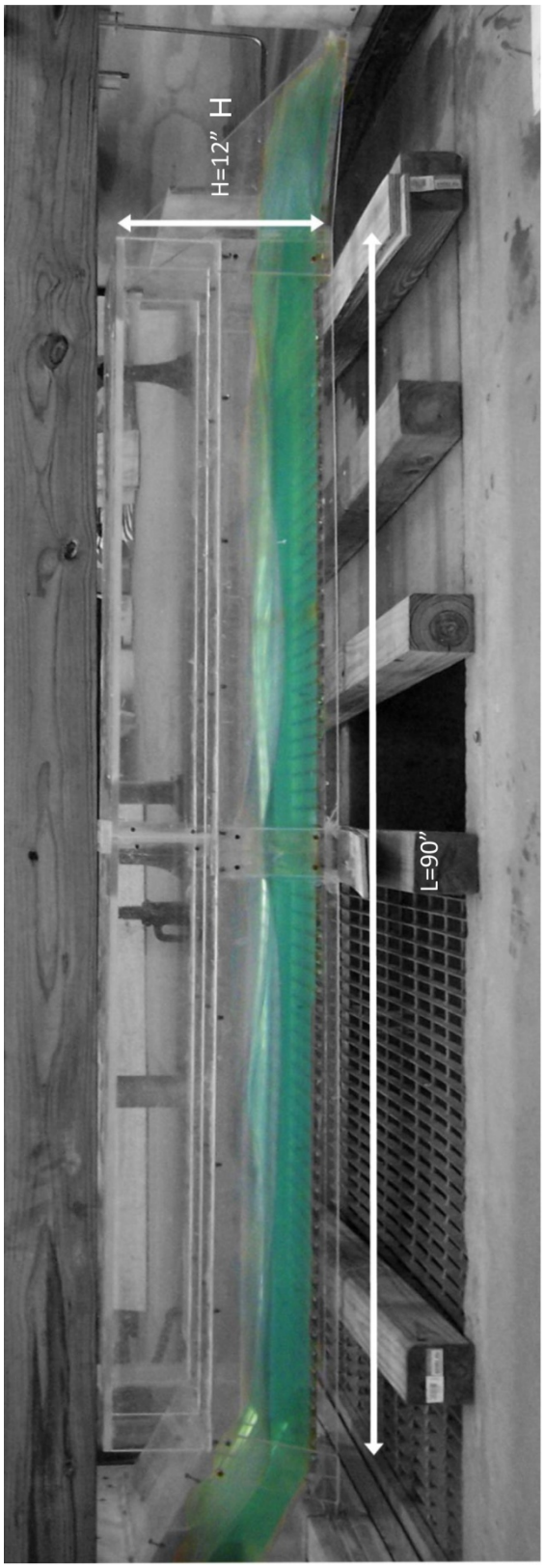

Figure 10. Example of extended channel height to apply open channel condition.

Figure 11. Downstream plywood channel after wingwall.

Figure 12. Reservoir and channel inlet for culvert model.

This Page Is Intentionally Blank

DATA COLLECTION

Many experiments were conducted to create energy dissipation within a broken-back culvert. Thirty-two experiments were done for this model with variations in length, height, width, and energy dissipaters used. Each experiment tested three scenarios. They were run with upstream heads of 0.8d, 1.0d, and 1.2d with each depth denoted by A, B, or C, respectively. For example, 8A represents the 8^{th} experiment run at 0.8d, 8B represents the 8^{th} experiment run at 1.0d, and 8C represents the 8^{th} experiment run at 1.2d. A SonTek 2D-side looking MicroADV sonar velocimeter was used to measure the velocity at the intake of the structure, after the hydraulic jump, and at the downstream end of the culvert. 2D-side looking denotes it has two receiver arms to give readings in the x and y planes. Also, a pitot tube was used to measure velocity at the toe before the hydraulic jump. The flow rates for all experiments were the same. For 0.8d, the flow rate was 1.0 cfs; for 1.0d, the flow rate was 1.3 cfs; and for 1.2d, the flow rate was 1.7 cfs. Also the velocity at the intake of the structure was the same for all experiments. For 0.8d, the velocity was 2.5 fps; for 1.0d, the velocity was 2.7 fps; and for 1.2d the velocity was 2.8 fps.

Experiments 1 through 17 were run on a model with 2 barrels measuring 6 inches by 6 inches in area and a length of 6.9 feet which represented under pressure flow condition. For Experiments 18 through 32, the height of the culvert was raised to 12 inches with the original length of 6.9 feet and width of 6 inches which represented the open channel condition. Different configurations of friction blocks, and sills were used in the experiments. All results are shown in Table 1 for pressure flow experiments and Table 2 for open channel flow experiments, and selected experiment photos can be seen in Appendix A.

In these experiments, the length of the hydraulic jump (L), the depth before the jump (Y_1), the depth after the jump (Y_2), the distance from the beginning of the hydraulic jump to the beginning of the sill (X), the depth of the water in the inclined channel (Y_s), and the depth of the water downstream of the culvert ($Y_{D/S}$) were measured. All dimensions were measured by using a rule and point gage. The flowrate was measured by a two plate manometer between which measures the pressure

difference in a fixed pipe opening size. As mentioned above, the velocity before the jump (V_1) was measured by a pitot tube and the velocity at the inlet of structure as seen in Figure 12 ($V_{u/s}$), the velocity after the jump (V_2), and the velocity downstream of culvert ($V_{D/S}$) were all measured by ADV.

The procedure of the experiment is as follows:

1. Install energy dissipation (such as sills or friction blocks) in the model
2. Set point gage to the correct height in the reserve (for example, Experiment 1A means the head equal to 0.8d)
3. Turn on pump in station
4. Adjust valve and coordinate the opening to obtain the amount of head for the experiment
5. Record the reading for flow rate (using a two plate manometer)
6. Run the model for 10 minutes before taking measurements (to allow for the flow to establish)
7. Measure Y_s, Y_1, Y_2, L, X, and $Y_{D/S}$, as seen in Figure 13
8. Measure velocities along the channel $V_{u/s}$, V_1, V_2, and $V_{D/S}$
9. Post process the raw ADV data to determine final velocity values

Post-processing the raw ADV data was essential to maintain data validity. A software program from the Bureau of Reclamation called WinADV was obtained to process the ADV data. The MicroADV was calibrated according to water temperature, salt content, and total suspended solids. The unit was calibrated to the manufacturer's specification for total suspended solids based on desired trace solution water content. At the end of each day of experiments, the reserve was drained to prevent mold growth which could affect the suspended solid concentration of the water. If this change in sediment concentration were to occur, it could minimally affect velocity readings.

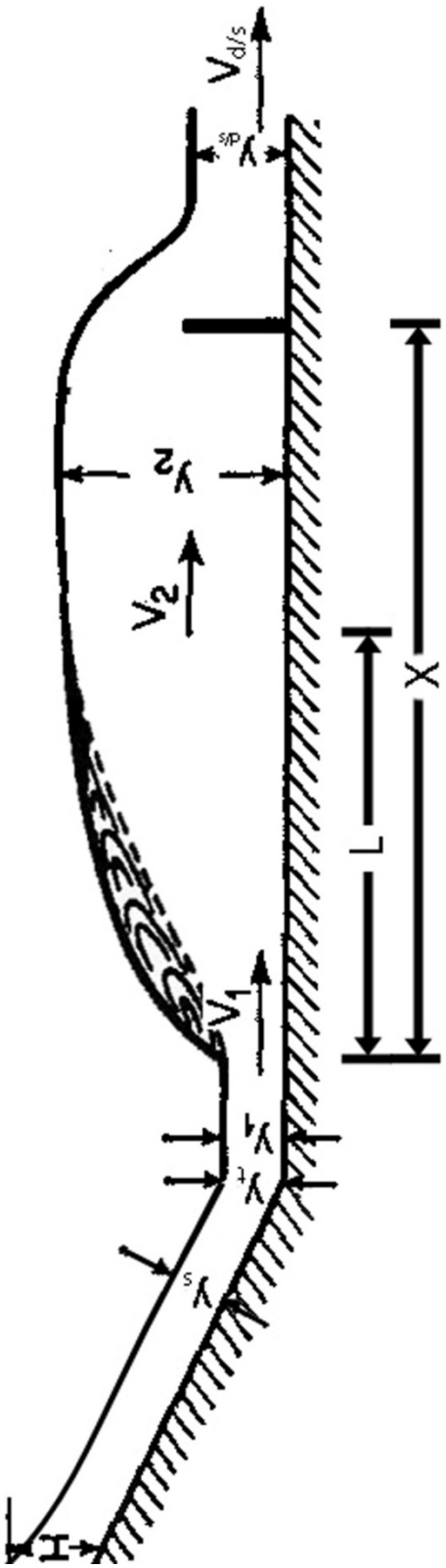

Figure 13. Hydraulic jump variables in a broken-back culvert.

This Page Is Intentionally Blank

DATA ANALYSIS

Eight experiments were selected from thirty-two experiments performed in the hydraulic laboratory. These experiments show model runs without friction blocks, the effect of a sill at the end of the model, and with friction blocks of different shapes as well as the sill. The friction blocks were comprised of three different shapes, including flat-faced friction blocks, semi-circular faced friction blocks, and C-shaped blocks (see Figure 9). After the effectiveness was evaluated, the numbers of blocks were varied by 15, 30, and 45.

In these experiments, the optimum sill height was determined first, the optimum sill location was found next, and finally the effectiveness of friction blocks in combination with the optimum sill parameters was determined.

Experiment 1 was run without any energy dissipation devices or sill in order to evaluate the hydraulic characteristics of the model, including the Froude number and supercritical flow conditions. This experiment is also an example of the current field practice to allow the kinetic energy of fluid to be transferred downstream without energy reduction. This experiment did not produce a hydraulic jump. The results can be found in Table 1, below.

Table 1. Experiment 1 using Pressure Flow Condition with no sill in the culvert.

H.J.	Run	H	W_{temp}	Q	$V_{u/s}$	Y_s	Y_{toe}	Y_1	Y_2	$Y_{d/s}$	Fr1	V_1	V_2	$V_{d/s}$	L	X	ΔE	THL	E_2/E_1
N	1A	0.8d	-	1.0092	2.500	2.50	2.50	-	-	2.13	2.2343	5.78698 P-tube	-	6.00533 P-tube	-	-	-	0.714598	-
N	1B	1.0d	-	1.3145	2.700	2.83	3.37	-	-	2.63	1.9791	5.95147 P-tube	-	6.419968 P-tube	-	-	-	0.648387	-
N	1C	1.2d	-	1.7117	2.800	4.13	4.00	-	-	3.13	1.8330	6.00533 P-tube	-	6.61755 P-tube	-	-	-	0.970876	-

The total head loss between upstream of structure and downstream of structure was calculated by applying the Bernoulli equation:

$$THL = \left(H + \frac{V_{u/s}^2}{2g} + Z \right) - \left(Y_{d/s} + \frac{V_{d/s}^2}{2g} \right)$$

Where:

THL = Total head loss, inches

H = Water depth upstream of the culvert, inches

Z = Drop between upstream and downstream the model was 0.3 feet, representing a 6 foot drop in the prototype.

The loss of energy or energy dissipation in the jump was calculated by taking the difference between the specific energy before the jump and after the jump

$$\Delta E = E_1 - E_2 = \frac{\left(Y_2 - Y_1\right)^3}{4Y_1Y_2}$$

The efficiency of the jump was calculated by taking the ratio of the specific energy before and after the jump:

$$\frac{E_2}{E_1} = \frac{\left(8F_{r1}^2 + 1\right)^{3/2} - 4F_{r1}^2 + 1}{8F_{r1}^2\left(2 + F_{r1}^2\right)}$$

Where the downstream depth was known, the following equation was used to calculate the upstream supercritical flow Froude number (Fr) of the hydraulic jump:

$$Fr_1 = \sqrt{\frac{\left(\frac{2Y_2}{Y_1} + 1\right)^2 - 1}{8}}$$

If the downstream depth was unknown, the following equation was used to calculate the Froude number (Fr) of the hydraulic jump:

$$Fr_1 = \frac{V_1}{\sqrt{gY_1}}$$

Experiment 2 was run with one 1.25-inch sill located 25 inches from the end of the culvert. Experiment 2 demonstrates the use of one sill to control the hydraulic jump under open channel and pressure flow conditions. Pressure flow is defined by the fluid excreting pressure against the top of the model. A hydraulic jump was observed in all three flow conditions. The results show that the Froude number values ranged from 1.8 to 2.3. These ranges of Froude number values are indicative of a weak hydraulic jump. The energy dissipation due to hydraulic jump ranges between 0.1 inches to 0.26 inches and the total head loss for the whole culvert ranges between 1.89 inches to 2.38 inches. Additional results can be seen in Table 2.

Table 2. Experiment 2 using Pressure Flow Condition with a 1.25 inch sill at 25 inches from the end of the culvert.

H.J.	Run	H	W_{temp}	Q	$V_{u/s}$	Y_s	Y_{toe}	Y_1	Y_2	$Y_{d/s}$	Fr1	V_1	V_2	$V_{d/s}$	L	X	ΔE	THL	E_2/E_1
Y	2A	0.8d	-	0.9893	2.500	2.50	2.40	2.55	4.90	2.90	2.2123	5.78688 P-tube	-	4.88139 P-tube	5.00	-	0.26	2.224602	0.874
Y	2B	1.0d	-	1.3853	2.700	2.88	3.38	3.25	5.90	3.25	2.0153	5.95147 P-tube	-	5.58874 P-tube	4.00	-	0.24	1.888382	0.907
Y	2C	1.2d	-	1.6930	2.800	4.25	4.00	3.90	6.00	3.40	1.8729	6.05871 P-tube	-	5.89712 P-tube	4.50	-	0.10	2.380865	0.929

Experiment 12 was run with one 1.25-inch sill located 25 inches from the end of the culvert. In addition, 30 flat faced friction blocks were placed in the horizontal portion of the channel in the pattern as shown in Figure 8. Experiment 12 demonstrates the use of one sill to control the hydraulic jump under open channel and pressure flow conditions. Pressure flow is defined by the fluid excreting pressure against the top of the model. A hydraulic jump was observed in all three flow conditions. The results show that the Froude number values ranged from 1.8 to 2.5. These ranges of Froude number

values are indicative of a weak hydraulic jump. The energy dissipation due to hydraulic jump ranges between 0.03 inches to 0.97 inches and the total head loss for the whole culvert ranges between 1.67 inches to 3.10 inches. Additional results can be seen in Table 3.

Table 3. Experiment 12 using Pressure Flow Condition with a 1.25 inch sill at 25 inches from the end of the culvert with 30 flat-faced friction blocks in front of the sill.

H.J.	Run	H	W_{temp}	Q	$V_{u/s}$	Y_s	Y_{toe}	Y_1	Y_2	$Y_{d/s}$	Fr1	V_1	V_2	$V_{d/s}$	L	X	ΔE	THL	E_2/E_1
Y	12A	0.8d	50.3	0.9812	2.500	2.50	2.38	2.00	5.50	2.50	2.4739	5.73096 P-tube	-	4.609989 P-tube	8.00	-	0.97	3.104597	0.829
Y	12B	1.0d	50.4	1.3621	2.700	3.50	3.75	4.13	5.50	3.25	1.8040	6.00533 P-tube	-	5.3232 P-tube	3.50	-	0.03	2.428300	0.940
Y	12C	1.2d	50.3	1.6883	2.800	3.88	4.00	3.88	6 (u.p.)	3.75	1.8777	6.05871 P-tube	-	6.05871 P-tube	7.00	-	0.10	1.670876	0.929

Experiment 15 was run with a 1.25-inch sill located 25 inches from the downstream end of the culvert. In addition, 30 curved friction blocks were placed in the horizontal portion of the channel in the pattern shown in Figure 8. Experiment 15 was chosen for two reasons: (1) a hydraulic jump formed inside the horizontal section of the model for all three flow conditions, and (2) it is an example of the field being under pressure due to the confines of the model. This experiment produced a hydraulic jump for all three conditions. The total head loss ranges between -0.68 inches to 2.24 inches. The results of this experiment are shown in Table 4.

Table 4. Experiment 15 using Pressure Flow Condition with a 1.25 inch sill at 25 inches from the end of the culvert with 30 curved-face friction blocks in front of the sill.

H.J.	Run	H	W_{temp}	Q	$V_{u/s}$	Y_s	Y_{toe}	Y_1	Y_2	$Y_{d/s}$	Fr1	V_1	V_2	$V_{d/s}$	L	X	ΔE	THL	E_2/E_1
Y	15A	0.8d	48.2	1.0132	2.500	2.50	2.63	2.38	6 (u.p.)	2.88	2.2678	5.73097 P-tube	-	4.88139 P-tube	12.00	-	0.83	2.244597	0.864
Y	15B	1.0d	47.0	1.3084	2.700	3.00	3.38	3.50	6 (u.p.)	3.25	1.8701	5.73097 P-tube	-	5.50164 P-tube	7.50	-	0.19	-0.681615	0.930
Y	15C	1.2d	47.1	1.7325	2.800	4.38	4.00	4.50	6 (u.p.)	4.25	1.7282	6.00530 P-tube	-	5.95147 P-tube	5.00	-	0.03	1.410870	0.951

Experiment 22 was run with a 1.75-inch sill in the middle of the culvert with an increased culvert height of 12 inches. Experiment 22 illustrates the open channel flow condition, the fluid at atmosphere pressure throughout the model, and the use of a single sill at the end to control the hydraulic jump. A hydraulic jump was observed in all three flow conditions. The results show that the Froude number values ranged from 1.7 to 1.9. This range of Froude number values is indicative of a weak type of hydraulic jump. In a weak jump, a series of small rollers develops on the surface of the jump, but the downstream water surface remains smooth (Chow, 1959). The energy dissipation due to the hydraulic jump ranges between 0.64 inches to 0.92 inches and the total head loss for the whole culvert ranges between 1.668 inches to 2.37 inches. Additional results can be seen in Table 5.

Table 5. Experiment 22 using Open Channel Condition with a 1.75 inch sill at the middle of the culvert.

H.J.	Run	H	W_{temp}	Q	$V_{u/s}$	Y_s	Y_{toe}	Y_1	Y_2	$Y_{d/s}$	Fr1	V_1	V_2	$V_{d/s}$	L	X	ΔE	THL	E_2/E_1
Y	22A	0.8d	56.3	0.9893	2.500	2.63	2.50	2.50	6.38	2.75	2.1289	4.94692 P-tube	2.40749 P-tube	4.88139 P-tube	8.50	38.50	0.92	2.374602	0.888
Y	22B	1.0d	56.8	1.3385	2.700	3.00	3.38	3.50	7.50	3.63	1.8350	5.4428 P-tube	3.10805 P-tube	5.50164 P-tube	12.00	-	0.61	1.688377	0.935
Y	22C	1.2d	57.4	1.6954	2.800	4.36	4.00	4.00	8.36	4.00	1.7970	5.5599 P-tube	3.0027 P-tube	5.95147 P-tube	14.00	-	0.62	1.660870	0.941

Experiment 26 was run with a 1.75-inch sill 25 inches from the end of the culvert with 30 flat faced friction blocks with an increased culvert height of 12 inches. Experiment 26 was chosen to show a single sill located midway in the horizontal barrel with friction blocks under an open channel flow condition. A hydraulic jump was observed in all three flow conditions. The results show that the Froude number values ranged from 1.7 to 2.1. These ranges of Froude number values are indicative of a weak hydraulic jump. The energy dissipation due to the hydraulic jump ranges between 0.89 inches to 0.96 inches and the total head loss for the whole culvert ranges between 2.11 inches to 2.23 inches. Additional results can be seen in Table 6.

Table 6. Experiment 26 using Open Channel Condition with a 1.75 inch sill at 25 inches from the end of the culvert with 30 flat-faced friction blocks in front of the sill.

H.J.	Run	H	W_{temp}	Q	$V_{u/s}$	Y_s	Y_{toe}	Y_1	Y_2	$Y_{d/s}$	Fr1	V_1	V_2	$V_{d/s}$	L	X	ΔE	THL	E_2/E_1
Y	26A	0.8d	56.8	0.9893	2.473	2.38	2.38	2.38	6.38	2.63	2.2211	5.32316 P-tube	2.7799 P-tube	5.011586 P-tube	14.00	54.00	1.05	2.229808	0.892
Y	26B	1.0d	56.8	1.3296	2.659	3.00	3.50	4.13	7.50	3.38	1.5990	5.6745 P-tube	3.30877 P-tube	5.3833 P-tube	13.00	51.00	0.31	2.137657	0.954
Y	26C	1.2d	57.1	1.7279	2.880	4.38	3.88	4.88	8.38	3.75	1.5274	5.89712 P-tube	3.20998 P-tube	5.89712 P-tube	14.00	48.50	0.26	2.115357	0.963

Experiment 27 was run with one 1.75-inch sill located 25 inches from the end of the culvert. In addition, 45 flat faced friction blocks were placed in the horizontal portion of the channel in the pattern shown in Figure 8. A hydraulic jump was observed in all three flow conditions. The results show that the Froude number values ranged from 1.7 to 2.1. These ranges of Froude number values are indicative of a weak hydraulic jump. The energy dissipation due to hydraulic jump ranges between 0.4 inches to 1.1 inches and the total head loss for the whole culvert ranges between 2.11 inches to 2.20 inches. Additional results can be seen in Table 7.

Table 7. Experiment 27 using Open Channel Condition with a 1.75 inch sill at 25 inches from the end of the culvert with 45 flat-faced friction blocks in front of the sill.

H.J.	Run	H	W_{temp}	Q	$V_{u/s}$	Y_s	Y_{toe}	Y_1	Y_2	$Y_{d/s}$	Fr1	V_1	V_2	$V_{d/s}$	L	X	ΔE	THL	E_2/E_1
Y	27A	0.8d	57.0	0.9893	2.473	2.63	2.38	2.38	6.50	2.75	2.2572	5.3833 P-tube	2.8934 P-tube	5.01159 P-tube	13.00	54.00	1.13	2.109801	0.888
Y	27B	1.0d	57.1	1.3355	2.671	3.00	3.50	3.50	7.38	3.25	1.8103	5.61747 P-tube	3.49799 P-tube	5.44280 P-tube	13.00	52.50	0.57	2.159348	0.935
Y	27C	1.2d	57.2	1.7094	2.849	3.88	4.00	4.38	8.25	3.75	1.6479	5.78688 P-tube	3.8486 P-tube	5.84230 P-tube	14.00	52.25	0.40	2.202360	0.956

Experiment 29 was run with a 1.75-inch sill located 25 inches from the end of the culvert. In addition, 30 curved faced friction blocks were placed in the horizontal portion of the channel in the pattern shown in Figure 8. A hydraulic jump was observed in all three flow conditions. The results show that the Froude number values ranged from 1.7 to 1.9. These ranges of Froude number values are indicative of a weak hydraulic jump. The energy dissipation due to the hydraulic jump ranges between 0.88 inches to 0.95 inches and the total head loss for the whole culvert ranges between -0.32 inches to 2.25 inches. Additional results can be seen in Table 8.

Table 8. Experiment 29 using Open Channel Condition with a 1.75 inch sill at 25 inches from the end of the culvert with 30 curved-face friction blocks in front of the sill.

H.J.	Run	H	W_{temp}	Q	$V_{u/s}$	Y_s	Y_{toe}	Y_1	Y_2	$Y_{d/s}$	Fr1	V_1	V_2	$V_{d/s}$	L	X	ΔE	THL	E_2/E_1
Y	29A	0.8d	59.1	0.9973	2.500	2.38	2.50	2.50	6.50	2.75	2.1633	5.01159 P-tube	2.53715 P-tube	4.94692 P-tube	10.00	56.00	0.98	2.254593	0.882
Y	29B	1.0d	59.7	1.3084	2.700	2.88	3.25	3.25	7.50	3.38	1.9536	5.55986 P-tube	2.89344 P-tube	5.32316 P-tube	12.00	53.00	0.79	-0.321621	0.917
Y	29C	1.2d	59.8	1.7140	2.800	4.13	4.00	4.13	8.38	4.13	1.7530	5.78688 P-tube	3.10805 P-tube	5.95147 P-tube	12.00	49.00	0.55	1.530870	0.947

Experiment 31 was run with one 1.75-inch sill located 25 inches from the end of the culvert and utilized the increased culvert height of 12 inches. In addition, 30 c-shaped friction blocks were placed in the horizontal portion of the channel in the pattern shown in Figure 8. A hydraulic jump was observed in all three flow conditions. The results show that the Froude number values ranged from 1.5 to 2.2. These ranges of Froude number values are indicative of a weak type of hydraulic jump. The energy dissipation due to the hydraulic jump ranges between 0.88 inches to 0.97 inches and the total head loss for the whole culvert ranges between 1.53 inches to 2.37 inches. Additional results can be seen in Table 9.

Table 9. Experiment 31 using Open Channel Condition with a 1.75 inch sill at 25 inches from the end of the culvert with 15 C-shaped friction blocks in front of the sill.

H.J.	Run	H	W_{temp}	Q	$V_{u/s}$	Y_s	Y_{toe}	Y_1	Y_2	$Y_{d/s}$	Fr1	V_1	V_2	$V_{d/s}$	L	X	ΔE	THL	E_2/E_1
Y	31A	0.8d	60.8	0.9937	2.500	2.63	2.50	2.50	6.50	2.88	2.1633	5.07543 P-tube	2.77992 P-tube	4.94690 P-tube	10.00	55.50	0.98	2.12463	0.882
Y	31B	1.0d	61.1	1.3175	2.700	3.00	3.38	4.00	7.50	3.25	1.6417	5.55986 P-tube	3.10803 P-tube	5.35330 P-tube	11.00	53.00	0.36	2.368418	0.962
Y	31C	1.2d	61.3	1.7302	2.800	4.00	3.88	5.00	8.50	4.25	1.5149	5.75899 P-tube	3.4047 P-tube	5.89712 P-tube	13.50	52.50	0.25	1.530865	0.977

This Page Is Intentionally Blank

RESULTS

PRESSURE FLOW CONDITION

After careful evaluation, Experiments 2 and 12 were selected from the data analysis portion for a pressure flow condition. These experiments were selected by examining many factors, including their relativity low downstream velocities (4 to 6 fps), high total hydraulic head losses, and hydraulic jump efficiency. It was found that these experiments yielded results most applicable to modifying existing culverts with the addition of sills and/or friction blocks. Figure 14 shows characteristics of the hydraulic jump for Experiment 2C in Table 10 and Figure 15 shows characteristics for Experiment 12C in Table 11.

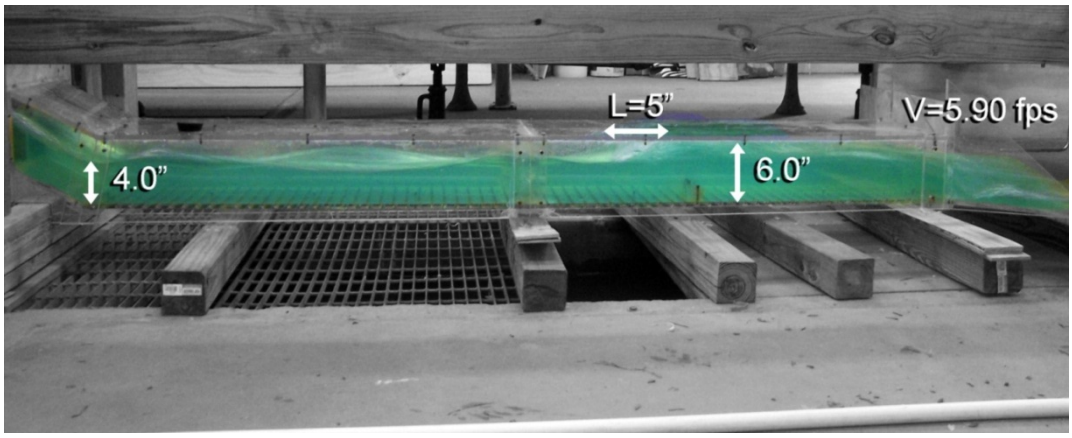

Figure 14. Characteristics of hydraulic jump for Experiment 2C under pressure flow condition.

Table 10. Selected factors for Experiment 2.

Experiment 2A For 0.8d	Experiment 2B For 1.0d	Experiment 2C For 1.2d
Y_2 = 4.90 in	Y_2 = 5.90 in	Y_2 = 6.00 in
$V_{d/s}$ = 4.88 fps	$V_{d/s}$ = 5.59 fps	$V_{d/s}$ = 5.90 fps
THL = 2.22 in.	THL = 1.89 in.	THL = 2.38 in.
E_1/E_2 = 0.87	E_1/E_2 = 0.91	E_1/E_2 = 0.93
Channel reduction = none	Channel reduction = none	Channel reduction = none

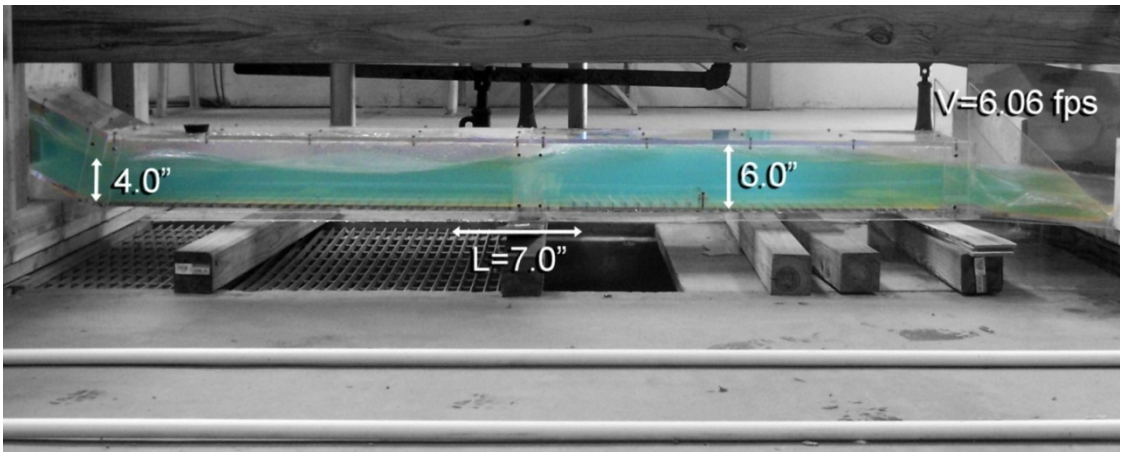

Figure 15. Characteristics of hydraulic jump for Experiment 12C under pressure flow condition.

Table 11. Selected factors for Experiment 12.

Experiment 12A For 0.8d	**Experiment 12B For 1.0d**	**Experiment 12C For 1.2d**
Y_2 = 5.5 in	Y_2 = 5.5 in	Y_2 = 6 in (under pressure)
$V_{d/s}$ = 4.61 fps	$V_{d/s}$ = 5.32 fps	$V_{d/s}$ = 6.06 fps
THL = 3.10 inches	THL = 2.43 inches	THL = 1.67 inches
E_1/E_2 = 0.83	E_1/E_2 = 0.94	E_1/E_2 = 0.93
Channel reduction = 24 in (40 ft)	Channel reduction = 12 in (20 ft)	Channel reduction = none

OPEN CHANNEL FLOW CONDITION

After careful evaluation, Experiments 22 and 26 were selected from the data analysis portion for an open channel flow condition. These experiments were selected by examining many factors, including their relativity low downstream velocities, high total hydraulic head losses, acceptable hydraulic jump efficiency, and possible reduction in channel length. Experiments 22 and 26 have the similar sill arrangements, with friction blocks added to the horizontal channel barrel in Experiment 26. It was found that these experiments yielded results most applicable to the new construction of culverts due to the increased ceiling height of the culvert. The culvert barrel could be reduced by reducing a section at the end of the channel where the water surface profile is more uniform. Figure 16 shows characteristics of the hydraulic jump for Experiment 22 in Table 12 and Figure 17 shows characteristics for Experiment 26 in Table 13.

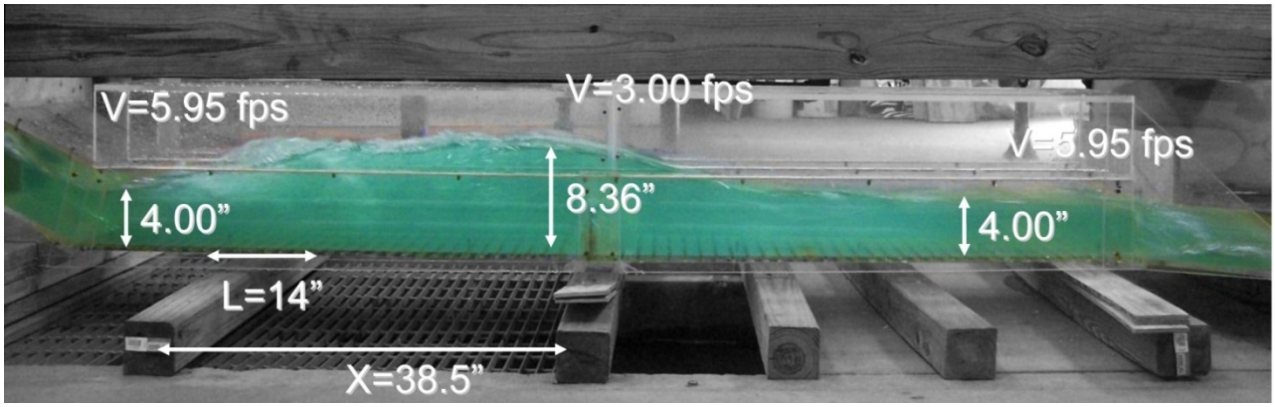

Figure 16. Characteristics of hydraulic jump for Experiment 22C under open channel flow condition.

Table 12. Selected factors for Experiment 22.

Experiment 22A For 0.8d	**Experiment 22B For 1.0d**	**Experiment 22C For 1.2d**
Y_2 = 6.38 in	Y_2 = 7.5 in	Y_2 = 8.36 in
$V_{d/s}$ = 4.88 fps	$V_{d/s}$ = 5.50 fps	$V_{d/s}$ = 5.95 fps
THL = 2.37 inches	THL = 1.69 inches	THL = 1.66 inches
E_1/E_2 = 0.89	E_1/E_2 = 0.94	E_1/E_2 = 0.94
Channel reduction = 34 in (56.0 ft)	Channel reduction = 34 in (56.0 ft)	Channel reduction = 25 in (42.0 ft)

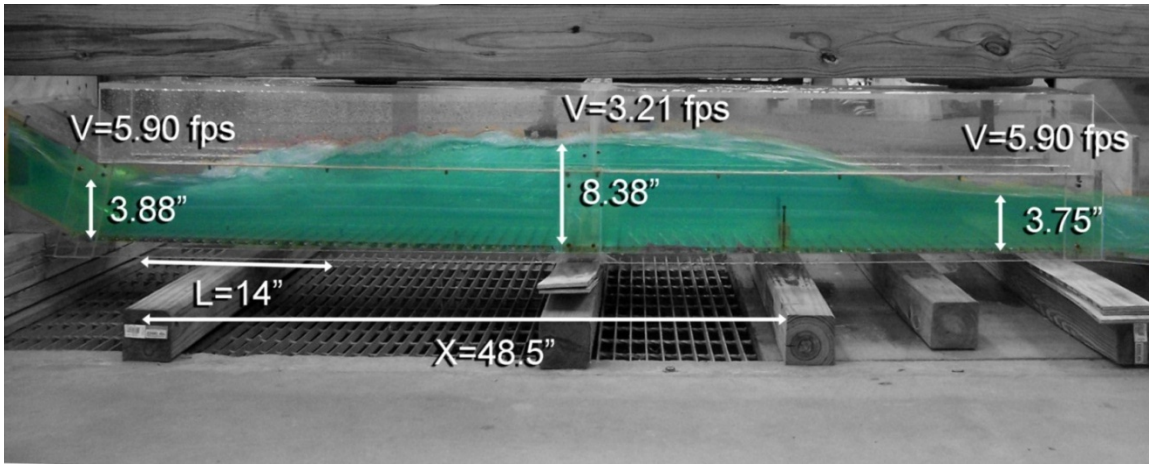

Figure 17. Characteristics of hydraulic jump for Experiment 26C under open channel flow condition.

Table 13. Selected factors for Experiment 26.

Experiment 26A For 0.8d	**Experiment 26B For 1.0d**	**Experiment 26C For 1.2d**
Y_2 = 6.38 in	Y_2 = 7.5 in	Y_2 = 8.38 in
$V_{d/s}$ = 5.01 fps	$V_{d/s}$ = 5.38 fps	$V_{d/s}$ = 5.90 fps
THL = 2.23 inches	THL = 2.14 inches	THL = 2.11 inches
E_1/E_2 = 0.89	E_1/E_2 = 0.95	E_1/E_2 = 0.96
Channel reduction = 20 in (33.3 ft)	Channel reduction = 20 in (33.3 ft)	Channel reduction = 12 in (20 ft)

CONCLUSIONS

A laboratory model was constructed to represent a broken-back culvert. The idealized prototype contains a 1 (vertical) to 2 (horizontal) slope, a 12-foot horizontal length of slanted part of culvert continuing down to a 138-foot flat culvert with a 1 percent slope. The model was made to 1:20 scale. The following dimensions are in terms of the prototype culvert. It was noted that the current practice of not using any energy dissipaters (as in Experiment 1) allowed all the energy to flow through the culvert instead of reducing or dissipating it. The following conclusions can be drawn based on the laboratory experiments for pressure flow conditions and open channel flow conditions:

Pressure Flow Conditions

1) For retrofitting an existing culvert, Experiment 2 is the best option for pressure flow condition. It consists of three flow conditions: 0.8, 1.0 and 1.2 times the upstream culvert depth of 10 feet. This scenario uses one sill with two small orifices at the bottom, so that water can be completely drained from the culvert. The sill is located 42 feet from the outlet face of the culvert.
2) Optimal placement of one sill, 2.1 ft. (1.25 inches) high, resulted in 91 percent energy dissipation as noted in Experiment 2C.
3) If one sill, 2.1 feet high, and 30 flat faced friction blocks are placed in the flat part of the culvert starting at formation of the hydraulic jump, energy dissipation of 93 percent occurs as noted in Experiment 12C.
4) The reduction of energy due to the region of friction blocks is marginal.
5) Experiment 2 offers similar performance to friction block experiments without the additional cost.
6) For Experiment 2, no reduction in culvert length can be made due to the full flow at the end of the culvert, as can be seen in Table 10.
7) For Experiment 12, reduction in culvert length can be made at the end of the culvert for 12A and 12B. But no reduction in culvert length can be made for 12C, as can be seen in Table 11.

Open Channel Flow Condition

8) For new culvert construction, Experiment 22 is the best option for an open channel flow condition. This option includes one sill with two small orifices at the bottom for draining the culvert completely. The sill is located 69 feet from the end of the culvert. The height of the culvert should be 14 feet to allow open channel condition in the culvert.

9) If one sill 3.0 feet high is placed in the flat part of the culvert, it results in 94 percent of energy loss as seen in Experiment 22C.

10) If one sill 3.0 feet high with 30 flat faced friction blocks are placed in the flat part of the culvert starting at initiation of hydraulic jump, energy dissipation of 96 percent occurs as seen in Experiment 26C.

11) The reduction of energy due to 30 friction blocks is marginal. The optimal 3.0 foot sill is the most economical option.

12) Experiment 22 shows an opportunity to reduce the culvert length at the end in the range of 42 to 56 feet. The 42-foot reduction was determined by eliminating the downstream segment of the culvert where the water surface is no longer uniform after the jump. The 56-foot reduction results from removing a portion of the downstream culvert from the sill to the beginning of the downstream wing-wall section. This option is important if there are problems with the right-of-way.

Comparison between 24-foot and 6-foot drop conditions:

13) The 24-foot drop was under an Oscillating jump condition while the 6 foot drop was under a weak jump condition.

14) 58-89 percent of the energy was dissipated in the 24-foot drop while 89-97 percent of the energy was dissipated in the 6 foot drop.

15) Under open channel conditions the 24-foot drop could have its length reduced by 15-44 feet, while the 6-foot drop could have its length reduced by 42-56 feet.

16) Under pressure flow conditions no reductions in length could be made for either the 24-foot or the 6-foot drop.

17) The best open channel flow scenario for the 24-foot drop was one sill 6 feet high at 40 feet from the outlet, but for the 6-foot drop one sill 3 feet high at 42 feet from the outlet.

18) The best pressure flow scenario for the 24-foot drop was two sills of 3.33 feet high at 45 feet from the outlet and 5 feet high at 25 feet from the outlet, but for the 6-foot drop was one sill of 2.1 feet high at 42 feet from the outlet.

19) For both drop conditions the flat faced friction blocks were the best shape, but they provide negligible impact on the jump efficiency.

This Page Is Intentionally Blank

REFERENCES

1. Alikhani, A., Behroz-Rad, R., and Fathi-Moghadam, M. (2010). Hydraulic jump in stilling basin with vertical end sill. International Journal of Physical Sciences. 5(1), 25-29.
2. Bhutto, H., Mirani, S. and Chandio, S. (1989). Characteristics of free hydraulic jump in rectangular channel. Mehran University Research Journal of Engineering and Technology, 8(2), 34 – 44.
3. Chanson, H. (2008). Acoustic Doppler velocimetery (ADV) in the field and in laboratory: practical experiences. International Meeting on Measurements and Hydraulics of Sewers, 49-66.
4. Chanson, H. (2009). Current knowledge in hydraulic jumps and related phenomena. European Journal of Mechanics B/Fluid. 29(2009), 191-210.
5. Chow, V.T. (1959). Open-channel Hydraulics. McGraw-Hill, New York, NY, 680 pages.
6. Eloubaidy, A., Al-baidbani, J., and Ghazali, A. (1999). Dissipation of hydraulic energy by curved baffle Blocks. Pertanika Journal Science Technology. 7 (1), 69-77 (1999).
7. Federal Highway Administration (2006). The Hydraulic Design of Energy Dissipaters for Culverts and Channels.
8. Finnemore, J. E., and Franzini, B. J., (2002) Fluid mechanics with engineering applications. McGraw-Hill, New York, NY, 790.
9. Gharanglk, A. and Chaudhry, M. (1991). Numerical simulation of hydraulic jump. Journal of Hydraulic Engineering. 117(9), 1195 – 1211.
10. Goring, D., Nikora, V. (2002). Despiking ascoustic doppler velocimeter data. Journal Of Hydraulic Engineering, 128(1), 117-128.
11. Hotchkiss, R. and Donahoo, K. (2001). Hydraulic design of broken-back culvert. Urban Drainage Modeling, American Society of Civil Engineers, 51 – 60.
12. Hotchkiss, R., Flanagan, P. and Donahoo, K. (2003). Hydraulic jumps in broken-back culvert. Transportation Research Record (1851), 35 – 44.

13. Hotchkiss, R. and Larson, E. (2005). Simple Methods for Energy Dissipation at Culvert Outlets. Impact of Global Climate Change. World Water and Environmental Resources Congress.
14. Hotchkiss, R., Thiele, E., Nelson, J., and Thompson, P. (2008). Culvert Hydraulics: Comparison of Current Computer Models and Recommended Improvements. Journal of the Transportation Research Board, No. 2060, Transportation Research Board of the National Academies, Washington, D.C, 2008, pp. 141-149.
15. Larson, E. (2004). Energy dissipation in culverts by forcing a hydraulic jump at the outlet. Master's Thesis, Washington State University.
16. Mignot, E. and Cienfuegos, R. (2010). Energy dissipation and turbulent production in weak hydraulic jumps. Journal of Hydraulic Engineering, ASCE, 136 (2), 116-121.
17. Mori, N. Suzuki, T., and Kakuno, S. (2007). Noise of acoustic doppler velocimeter data in bubbly flows. Journal of Engineering Mechanics, 133(1), 122-125.
18. Ohtsu I., Yasuda, Y., and Hashiba, H. (1996). Incipient jump conditions for flows over a vertical sill. Journal of Hydraulic Engineering, ASCE. 122(8) 465-469. doi: 10.1061/(ASCE)0733-29(1996)122:8(465).
19. Ohtsu, I et al. (2001). Hydraulic condition for undular jump formation. Journal of Hydraulic Research. 39(2), 203-209.
20. Pagliara, S., Lotti, I., and Palermo, M. (2008). Hydraulic jump on rough bed of stream rehabilitation structures. Journal of Hydro-environment Research 2(1), 29-38.
21. Rusch, R. (2008) Personal communication, Oklahoma Department of Transportation.
22. SonTek/YSI, Inc. ADVField/Hydra System Manual (2001).
23. Tyagi, A. K. and Schawn, B. (2002). A Prioritizing Methodology for Scour-critical Culverts in Oklahoma. Oklahoma Transportation Center.
24. Tyagi, A.K., et al., (2009), "Laboratory Modeling of Energy Dissipation in Broken-back Culverts – Phase I," Oklahoma Transportation Center, Oklahoma, 82 pp.
25. Tyagi, A.K. et al., (2010a). Energy Dissipation in Broken-back Culverts under Open Channel Flow Conditions. Am. Soc. Civil Engineers International Perspective on Current and Future State of Water Resources, 10.

26. Tyagi, A.K., Al-Madhhachi, A., and Brown, J. (2010b). Energy Dissipation in Broken-back Culverts under Pressure Flow Conditions. J. Hyd. Eng. (submitted for peer review).
27. Utah Department of Transportation (2004.) Manual of Instruction – Roadway Drainage and Culverts.
28. Varol, F., Cevik, E., and Yuksel, Y. (2009). The effect of water jet on the hydraulic jump. Thirteenth International Water Technology Conference, IWTC. 13 (2009), 895-910, Hurghada, Egypt.
29. Wahl, T. (2000). Analyzing ADV data using WinADV. 2000 joint water resources engineering and water resources planning and management, July 30- August 2, 2000- Minneapolis, Minnesota.
30. Wahl, T. (2003). Discussion of “Despiking acoustic Doppler velocimeter data” by Goring, D. and Nikora, V. Journal of Hydraulic Engineering,129(6), 484-487.

This Page Is Intentionally Blank

Appendix A

Laboratory Experiments for Hydraulic Jump

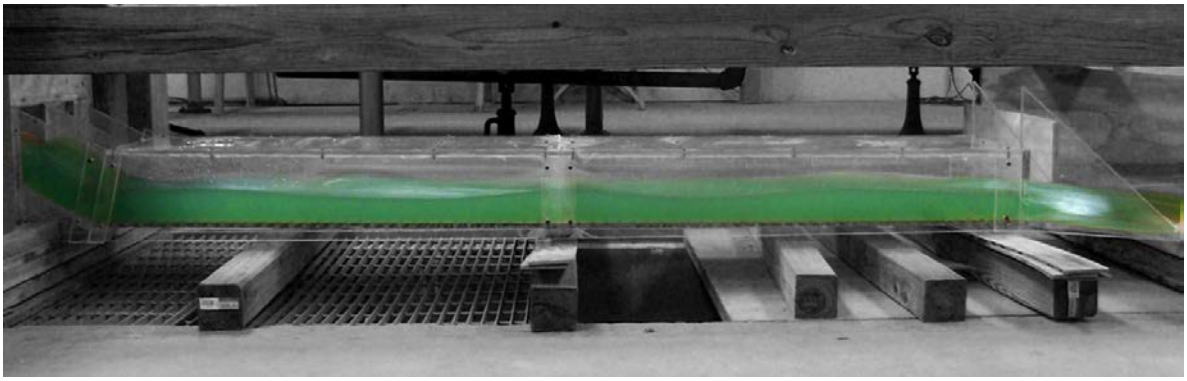

Figure A1. Experiment 1A

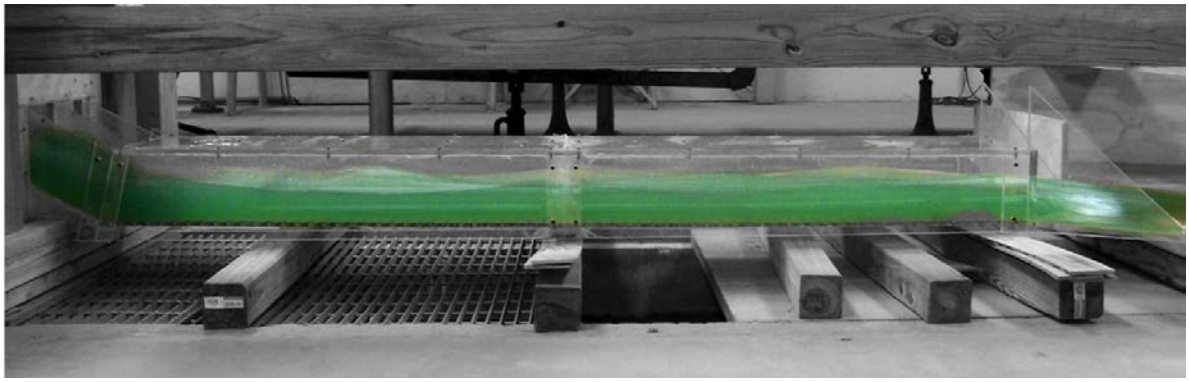

Figure A2. Experiment 1B

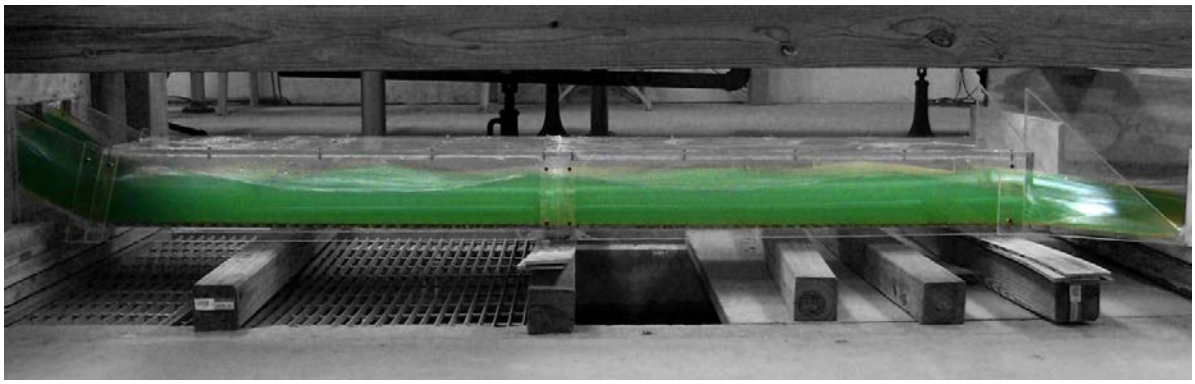

Figure A3. Experiment 1C

Table A1. Experiment 1 using Pressure Flow Condition with no sill in the culvert.

H.J.	Run	H	W_{temp}	Q	$V_{u/s}$	Y_s	Y_{toe}	Y_1	Y_2	$Y_{d/s}$	Fr1	V_1	V_2	$V_{d/s}$	L	X	ΔE	THL	E_2/E_1
N	1A	0.8d	-	1.0092	2.500	2.50	2.50	-	-	2.13	2.2343	5.78698 P-tube	-	6.00533 P-tube	-	-	-	0.714598	-
N	1B	1.0d	-	1.3145	2.700	2.83	3.37	-	-	2.63	1.9791	5.95147 P-tube	-	6.419968 P-tube	-	-	-	0.648387	-
N	1C	1.2d	-	1.7117	2.800	4.13	4.00	-	-	3.13	1.8330	6.00533 P-tube	-	6.61755 P-tube	-	-	-	0.970876	-

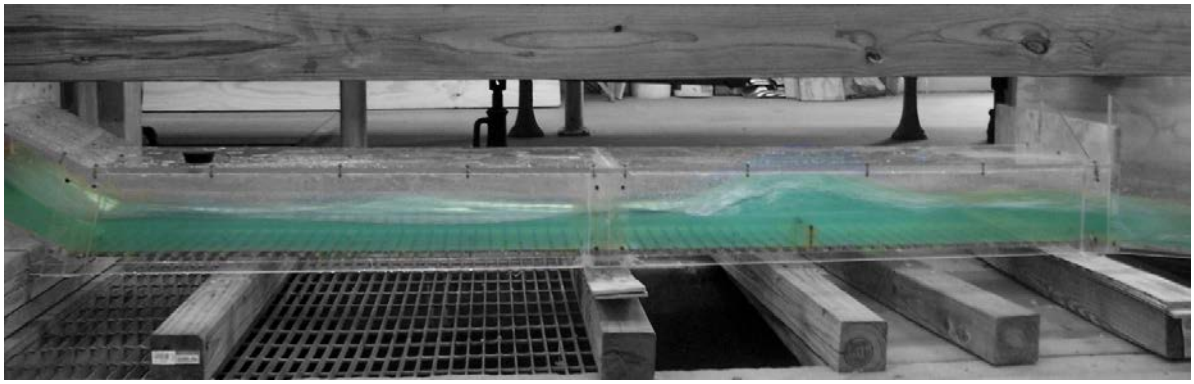

Figure A4. Experiment 2A

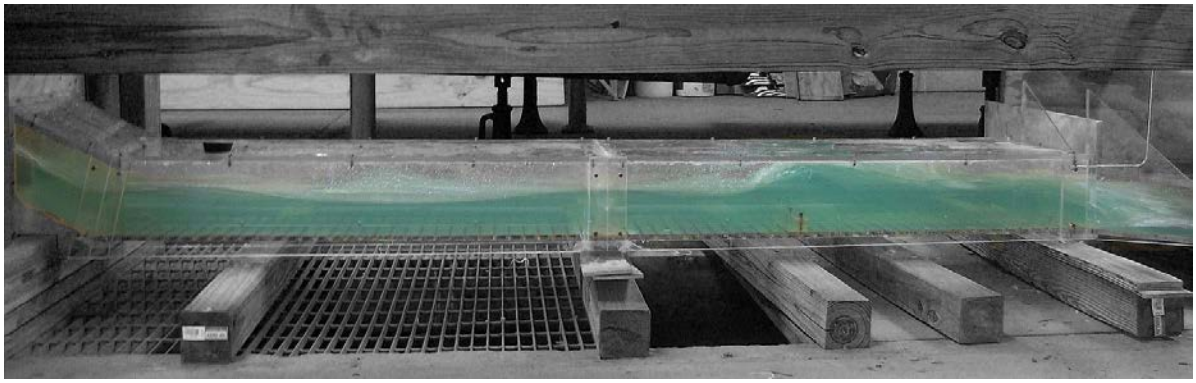

Figure A5. Experiment 2B

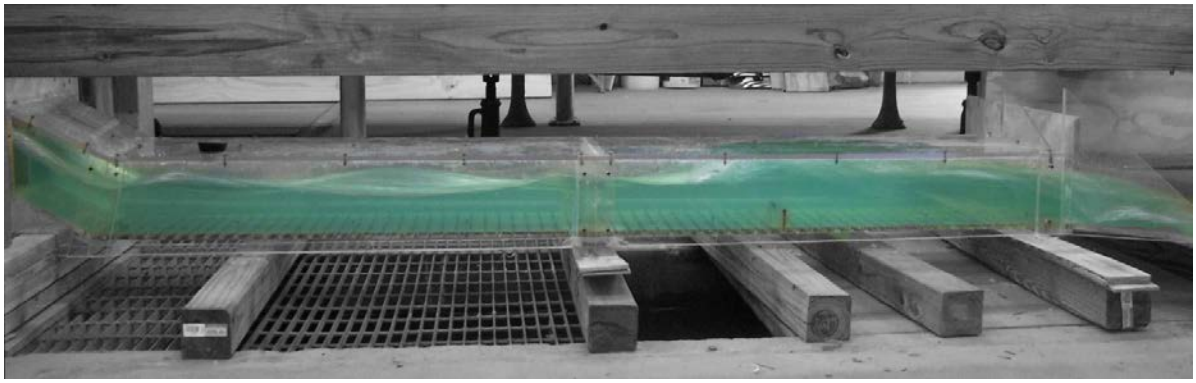

Figure A6. Experiment 2C

Table A2. Experiment 2 using Pressure Flow Condition with a 1.25 inch sill at 25 inches from the end of the culvert.

H.J.	Run	H	W_{temp}	Q	$V_{u/s}$	Y_s	Y_{toe}	Y_1	Y_2	$Y_{d/s}$	Fr1	V_1	V_2	$V_{d/s}$	L	X	ΔE	THL	E_2/E_1
Y	2A	0.8d	-	0.9893	2.500	2.50	2.40	2.55	4.90	2.90	2.2123	5.78688 P-tube	-	4.88139 P-tube	5.00	-	0.26	2.224602	0.874
Y	2B	1.0d	-	1.3853	2.700	2.88	3.38	3.25	5.90	3.25	2.0153	5.95147 P-tube	-	5.58874 P-tube	4.00	-	0.24	1.888382	0.907
Y	2C	1.2d	-	1.6930	2.800	4.25	4.00	3.90	6.00	3.40	1.8729	6.05871 P-tube	-	5.89712 P-tube	4.50	-	0.10	2.380865	0.929

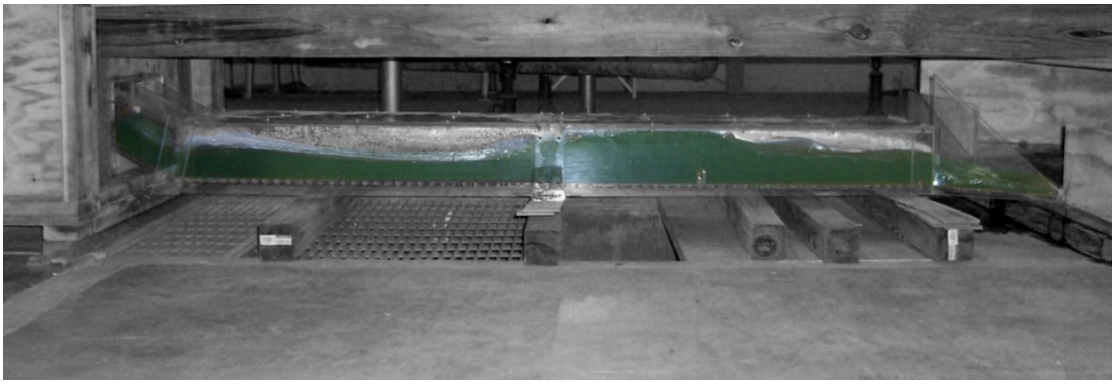

Figure A7. Experiment 3A

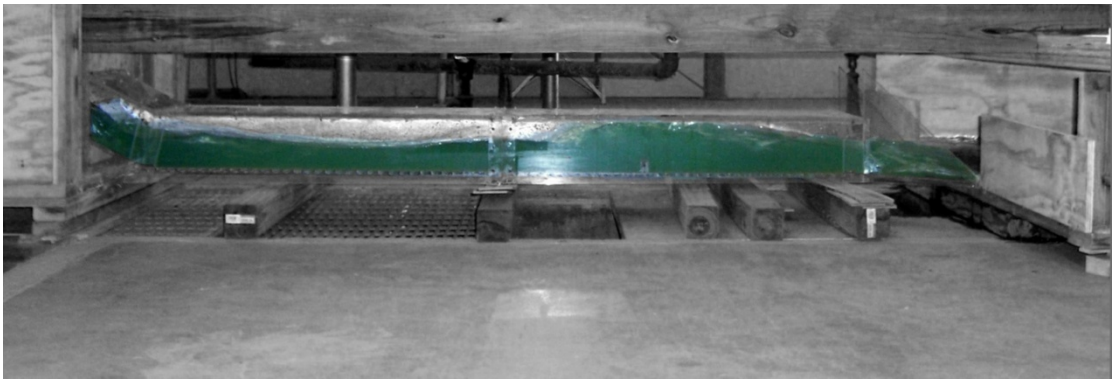

Figure A8. Experiment 3B

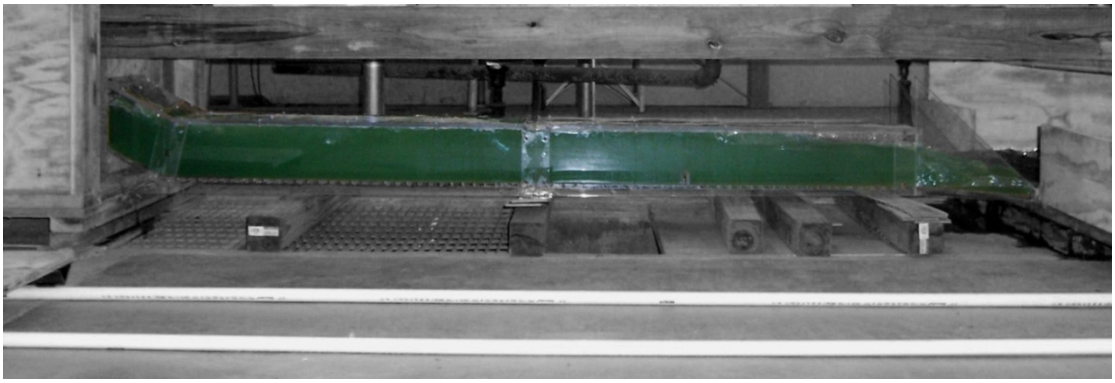

Figure A9. Experiment 3C

Table A3. Experiment 3 using Pressure Flow Condition with a 1.5 inch sill at 25 inches from the end of the culvert.

H.J.	Run	H	W_{temp}	Q	$V_{u/s}$	Y_s	Y_{toe}	Y_1	Y_2	$Y_{d/s}$	Fr1	V_1	V_2	$V_{d/s}$	L	X	ΔE	THL	E_2/E_1
Y	3A	0.8d	53.5	1.0092	2.500	2.75	2.50	2.00	5.25	2.87	2.2127	5.73097 P-tube	-	4.81498 P-tube	9.50	-	0.82	2.374590	0.874
Y	3B	1.0d	53.5	1.3255	2.700	4.38	3.50	3.50	6 (u.p.)	3.00	1.9420	5.95147 P-tube	-	5.41313 P-tube	8.50	-	0.19	2.498389	0.919
Y (Drown)	3C	1.2d	53.5	1.6598	2.800	4.65	6.00	4.65 (slope)	6 (u.p.)	4.50	1.2443	4.39545 P-tube (U.P.)	-	6.216108 P-tube	2.50	-	0.02	0.560870	0.996

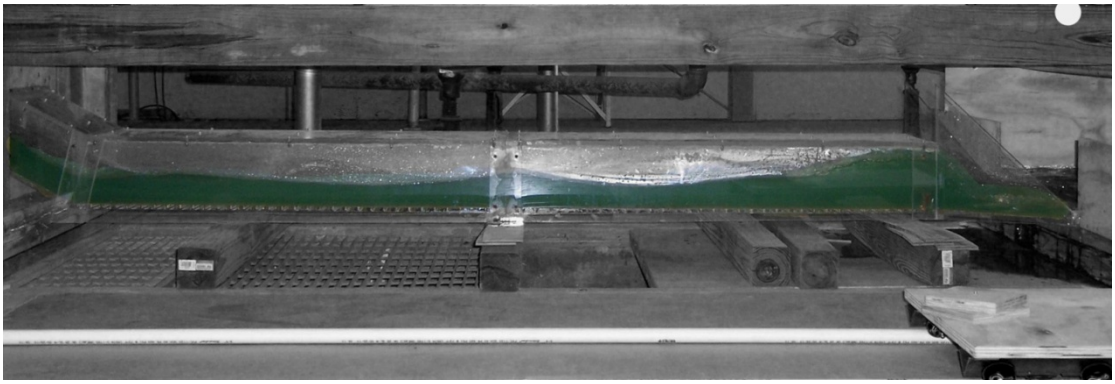

Figure A10. Experiment 4A

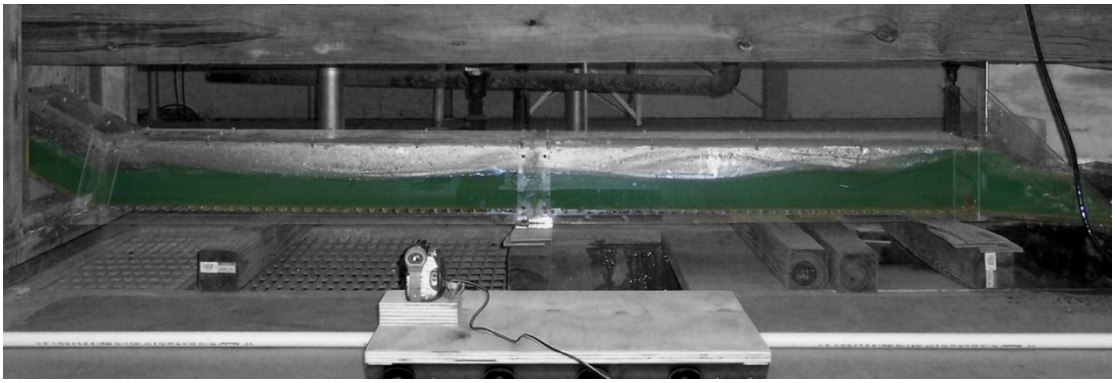

Figure A11. Experiment 4B

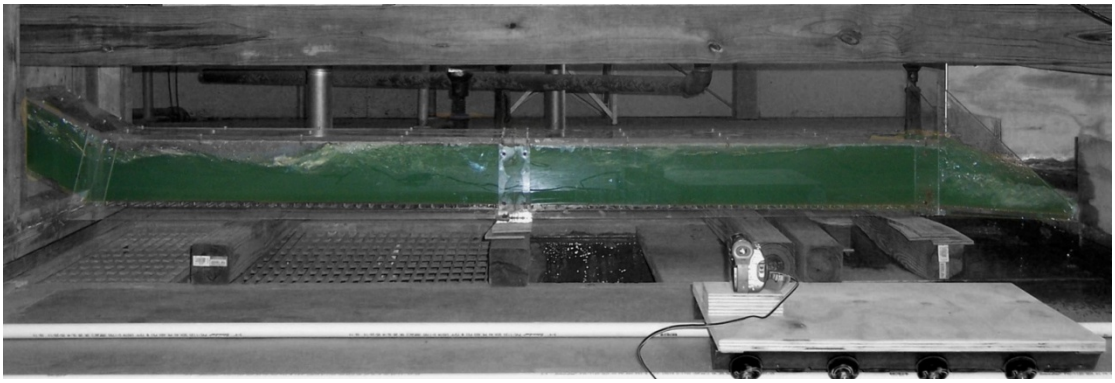

Figure A12. Experiment 4C

Table A4. Experiment 4 using Pressure Flow Condition with a 1.5 inch sill at the end of the culvert.

H.J.	Run	H	W_{temp}	Q	$V_{u/s}$	Y_s	Y_{toe}	Y_1	Y_2	$Y_{d/s}$	Fr1	V_1	V_2	$V_{d/s}$	L	X	ΔE	THL	E_2/E_1
Y	4A	0.8d	-	1.0132	2.500	2.25	2.13	2.13	4.75	4.75	2.4234	5.78688 P-tube	-	5.501636 P-tube	8.50	-	0.45	-0.825403	0.838
N	4B	1.0d	-	1.2962	2.700	2.87	2.38	2.25	5.50	5.50	2.4221	5.95147 P-tube	-	5.6831 corr = 80%	-	-	0.69	-0.559806	0.838
Y	4C	1.2d	-	1.7024	2.800	3.87	3.75	3.75	6 (u.p.)	6 (u.p.)	1.7158	5.442793 P-tube	-	5.7316 corr = 78%	5 (slope)	-	0.13	0.139521	0.952

Table A5. Experiment 5 using Pressure Flow Condition with a 2 inch sill at the end of the culvert.

H.J.	Run	H	W_{temp}	Q	$V_{u/s}$	Y_s	Y_{toe}	Y_1	Y_2	$Y_{d/s}$	Fr1	V_1	V_2	$V_{d/s}$	L	X	ΔE	THL	E_2/E_1
Y	5A	0.8d	57.4	1.0210	2.500	2.50	2.38*	2.38	6 (u.p.)	6 (u.p.)	2.3118	5.8423 P-tube	-	4.6099 P-tube	15.50	-	0.83	-0.395	0.857
Y (Toe)	5B	1.0d	57.4	1.3266	2.700	3.00	3.00*	3.00	6 (u.p.)	6 (u.p.)	1.6248	4.609989 P-tube	-	5.7309 P-tube	8.00	-	0.38	-1.161	0.964
Y (Drown)	5C	1.2d	56.8	1.5912	2.800	6.00	6.00*	5.25	6 (u.p.)	6 (u.p.)	1.2442	4.669892 P-tube	-	6.666 P-tube	3.00	-	0.00	-2.019	0.996

Table A7. Experiment 7 using Pressure Flow Condition with a 1.75 inch sill at the end of the culvert.

H.J.	Run	H	W_{temp}	Q	$V_{u/s}$	Y_s	Y_{toe}	Y_1	Y_2	$Y_{d/s}$	Fr1	V_1	V_2	$V_{d/s}$	L	X	ΔE	THL	E_2/E_1
Y	7A	0.8d	-	0.9933	2.500	2.88	2.38	2.25	6.00	6.00	2.3551	5.7869 P-tube	-	4.24641 P-tube	10.00	-	0.98	0.204597	0.849
Y	7B	1.0d	-	1.3084	2.700	2.88	3.25	2.75	6 (u.p.)	6.00	1.7725	4.81498 P-tube	-	5.95147 P-tube	7.00	-	0.52	-1.641614	0.944
Y (Drown)	7C	1.2d	49.7	1.6717	2.800	5.00	6 (u.p.)	6 (u.p.)	6 (u.p.)	6 (u.p.)	1.0954	4.39545 P-tube	-	6.216101 P-tube	2.00	-	0.00	-0.939114	1.000

Table A8. Experiment 8 using Pressure Flow Condition with a 1.25 inch sill at 25 inches from the end of the culvert and a 1.5 inch sill at the end of the culvert.

H.J.	Run	H	W_{temp}	Q	$V_{u/s}$	Y_s	Y_{toe}	Y_1	Y_2	$Y_{d/s}$	Fr1	V_1	V_2	$V_{d/s}$	L	X	ΔE	THL	E_2/E_1
Y	8A	0.8d	50.8	0.9973	2.500	2.25	2.50	3.00	5.25	5.00	2.0976	5.9515 P-tube	-	4.5396 P-tube	6.00	-	0.18	0.724602	0.893
Y	8B	1.0d	50.9	1.3650	2.700	3.00	3.50	3.25	6 (u.p.)	6 (u.p.)	1.9969	5.8971 P-tube	-	5.2008 P-tube	7.00	-	0.27	-0.081675	0.910
Y (Drown)	8C	1.2d	51.1	1.6788	2.800	4.25	4.50	4.50	6 (u.p.)	6 (u.p.)	1.4236	4.9469 P-tube	-	5.9515 P-tube	4.00	-	0.03	-0.339196	0.985

Photos for Experiments 5, 7, and 8 have been excluded because they exhibit a drowned jump.

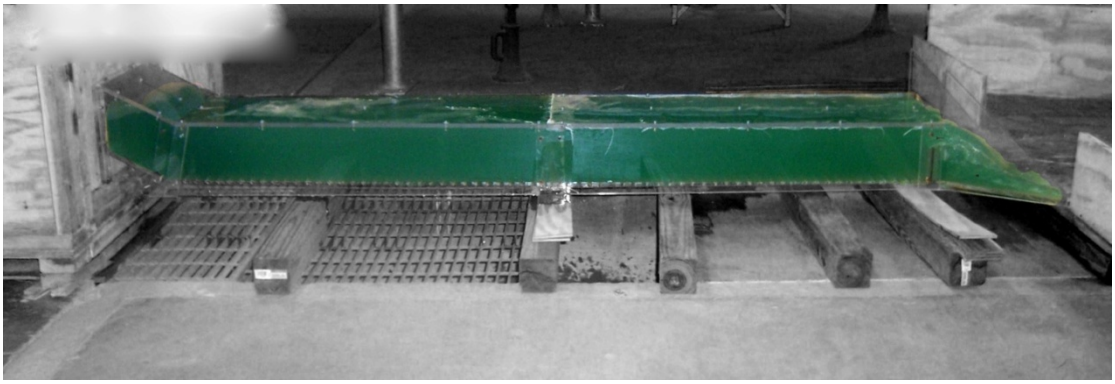

Figure A13. Experiment 6A

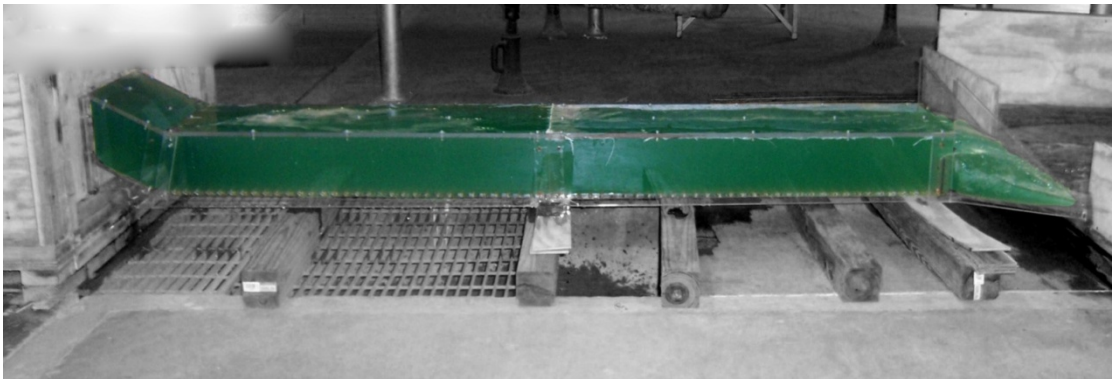

Figure A14. Experiment 6B

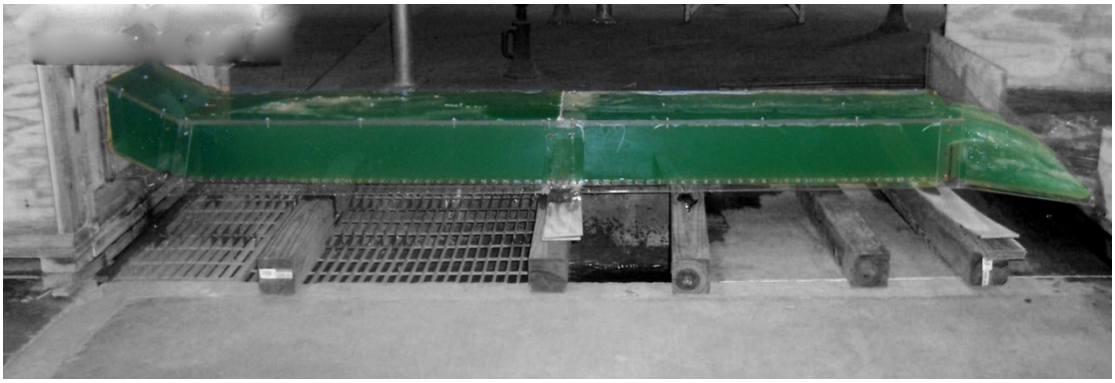

Figure A15. Experiment 6C

Table A6. Experiment 6 using Pressure Flow Condition with a 1.25 inch sill at the end of the culvert.

H.J.	Run	H	W_{temp}	Q	$V_{u/s}$	Y_s	Y_{toe}	Y_1	Y_2	$Y_{d/s}$	Fr1	V_1	V_2	$V_{d/s}$	L	X	ΔE	THL	E_2/E_1
N	6A	0.8d	-	0.9893	2.500	2.75	2.50	2.25	4.50	4.50	2.3777	5.84226 P-tube	-	5.73096 P-tube	-	-	0.28	-1.055386	0.846
N	6B	1.0d	-	1.3145	2.700	2.87	3.25	2.13	4.50	4.50	2.9263	6.9959 P-tube	-	6.1116 P-tube	-	-	0.35	-0.501551	0.755
N	6C	1.2d	-	1.7117	2.800	4.13	3.87	3.13	5.00	5.00	2.0906	6.0587 P-tube	-	6.41997 P-tube	-	-	0.10	-0.419133	0.894

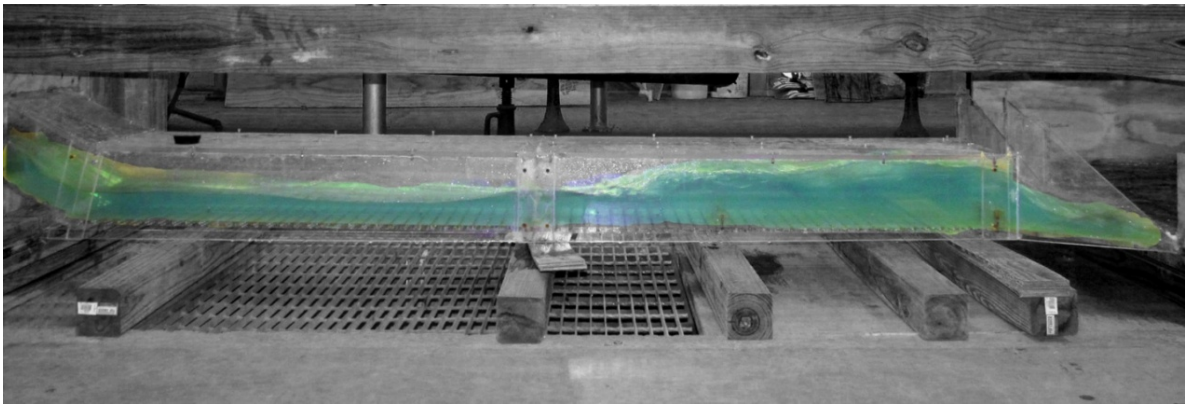

Figure A16. Experiment 9A

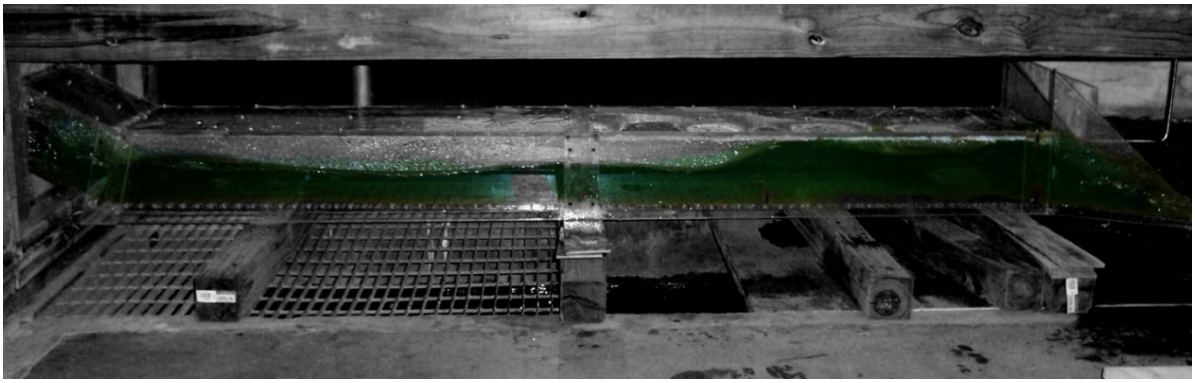

Figure A17. Experiment 9B

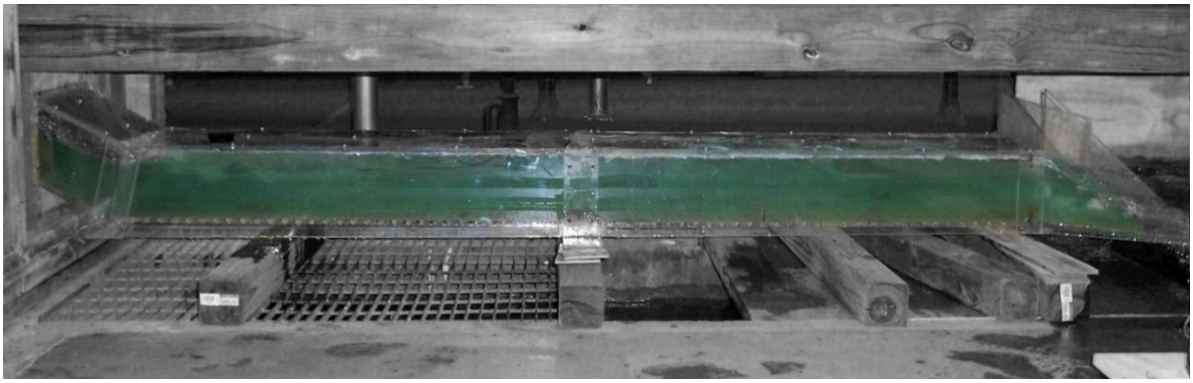

Figure A18. Experiment 9C

Table A9. Experiment 9 using Pressure Flow Condition with a 1 inch sill 25 inches from the end of the culvert and a 1.5 inch sill at the end of the culvert.

H.J.	Run	H	W_{temp}	Q	$V_{u/s}$	Y_s	Y_{toe}	Y_1	Y_2	$Y_{d/s}$	Fr1	V_1	V_2	$V_{d/s}$	L	X	ΔE	THL	E_2/E_1
Y	9A	0.8d	50.8	1.0053	2.513	2.50	2.50	2.50	5.00	5.50	2.2127	5.73097 P-tube	-	4.5396 P-tube	4.00	-	0.31	0.236980	0.874
Y	9B	1.0d	48.5	1.3084	2.617	2.75	3.00	3.00	5.50	6 (u.p.)	2.1354	6.0587 P-tube	-	4.60999 P-tube	3.50	-	0.24	0.915957	0.887
Y	9C	1.2d	48.4	1.7047	2.841	4.25	4.63	4.63	6 (u.p.)	6.00	1.4035	4.94692 P-tube	-	5.01158 P-tube	2.50	-	0.02*	1.624154	0.987

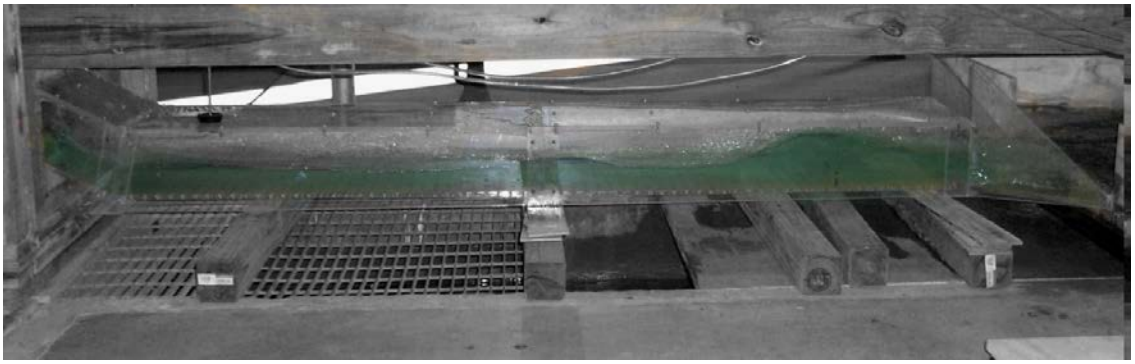

Figure A19. Experiment 10A

Figure A20. Experiment 10B

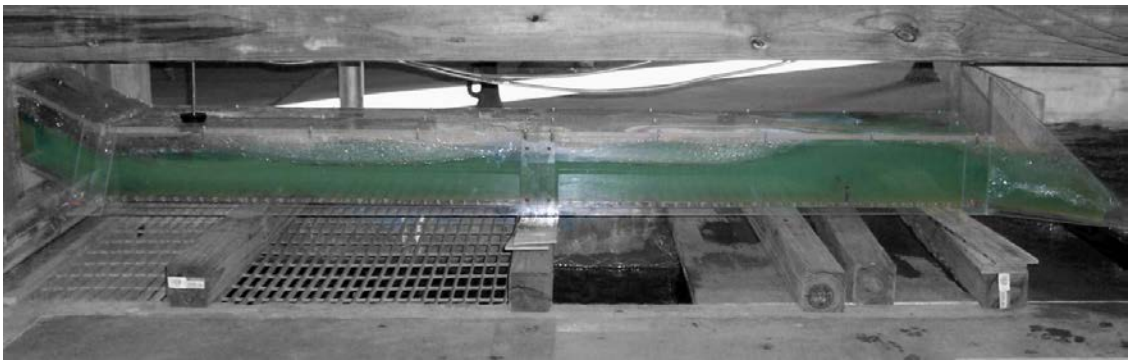

Figure A21. Experiment 10C

Table A10. Experiment 10 using Pressure Flow Condition with a 1.25 inch sill 13 inches from the end of the culvert.

H.J.	Run	H	W_{temp}	Q	$V_{u/s}$	Y_s	Y_{toe}	Y_1	Y_2	$Y_{d/s}$	Fr1	V_1	V_2	$V_{d/s}$	L	X	ΔE	THL	E_2/E_1
Y	10A	0.8d	49.0	0.9933	2.483	2.25	2.50	2.25	5.00	2.83	2.3094	5.6745 P-tube	-	4.74763 P-tube	4.50	-	0.46	2.519045	0.857
Y	10B	1.0d	48.9	1.3355	2.671	3.00	3.37	2.75	5.63	3.75	2.1507	5.84226 P-tube	-	5.26232 P-tube	2.50	-	0.39	2.019359	0.884
Y	10C	1.2d	49.1	1.6930	2.822	4.00	3.88	3.38	6 (u.p.)	4.00	1.9762	5.9515 P-tube	-	6.05871 P-tube	5.00	-	0.22	1.443572	0.913

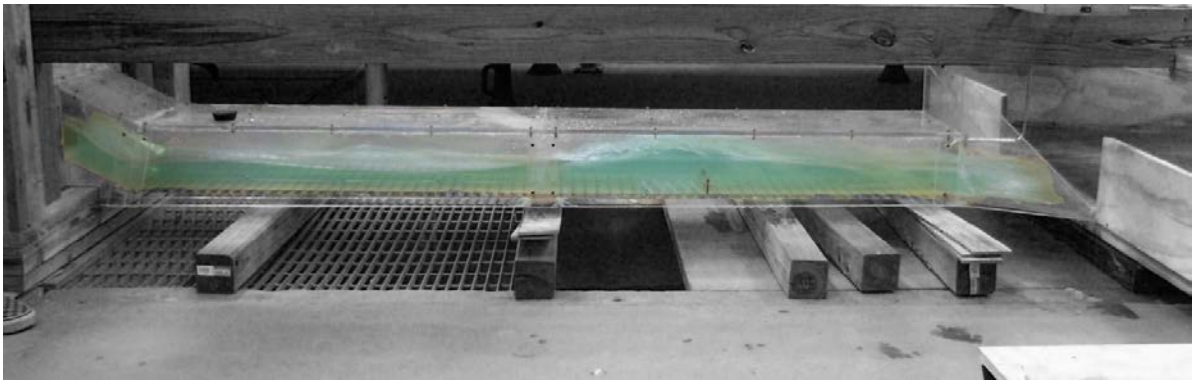

Figure A22. Experiment 11A

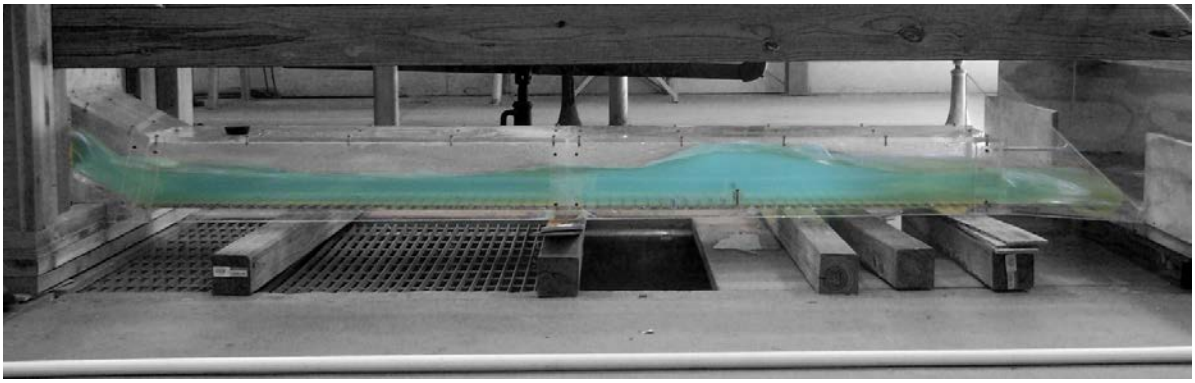

Figure A23. Experiment 11B

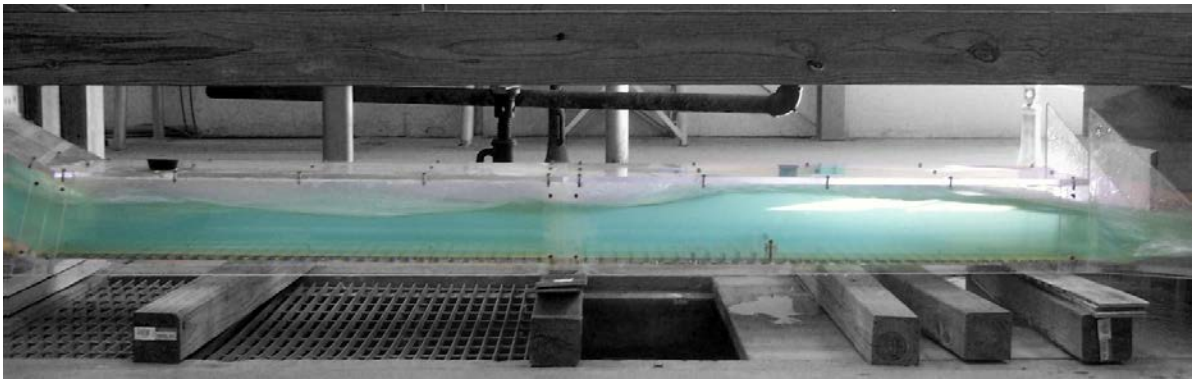

Figure A24. Experiment 11C

Table A11. Experiment 11 using Pressure Flow Condition with a 1.25 inch sill 25 inches from the end of the culvert and 15 flat-faced friction blocks in front of the sill.

H.J.	Run	H	W_{temp}	Q	$V_{u/s}$	Y_s	Y_{toe}	Y_1	Y_2	$Y_{d/s}$	Fr1	V_1	V_2	$V_{d/s}$	L	X	ΔE	THL	E_2/E_1
Y	11A	0.8d	49.3	0.9893	2.500	2.75	2.38	3.00	5.00	2.50	2.0199	5.73100 P-tube	-	4.67932 P-tube	5.75	-	0.13	2.984590	0.906
Y (?)	11B	1.0d	49.7	1.3205	2.700	2.75	3.50	3.50	5.00	3.00	1.9243	5.89710 P-tube	-	5.73097 P-tube	4.50	-	0.05	-1.161615	0.921
Y (?)	11C	1.2d	49.8	1.7302	2.800	4.25	4.00	4.25	5.38	4.00	1.7624	5.95150 P-tube	-	6.11163 P-tube	4.00	-	0.02	1.300866	0.946

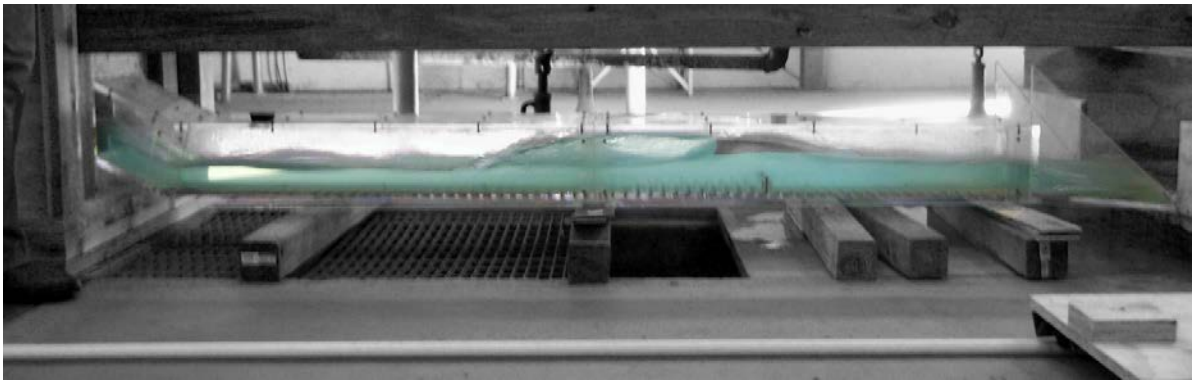

Figure A25. Experiment 12A

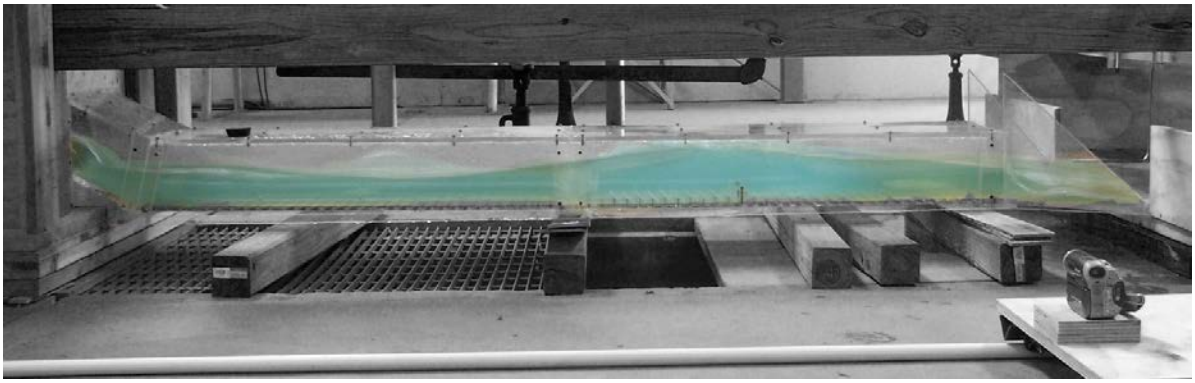

Figure A26. Experiment 12B

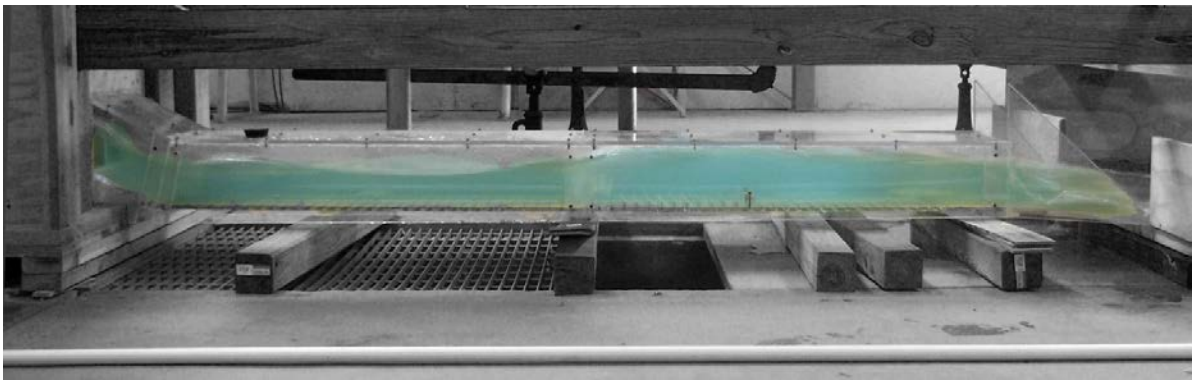

Figure A27. Experiment 12C

Table A12. Experiment 12 using Pressure Flow Condition with a 1.25 inch sill at 25 inches from the end of the culvert with 30 flat-faced friction blocks in front of the sill.

H.J.	Run	H	W_{temp}	Q	$V_{u/s}$	Y_s	Y_{toe}	Y_1	Y_2	$Y_{d/s}$	Fr1	V_1	V_2	$V_{d/s}$	L	X	ΔE	THL	E_2/E_1
Y	12A	0.8d	50.3	0.9812	2.500	2.50	2.38	2.00	5.50	2.50	2.4739	5.73096 P-tube	-	4.609989 P-tube	8.00	-	0.97	3.104597	0.829
Y	12B	1.0d	50.4	1.3621	2.700	3.50	3.75	4.13	5.50	3.25	1.8040	6.00533 P-tube	-	5.3232 P-tube	3.50	-	0.03	2.428300	0.940
Y	12C	1.2d	50.3	1.6883	2.800	3.88	4.00	3.88	6 (u.p.)	3.75	1.8777	6.05871 P-tube	-	6.05871 P-tube	7.00	-	0.10	1.670876	0.929

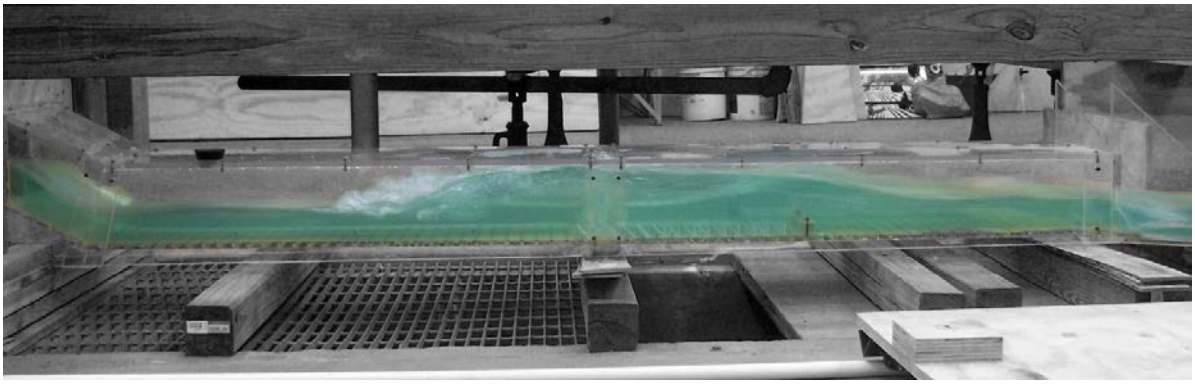

Figure A28. Experiment 13A

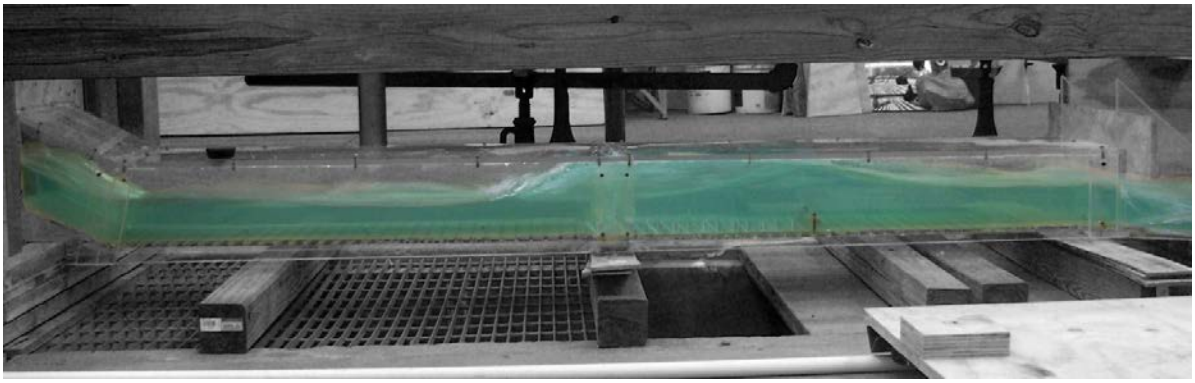

Figure A29. Experiment 13B

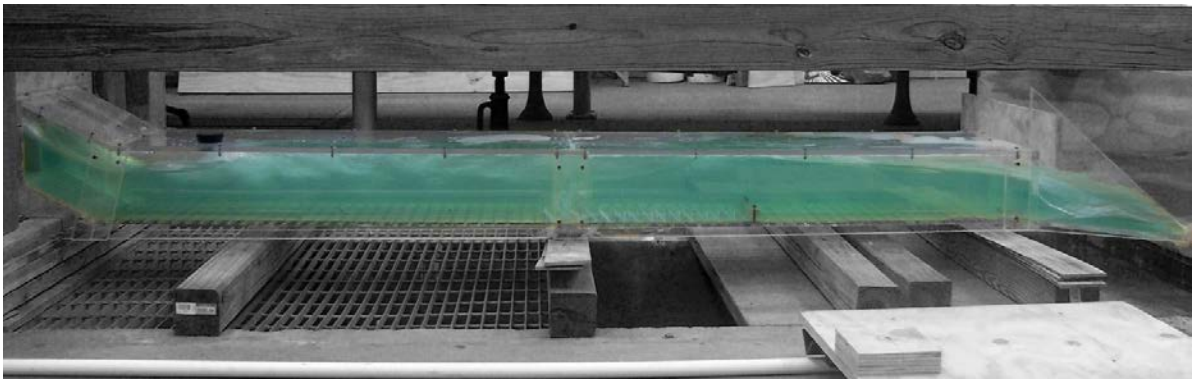

Figure A30. Experiment 13C

Table A13. Experiment 13 using Pressure Flow Condition with a 1.25 inch sill at 25 inches from the end of the culvert with 45 flat-faced friction blocks in front of the sill.

H.J.	Run	H	W_{temp}	Q	$V_{u/s}$	Y_s	Y_{toe}	Y_1	Y_2	$Y_{d/s}$	Fr1	V_1	V_2	$V_{d/s}$	L	X	ΔE	THL	E_2/E_1
Y	13A	0.8d	50.5	0.9933	2.500	2.63	2.50	2.38	6.00	2.63	2.2454	5.67450 P-tube	-	4.74763 P-tube	10.00	-	0.83	2.734598	0.868
Y	13B	1.0d	50.5	1.3145	2.700	2.88	2.38	3.13	6 (u.p.)	3.38	2.0348	5.89710 P-tube	-	5.32316 P-tube	8.00	-	0.31	-0.321621	0.904
Y	13C	1.2d	50.6	1.7187	2.800	4.25	4.13	4.13	6 (u.p.)	4.25	1.7878	5.95150 P-tube	-	5.89710 P-tube	7.00	-	0.07	1.530909	0.942

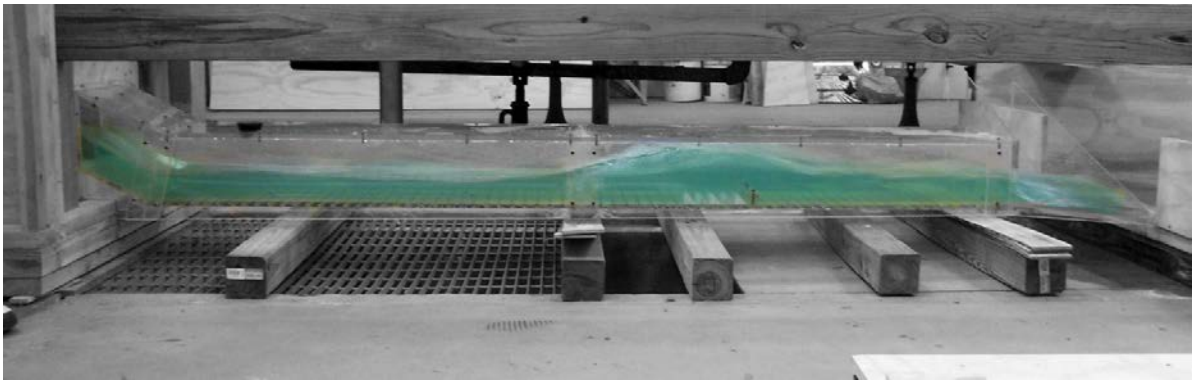

Figure A31. Experiment 14A

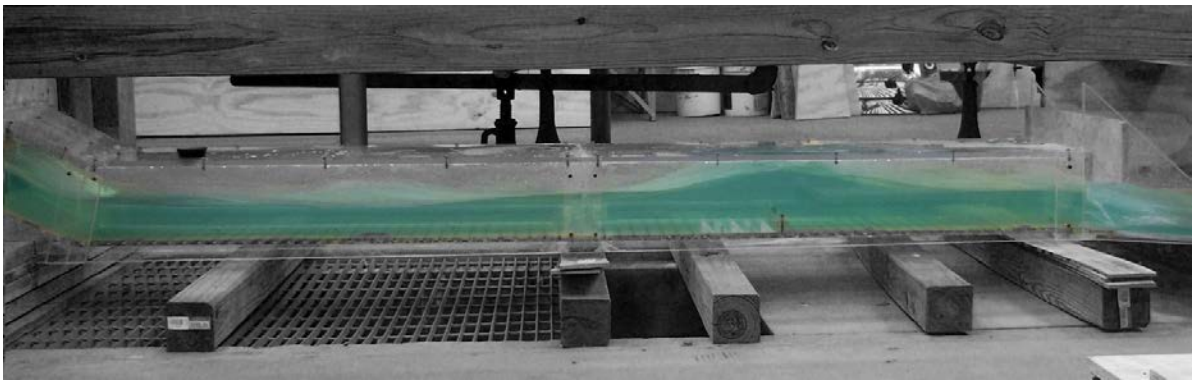

Figure A32. Experiment 14B

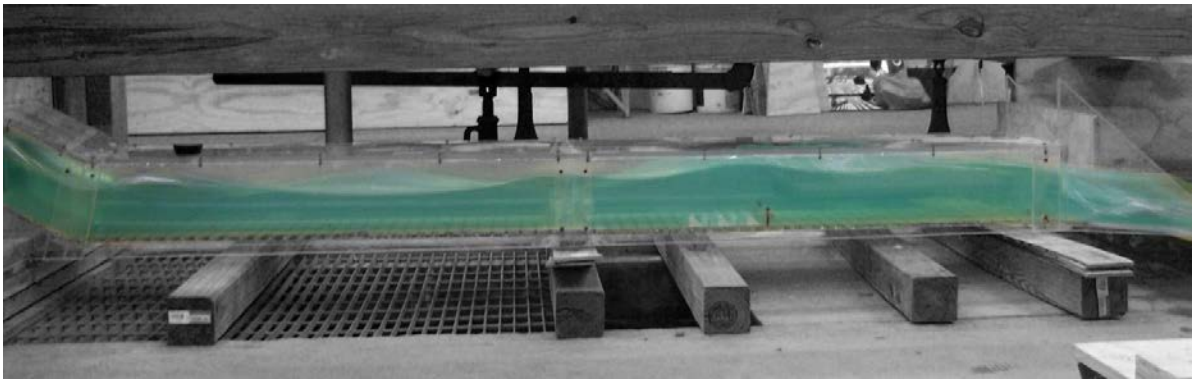

Figure A33. Experiment 14C

Table A14. Experiment 14 using Pressure Flow Condition with a 1.25 inch sill at 25 inches from the end of the culvert with 15 curved-face friction blocks in front of the sill.

H.J.	Run	H	W_{temp}	Q	$V_{u/s}$	Y_s	Y_{toe}	Y_1	Y_2	$Y_{d/s}$	Fr1	V_1	V_2	$V_{d/s}$	L	X	ΔE	THL	E_2/E_1
Y	14A	0.8d	48.2	0.9933	2.500	2.50	2.38	2.88	5.25	3.75	2.0616	5.730968 P-tube	- -	4.81498 P-tube	7.00	-	0.22	1.494590	0.899
Y (?)	14B	1.0d	48.3	1.3084	2.700	3.00	3.38	3.50	5.00	3.00	1.9243	5.897118 P-tube	- -	5.559856 P-tube	4.00	-	0.05	2.198385	0.921
Y (?)	14C	1.2d	48.1	1.7047	2.800	4.20	4.00	4.25	5.50	3.50	1.7783	6.00533 P-tube	- -	6.05871 P-tube	5.00	-	0.02	1.920876	0.943

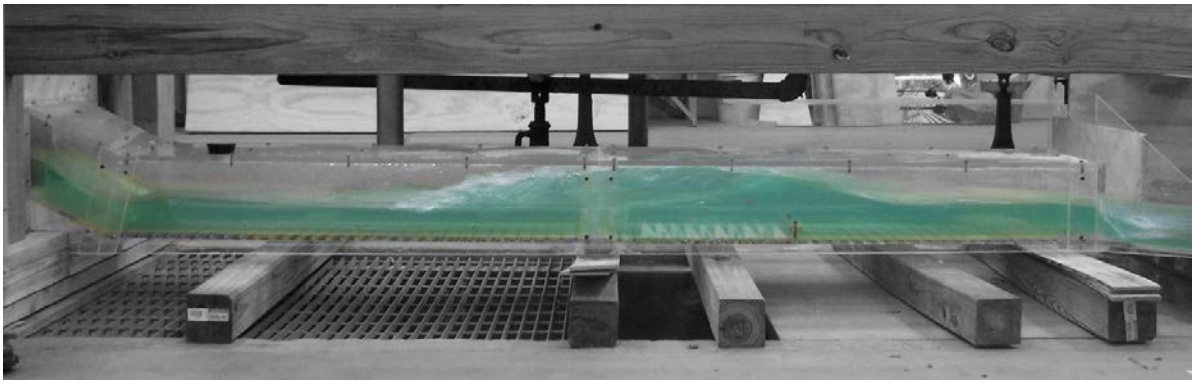

Figure A34. Experiment 15A

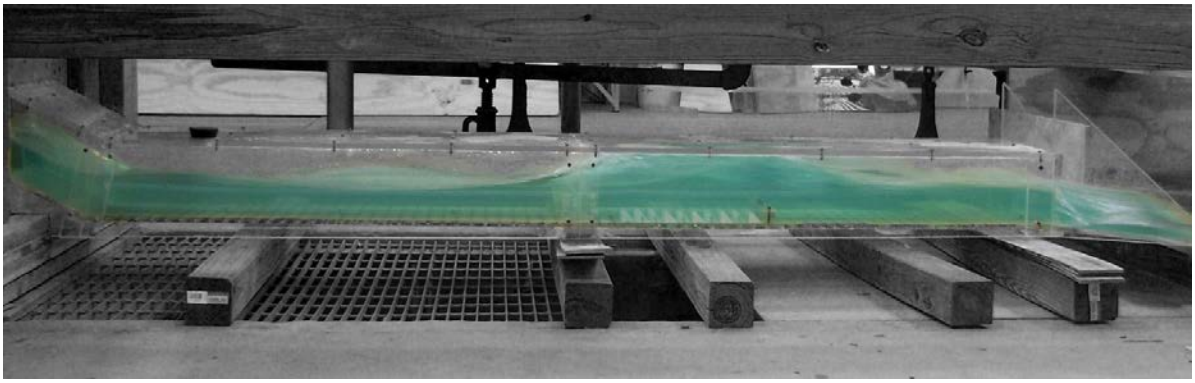

Figure A35. Experiment 15B

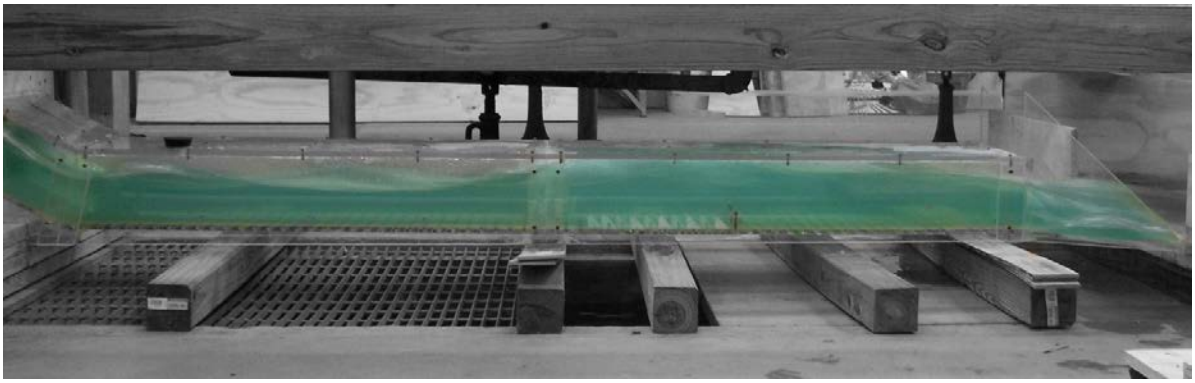

Figure A36. Experiment 15C

Table A15. Experiment 15 using Pressure Flow Condition with a 1.25 inch sill at 25 inches from the end of the culvert with 30 curved-face friction blocks in front of the sill.

H.J.	Run	H	W_{temp}	Q	$V_{u/s}$	Y_s	Y_{toe}	Y_1	Y_2	$Y_{d/s}$	Fr1	V_1	V_2	$V_{d/s}$	L	X	ΔE	THL	E_2/E_1
Y	15A	0.8d	48.2	1.0132	2.500	2.50	2.63	2.38	6 (u.p.)	2.88	2.2678	5.73097 P-tube	-	4.88139 P-tube	12.00	-	0.83	2.244597	0.864
Y	15B	1.0d	47.0	1.3084	2.700	3.00	3.38	3.50	6 (u.p.)	3.25	1.8701	5.73097 P-tube	-	5.50164 P-tube	7.50	-	0.19	-0.681615	0.930
Y	15C	1.2d	47.1	1.7325	2.800	4.38	4.00	4.50	6 (u.p.)	4.25	1.7282	6.00530 P-tube	-	5.95147 P-tube	5.00	-	0.03	1.410870	0.951

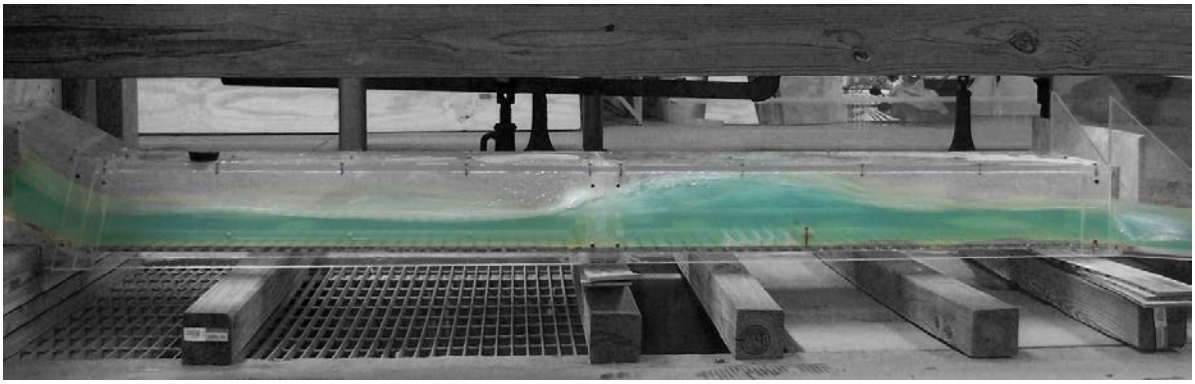

Figure A37. Experiment 16A

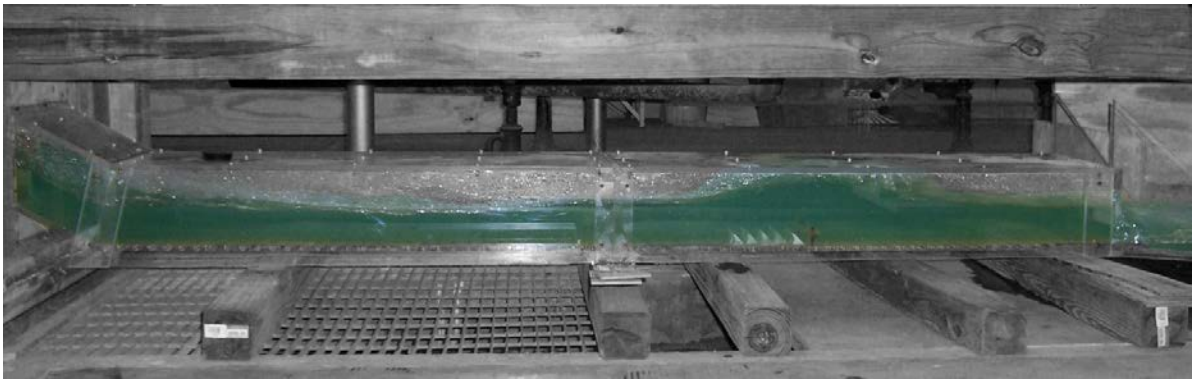

Figure A38. Experiment 16B

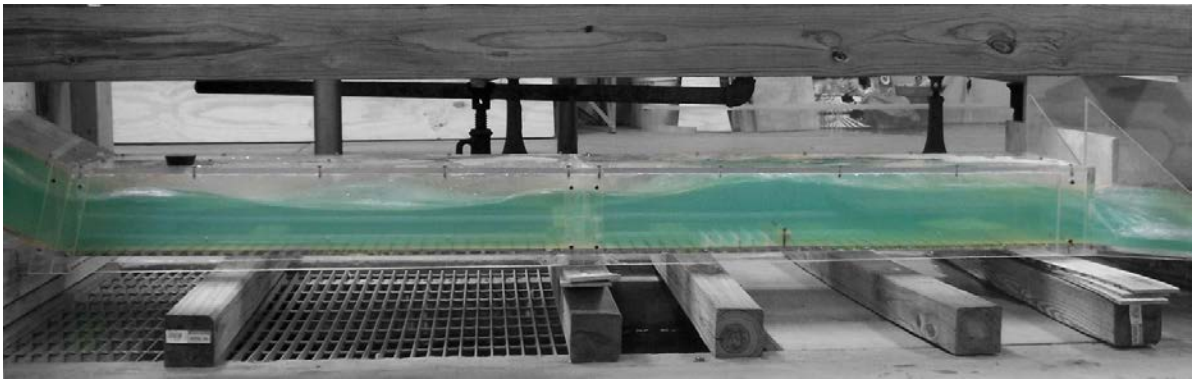

Figure A39. Experiment 16C

Table A16. Experiment 16 using Pressure Flow Condition with a 1.25 inch sill at 25 inches from the end of the culvert with 15 C-shaped friction blocks in front of the sill.

H.J.	Run	H	W_{temp}	Q	$V_{u/s}$	Y_s	Y_{toe}	Y_1	Y_2	$Y_{d/s}$	Fr1	V_1	V_2	$V_{d/s}$	L	X	ΔE	THL	E_2/E_1
Y	16A	0.8d	47.0	1.0013	2.500	2.63	2.38	3.13	4.88	2.63	1.9775	5.730969 P-tube	-	4.747631 P-tube	7.00	-	0.09	2.734596	0.913
Y (?)	16B	1.0d	46.9	1.3355	2.700	3.00	3.38	3.50	5.00	3.00	1.9243	5.897118 P-tube	-	5.674504 P-tube	4.00	-	0.05	1.958385	0.921
Y (?)	16C	1.2d	47.0	1.7256	2.800	4.20	4.00	4.25	5.50	3.50	1.7941	6.058713 P-tube	-	6.058713 P-tube	5.00	-	0.02	1.920870	0.941

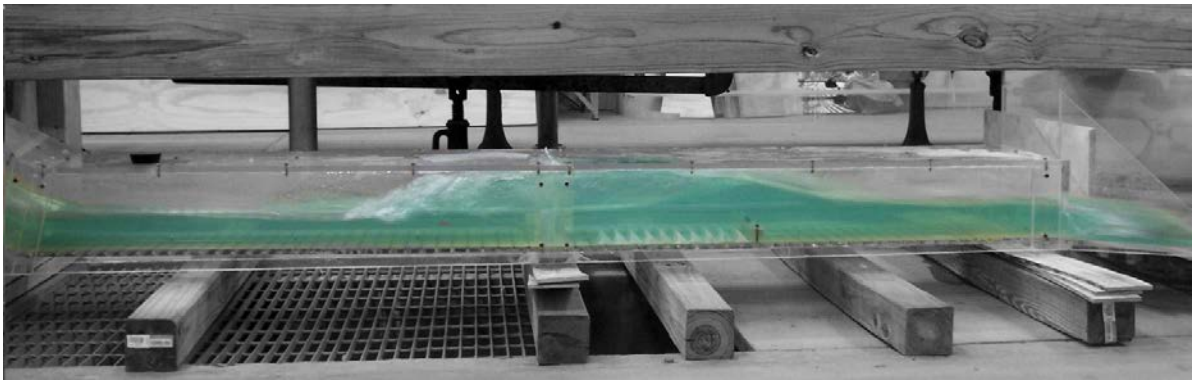

Figure A40. Experiment 17A

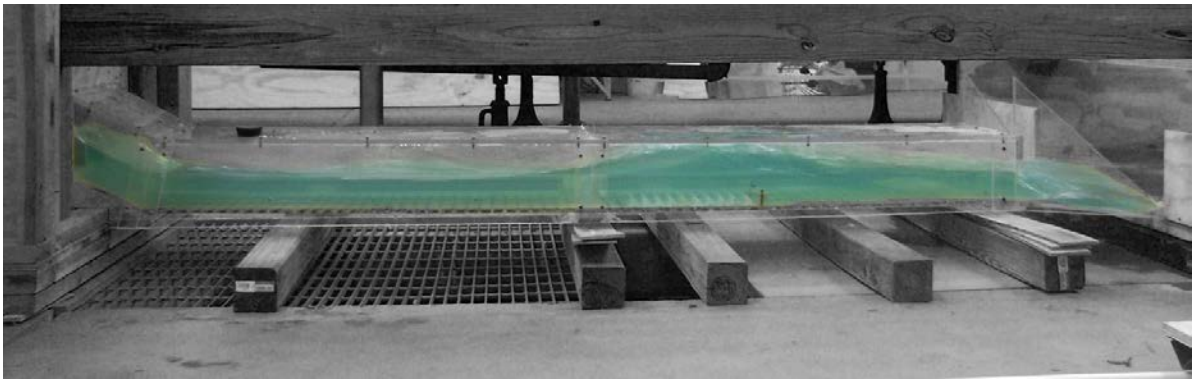

Figure A41. Experiment 17B

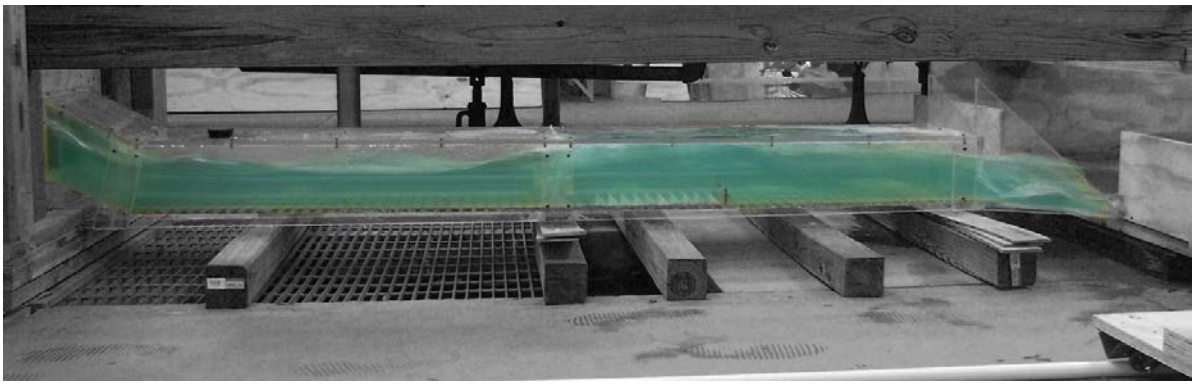

Figure A42. Experiment 17C

Table A17. Experiment 17 using Pressure Flow Condition with a 1.25 inch sill at 25 inches from the end of the culvert with 30 C-shaped friction blocks in front of the sill.

H.J.	Run	H	W_{temp}	Q	$V_{u/s}$	Y_s	Y_{toe}	Y_1	Y_2	$Y_{d/s}$	Fr1	V_1	V_2	$V_{d/s}$	L	X	ΔE	THL	E_2/E_1
Y	17A	0.8d	47.8	1.0092	2.500	2.25	2.63	2.38	6.00	2.75	2.3118	5.84226 P-tube	-	4.88139 P-tube	12.50	-	0.83	2.374596	0.876
Y (?)	17B	1.0d	47.8	1.3325	2.700	3.00	3.38	4.13	6 (u.p.)	2.83	1.7714	5.89712 P-tube	-	5.50164 P-tube	3.50	-	0.07	-0.681615	0.916
Y	17C	1.2d	48.0	1.7348	2.800	4.38	4.00	3.88	6 (u.p.)	4.38	1.8941	6.11163 P-tube	-	6.05871 P-tube	6.50	-	0.10	1.040870	0.930

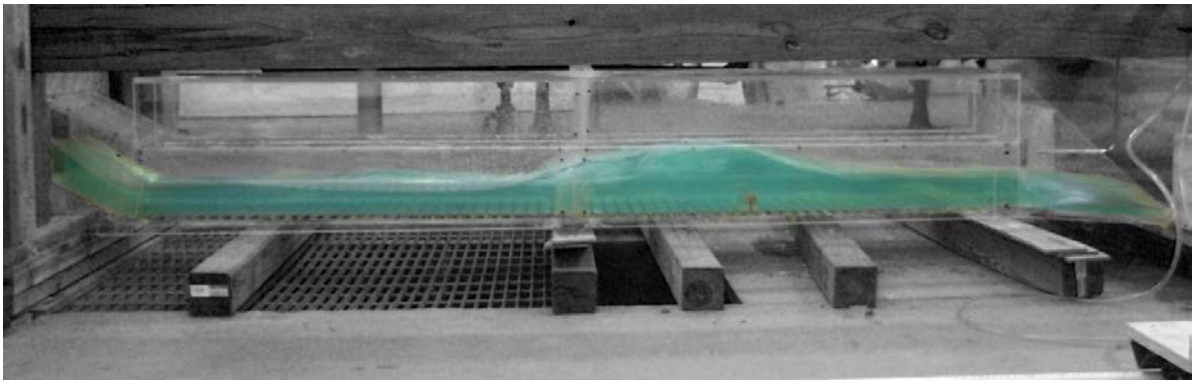

Figure A43. Experiment 18A

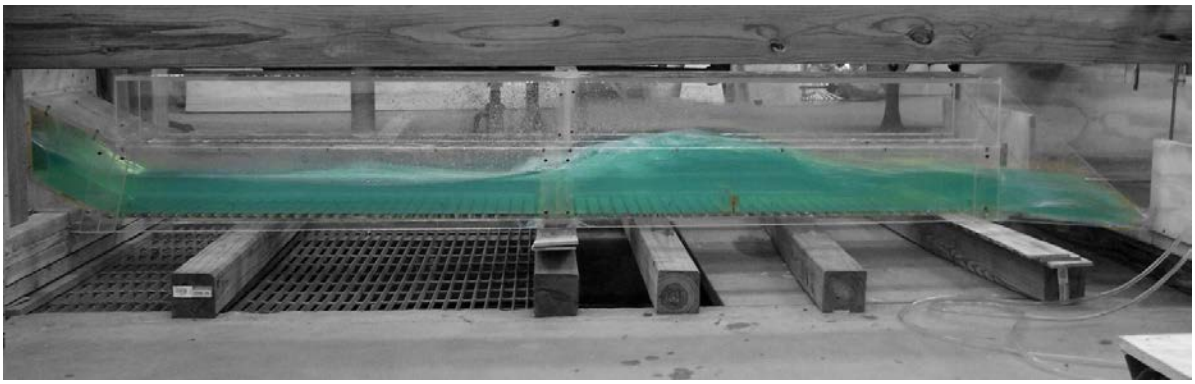

Figure A44. Experiment 18B

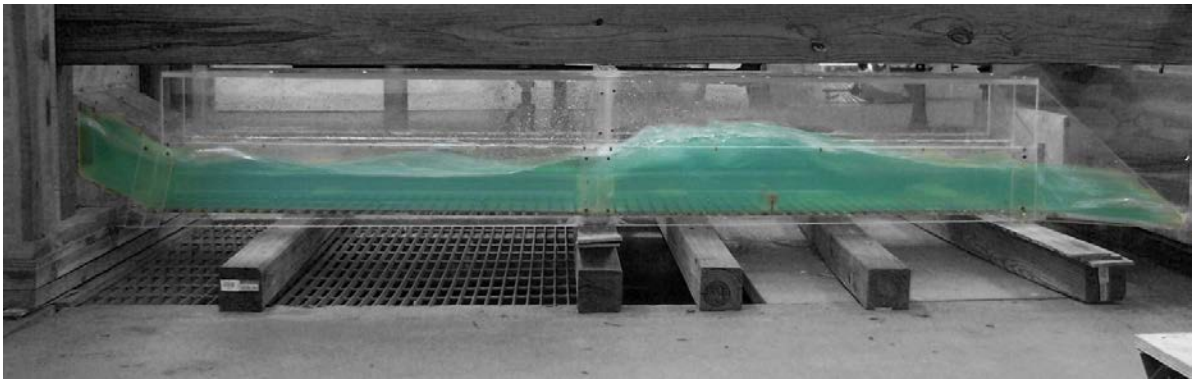

Figure A45. Experiment 18C

Table A18. Experiment 18 using Open Channel Condition with a 1.5 inch sill at 25 inches from the end of the culvert.

H.J.	Run	H	W_{temp}	Q	$V_{u/s}$	Y_s	Y_{toe}	Y_1	Y_2	$Y_{d/s}$	Fr1	V_1	V_2	$V_{d/s}$	L	X	ΔE	THL	E_2/E_1
Y	18A	0.8d	49.6	1.0053	2.500	2.50	2.63	2.38	5.63	2.75	1.9952	5.786882 P-tube	3.49799 P-tube	4.946918 P-tube	9.00	24.75	0.64	2.254597	0.910
Y	18B	1.0d	50.2	1.3145	2.700	2.88	3.38	3.38	6.38	3.25	1.6508	6.00533 P-tube	4.09194 P-tube	5.323157 P-tube	8.00	19.75	0.31	2.428385	0.961
Y	18C	1.2d	50.6	1.7163	2.800	4.38	3.88	5.00	7.25	3.75	1.3328	6.41997 P-tube	3.6775 P-tube	5.730968 P-tube	8.50	17.50	0.08	2.390871	0.992

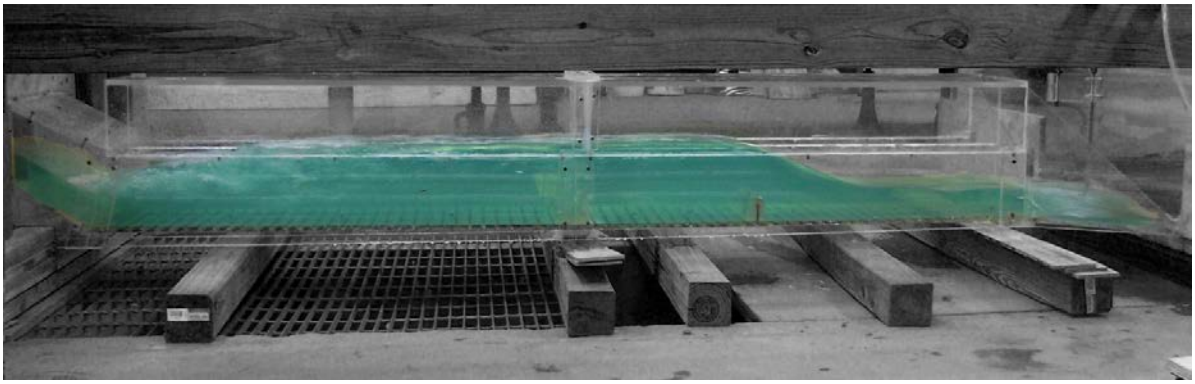

Figure A46. Experiment 19A

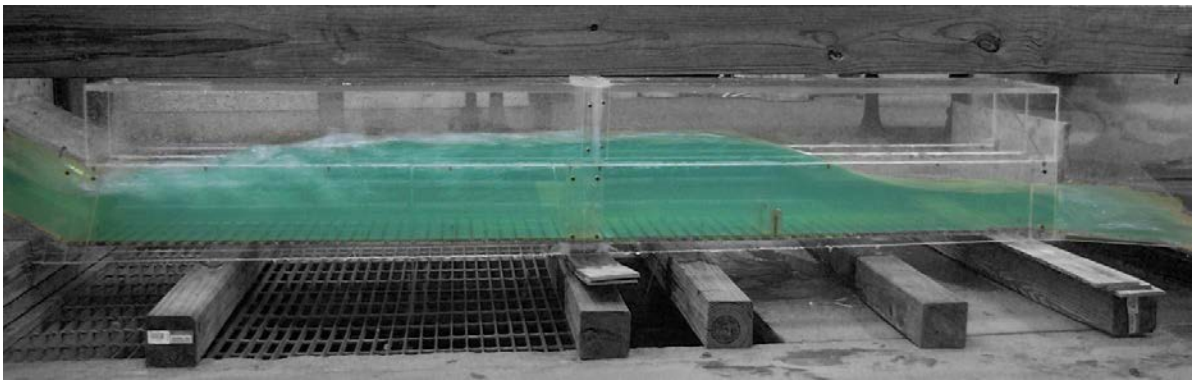

Figure A47. Experiment 19B

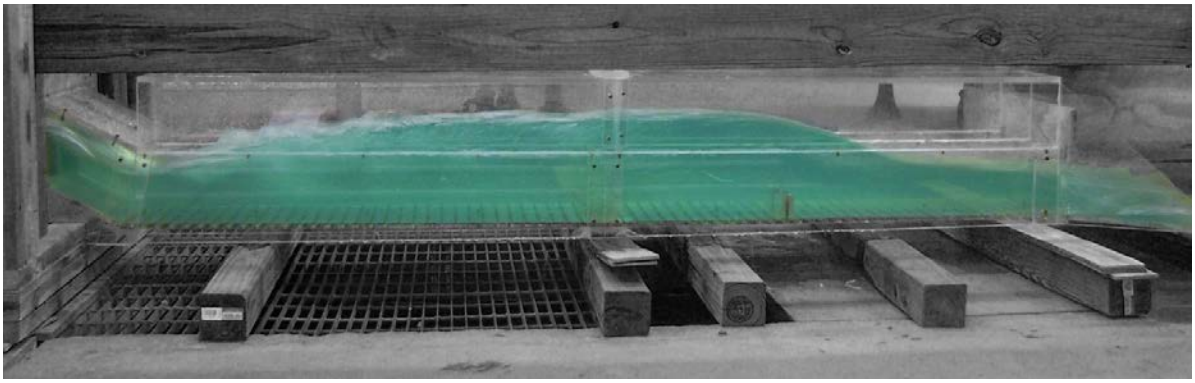

Figure A48. Experiment 19C

Table A19. Experiment 19 using Open Channel Condition with a 2 inch sill at 25 inches from the end of the culvert.

H.J.	Run	H	W_{temp}	Q	$V_{u/s}$	Y_s	Y_{toe}	Y_1	Y_2	$Y_{d/s}$	Fr1	V_1	V_2	$V_{d/s}$	L	X	ΔE	THL	E_2/E_1
Y (toe)	19A	0.8d	52.2	0.9933	2.500	2.25	N/A	2.00 (toe)	5.88	2.50	2.4066	4.78142 P-tube	1.9657 P-tube	5.13848 P-tube	6.50	-	1.24	2.144601	0.841
Y	19B	1.0d	52.5	1.3385	2.700	3.00	3.63	3.63	7.50	3.00	1.7797	5.38331 P-tube	2.53772 P-tube	5.55986 P-tube	10.00	54.00	0.53	-0.801615	0.943
Y	19C	1.2d	52.8	1.7094	2.800	4.25	4.13	4.13	8.75	3.75	1.8176	5.38331 P-tube	2.8934 P-tube	6.11163 P-tube	12.00	55.00	0.68	1.550870	0.938

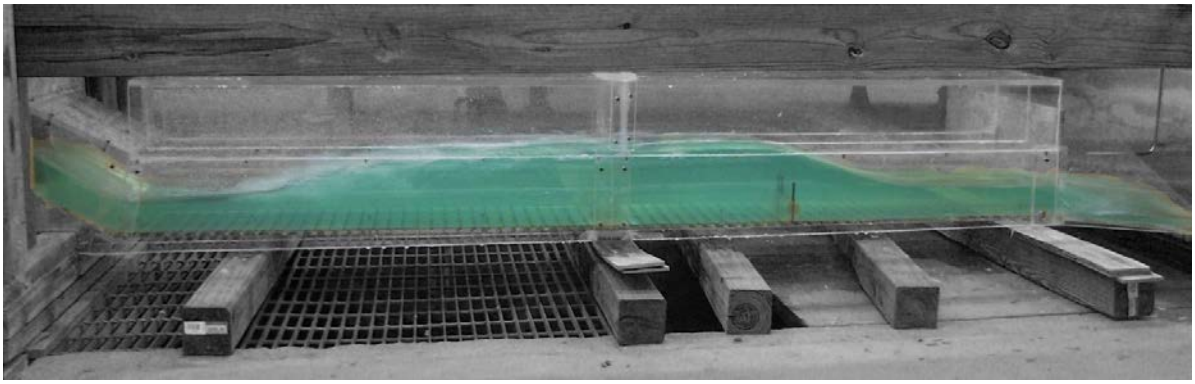

Figure A49. Experiment 20A

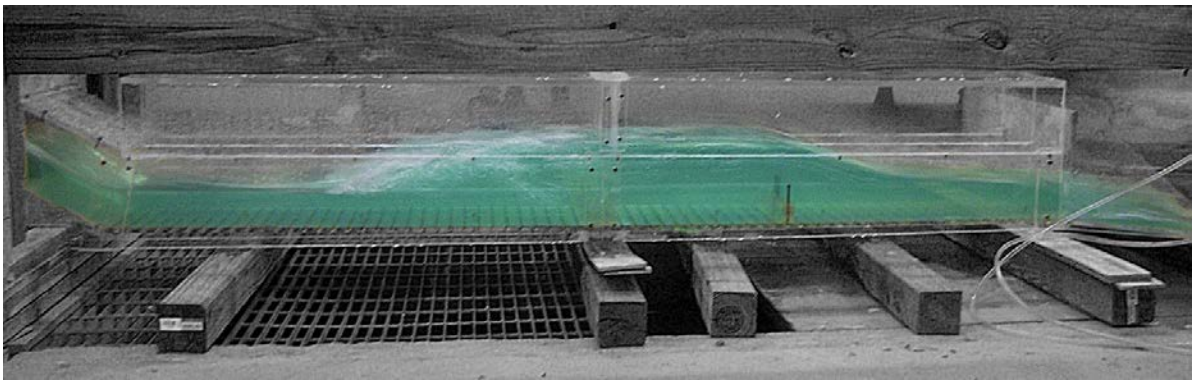

Figure A50. Experiment 20B

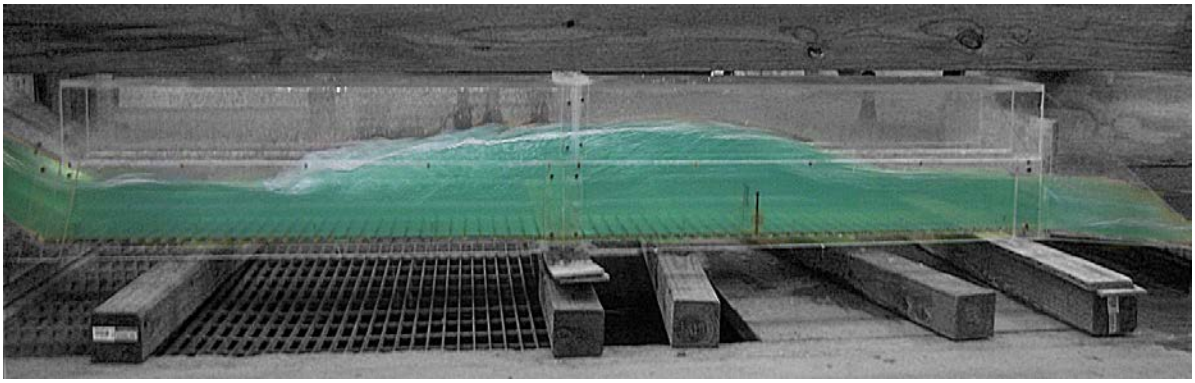

Figure A51. Experiment 20C

Table A20. Experiment 20 using Open Channel Condition with a 1.75 inch sill at 25 inches from the end of the culvert.

H.J.	Run	H	W_{temp}	Q	$V_{u/s}$	Y_s	Y_{toe}	Y_1	Y_2	$Y_{d/s}$	Fr1	V_1	V_2	$V_{d/s}$	L	X	ΔE	THL	E_2/E_1
Y	20A	0.8d	53.2	1.0013	2.500	2.75	2.50	3.00	6.38	2.75	1.8234	5.786882 P-tube	2.53772 P-tube	4.88139 P-tube	10.00	44.75	0.50	2.374602	0.937
Y	20B	1.0d	53.3	1.2931	2.700	3.00	3.25	3.00	7.25	3.25	2.0319	5.95147 P-tube	2.89344 P-tube	5.38331 P-tube	11.00	43.50	0.88	2.308380	0.904
Y	20C	1.2d	52.8	1.7302	2.800	4.50	3.88	3.75	8.38	3.88	1.9011	5.897118 P-tube	2.77995 P-tube	5.924356 P-tube	15.00	46.25	0.79	1.840871	0.925

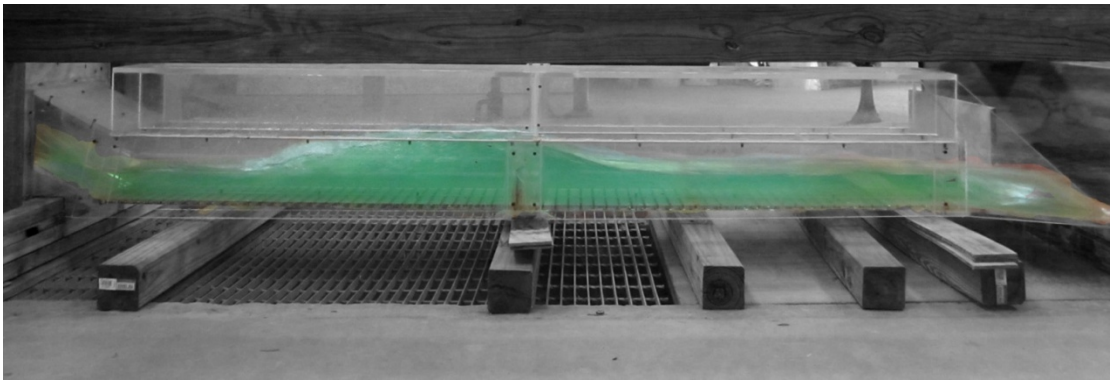

Figure A52. Experiment 21A

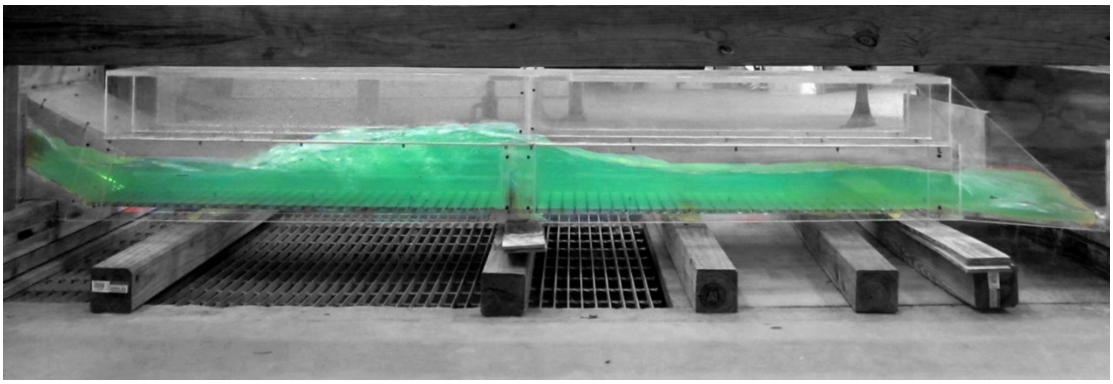

Figure A53. Experiment 21B

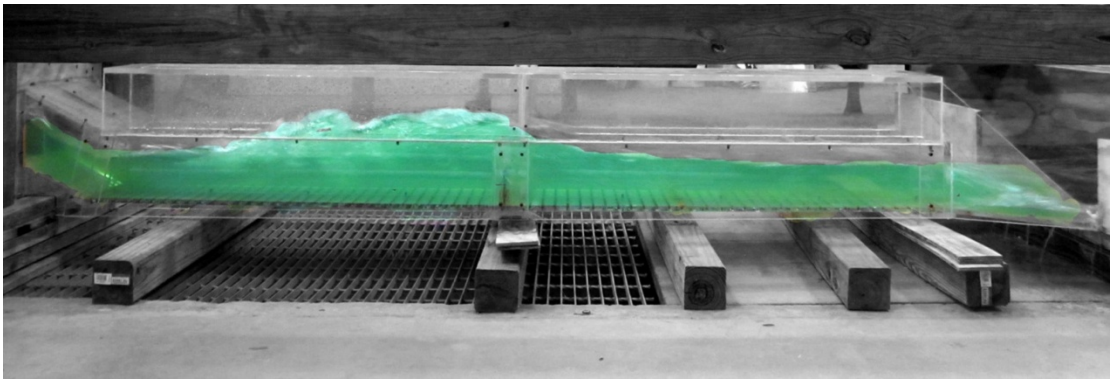

Figure A54. Experiment 21C

Table A21. Experiment 21 using Open Channel Condition with a 1.5 inch sill at the middle of the culvert.

H.J.	Run	H	W_{temp}	Q	$V_{u/s}$	Y_s	Y_{toe}	Y_1	Y_2	$Y_{d/s}$	Fr1	V_1	V_2	$V_{d/s}$	L	X	ΔE	THL	E_2/E_1
Y	21A	0.8d	53.9	1.0092	2.500	2.63	2.38	2.38	5.75	2.75	2.0314	5.55985 P-tube	3.20998 P-tube	4.81498 P-tube	10.00	-	0.70	2.494596	0.904
Y	21B	1.0d	54.8	1.3504	2.700	3.65	3.65	3.00	6.88	3.50	1.9433	6.31886 P-tube	3.20998 P-tube	5.38330 P-tube	11.00	-	0.71	-0.441600	0.918
Y	21C	1.2d	55.4	1.7394	2.800	4.50	4.00	3.75	7.88	4.00	1.8051	6.2677 P-tube	4.0125 P-tube	5.89710 P-tube	11.50	-	0.60	1.780909	0.940

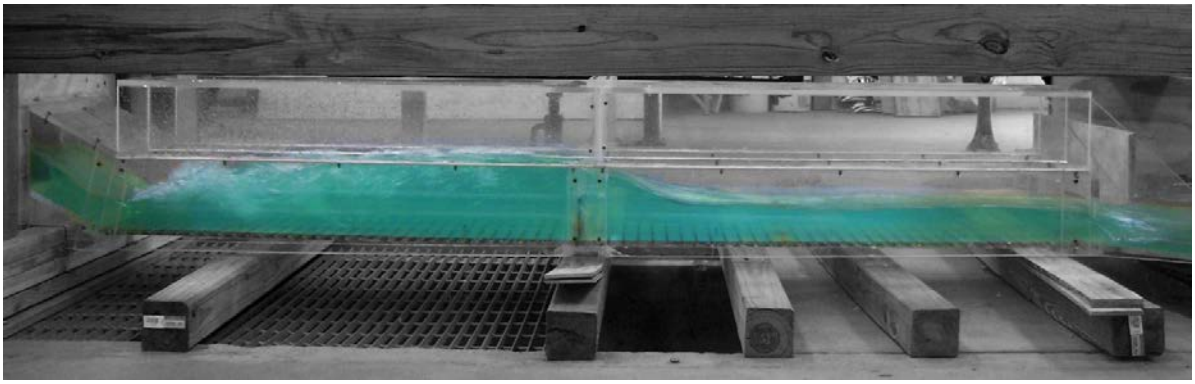

Figure A55. Experiment 22A

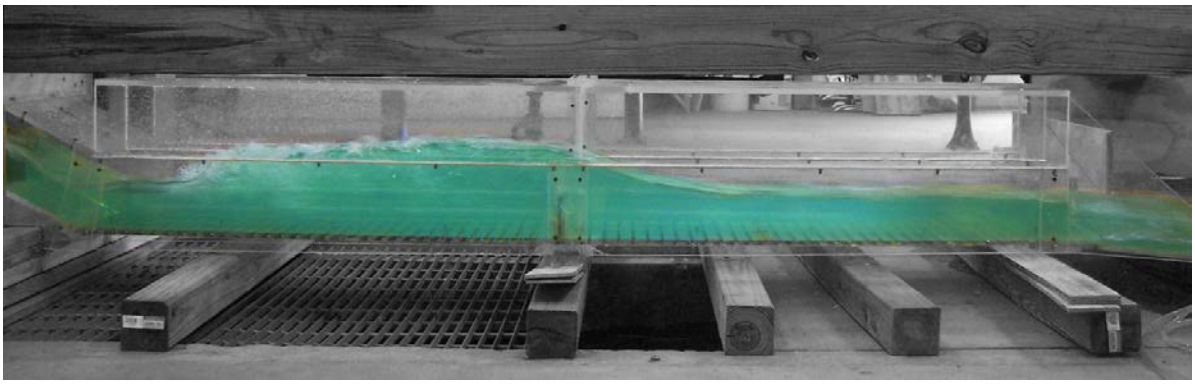

Figure A56. Experiment 22B

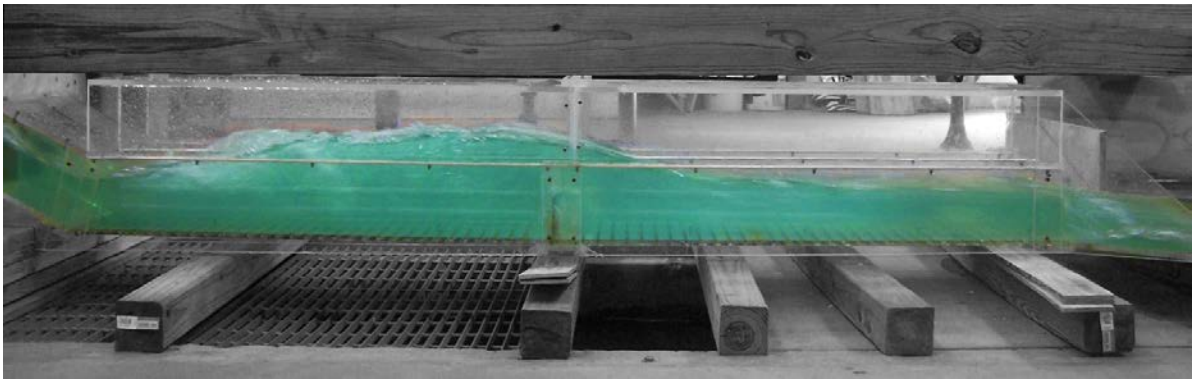

Figure A57. Experiment 22C

Table A22. Experiment 22 using Open Channel Condition with a 1.75 inch sill at the middle of the culvert.

H.J.	Run	H	W_{temp}	Q	$V_{u/s}$	Y_s	Y_{toe}	Y_1	Y_2	$Y_{d/s}$	Fr1	V_1	V_2	$V_{d/s}$	L	X	ΔE	THL	E_2/E_1
Y	22A	0.8d	56.3	0.9893	2.500	2.63	2.50	2.50	6.38	2.75	2.1289	4.94692 P-tube	2.40749 P-tube	4.88139 P-tube	8.50	38.50	0.92	2.374602	0.888
Y	22B	1.0d	56.8	1.3385	2.700	3.00	3.38	3.50	7.50	3.63	1.8350	5.4428 P-tube	3.10805 P-tube	5.50164 P-tube	12.00	-	0.61	1.688377	0.935
Y	22C	1.2d	57.4	1.6954	2.800	4.36	4.00	4.00	8.36	4.00	1.7970	5.5599 P-tube	3.0027 P-tube	5.95147 P-tube	14.00	-	0.62	1.660870	0.941

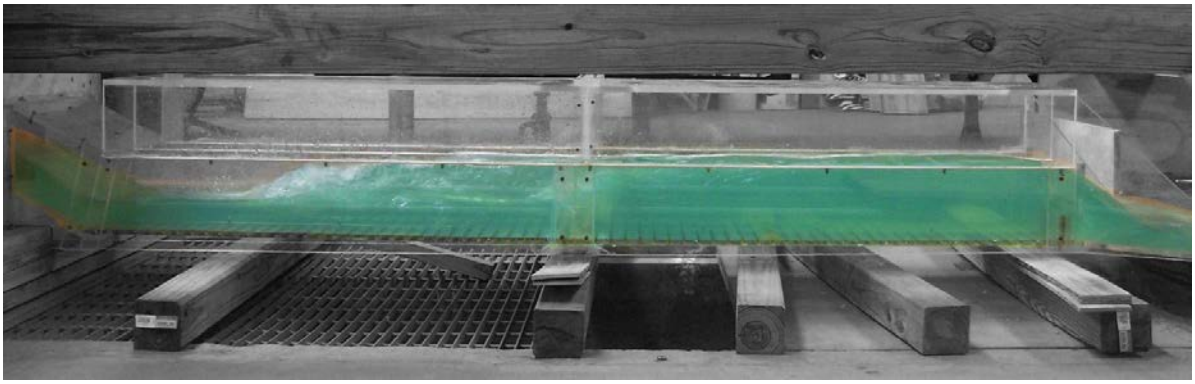

Figure A58. Experiment 23A

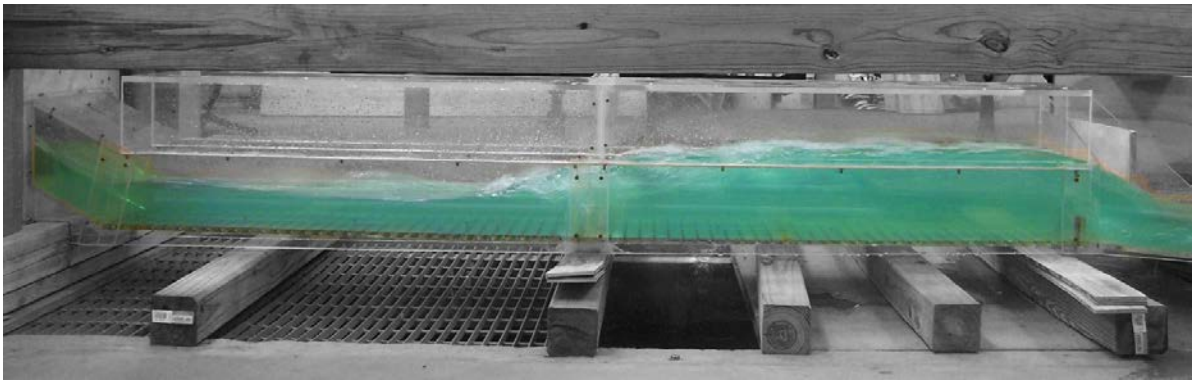

Figure A59. Experiment 23B

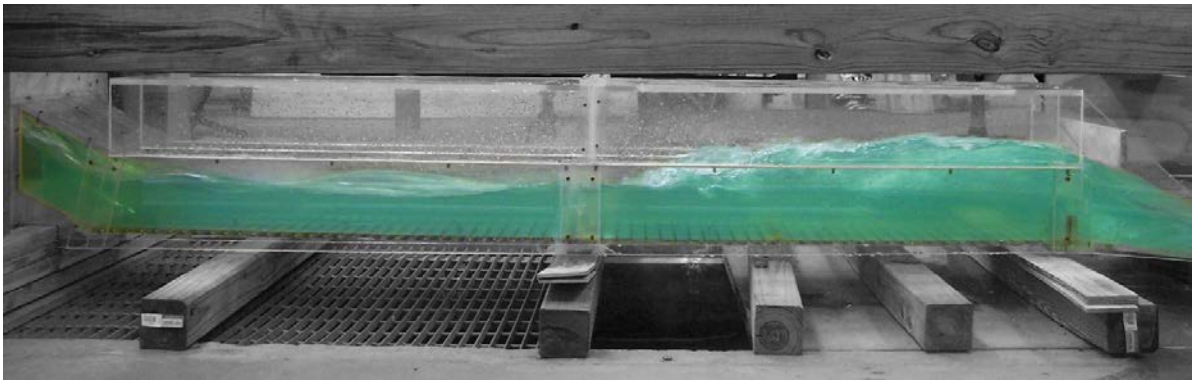

Figure A60. Experiment 23C

Table A23. Experiment 23 using Open Channel Condition with a 2 inch sill at the end of the culvert.

H.J.	Run	H	W_{temp}	Q	$V_{u/s}$	Y_s	Y_{toe}	Y_1	Y_2	$Y_{d/s}$	Fr1	V_1	V_2	$V_{d/s}$	L	X	ΔE	THL	E_2/E_1
Y	23A	0.8d	57.4	0.9973	2.500	2.63	2.38	2.88	6.13	6.50	1.8247	5.7869 P-tube	2.6004 P-tube	4.81498 P-tube	13.00	-	0.49	-1.25541	0.937
Y	23B	1.0d	57.5	1.3205	2.700	3.00	3.38	2.88	7.13	6.75	2.0742	6.13791 P-tube	3.498 P-tube	5.32316 P-tube	12.00	-	0.93	-0.321621	0.897
Y	23C	1.2d	57.8	1.7279	2.800	4.36	3.88	4.25	7.88	7.25	1.6266	6.3696 P-tube	3.2099 P-tube	5.53082 P-tube	10.50	-	0.36	-0.689130	0.964

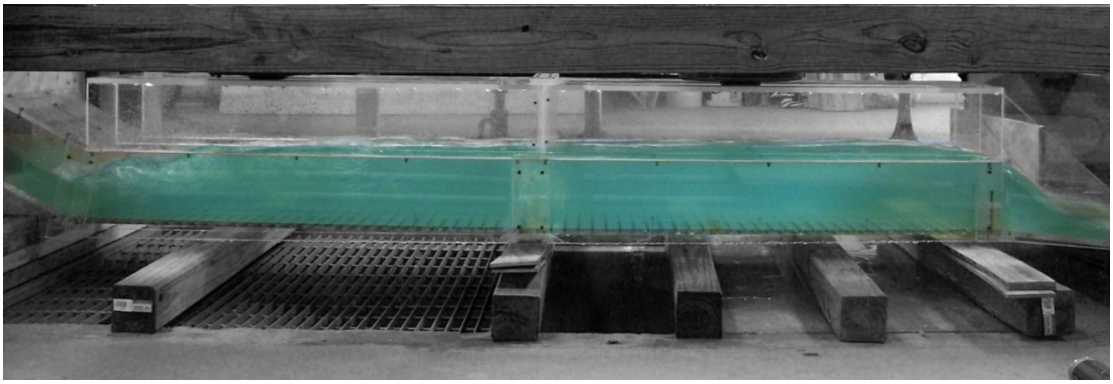

Figure A61. Experiment 24A

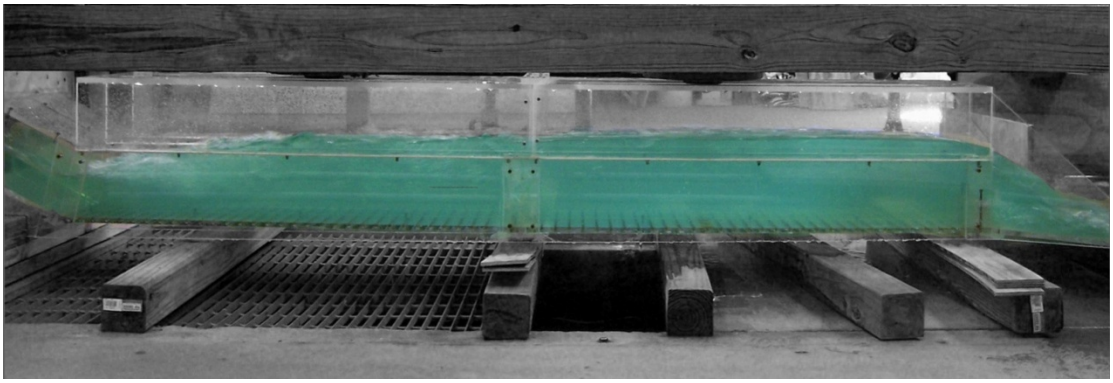

Figure A62. Experiment 24B

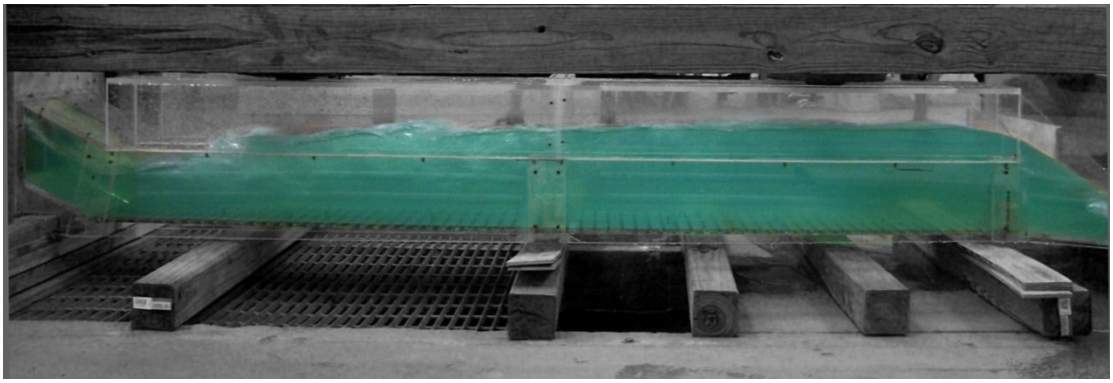

Figure A63. Experiment 24C

Table A24. Experiment 24 using Open Channel Condition with a 2.5 inch sill at the end of the culvert.

H.J.	Run	H	W_{temp}	Q	$V_{u/s}$	Y_s	Y_{toe}	Y_1	Y_2	$Y_{d/s}$	Fr1	V_1	V_2	$V_{d/s}$	L	X	ΔE	THL	E_2/E_1
Y (slope)	24A	0.8d	57.8	0.9812	2.500	2.63	4.50	2.63	6.63	6.38	2.1066	4.4687 P-tube	2.2698 P-tube	4.5396 P-tube	10.00	-	0.92	-0.655398	0.892
Y (toe)	24B	1.0d	58.0	1.3266	2.700	3.00	3.25	3.38	7.25	6.63	1.8366	5.3833 P-tube	2.8934 P-tube	5.1385 P-tube	13.00	82.50	0.59	-0.591649	0.935
Y	24C	1.2d	57.8	1.7210	2.800	4.36	4.00	4.25	8.63	8.13	1.7541	5.6745 P-tube	3.10805 P-tube	5.2623 P-tube	15.00	78.50	0.57	-1.029093	0.947

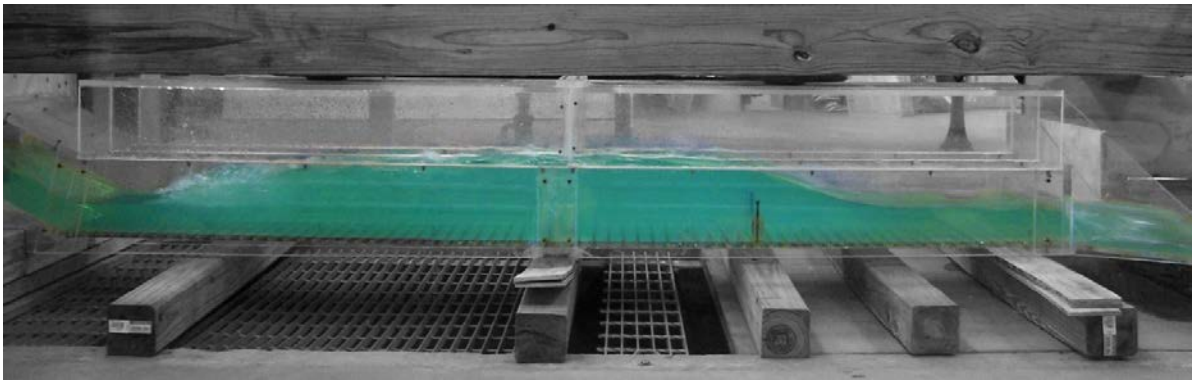

Figure A64. Experiment 25A

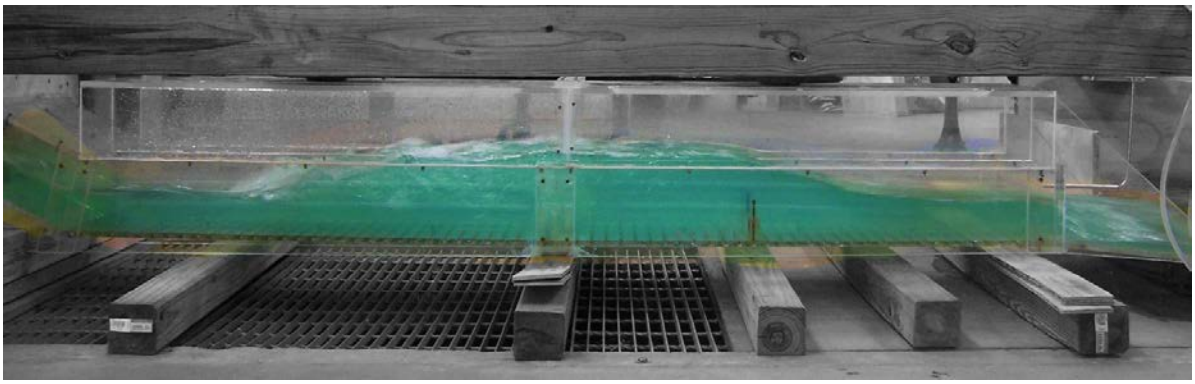

Figure A65. Experiment 25B

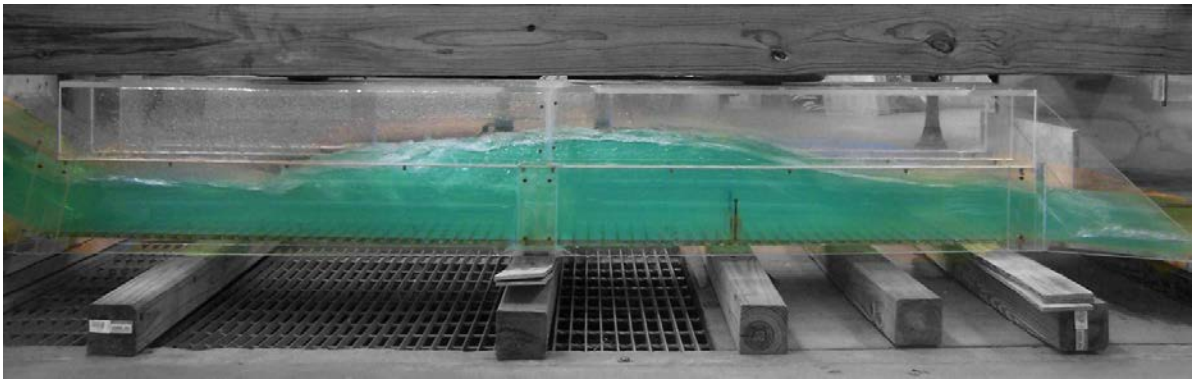

Figure A66. Experiment 25C

Table A25. Experiment 25 using Open Channel Condition with a 1.75 inch sill at 25 inches from the end of the culvert with 15 flat-faced friction blocks in front of the sill.

H.J.	Run	H	W_{temp}	Q	$V_{u/s}$	Y_s	Y_{toe}	Y_1	Y_2	$Y_{d/s}$	Fr1	V_1	V_2	$V_{d/s}$	L	X	ΔE	THL	E_2/E_1
Y	25A	0.8d	56.1	1.0053	2.500	2.63	2.38	3.00	6.50	2.75	1.8522	5.5598 P-tube	2.5377 P-tube	5.01159 P-tube	12.00	49.75	0.55	2.134597	0.905
Y	25B	1.0d	56.2	1.3205	2.700	3.13	3.38	3.25	7.38	3.25	1.9271	5.73097 P-tube	2.7799 P-tube	5.44279 P-tube	11.00	41.25	0.73	-0.561608	0.907
Y	25C	1.2d	56.4	1.7371	2.800	4.25	3.88	3.88	8.38	3.88	1.8472	5.9515 P-tube	2.83725 P-tube	5.84226 P-tube	13.00	40.50	0.70	2.020869	0.920

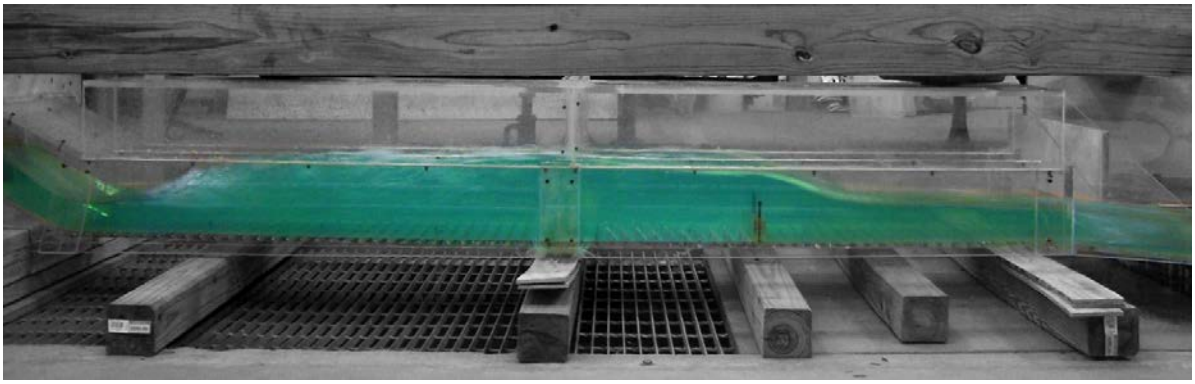

Figure A67. Experiment 26A

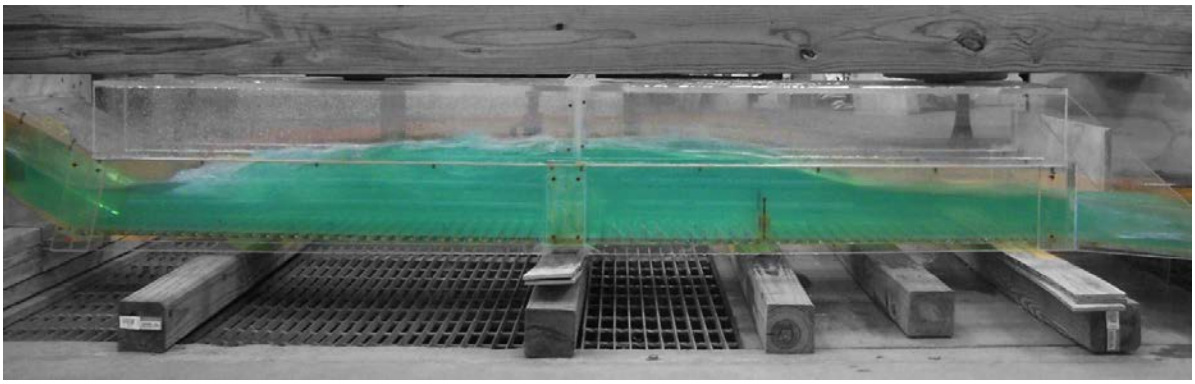

Figure A68. Experiment 26B

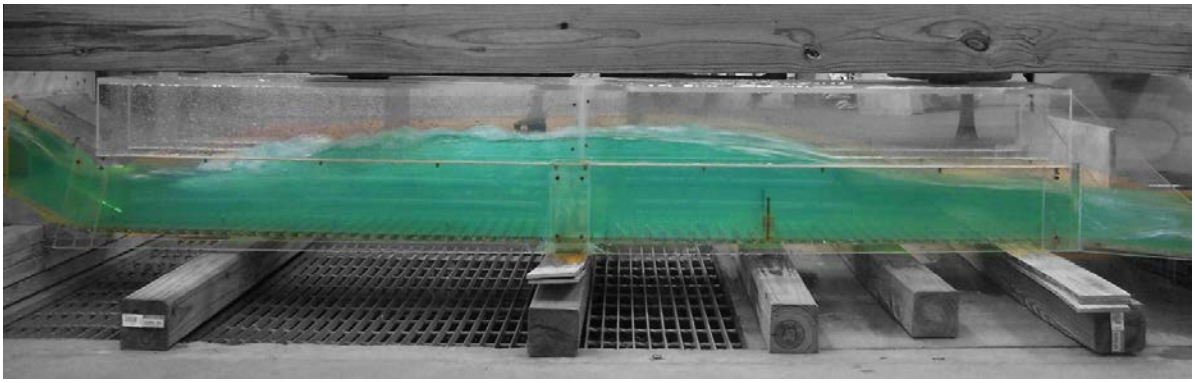

Figure A69. Experiment 26C

Table A26. Experiment 26 using Open Channel Condition with a 1.75 inch sill at 25 inches from the end of the culvert with 30 flat-faced friction blocks in front of the sill.

H.J.	Run	H	W_{temp}	Q	$V_{u/s}$	Y_s	Y_{toe}	Y_1	Y_2	$Y_{d/s}$	Fr1	V_1	V_2	$V_{d/s}$	L	X	ΔE	THL	E_2/E_1
Y	26A	0.8d	56.8	0.9893	2.473	2.38	2.38	2.38	6.38	2.63	2.2211	5.32316 P-tube	2.7799 P-tube	5.011586 P-tube	14.00	54.00	1.05	2.229808	0.892
Y	26B	1.0d	56.8	1.3296	2.659	3.00	3.50	4.13	7.50	3.38	1.5990	5.6745 P-tube	3.30877 P-tube	5.3833 P-tube	13.00	51.00	0.31	2.137657	0.954
Y	26C	1.2d	57.1	1.7279	2.880	4.38	3.88	4.88	8.38	3.75	1.5274	5.89712 P-tube	3.20998 P-tube	5.89712 P-tube	14.00	48.50	0.26	2.115357	0.963

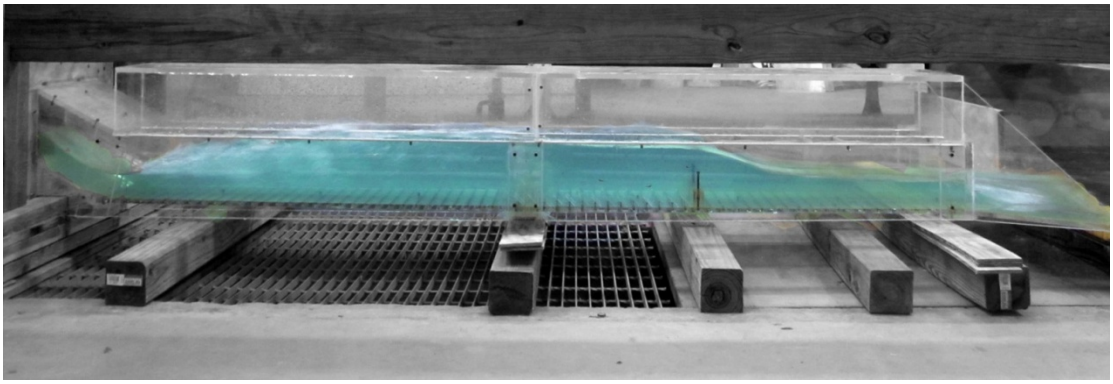

Figure A70. Experiment 27A

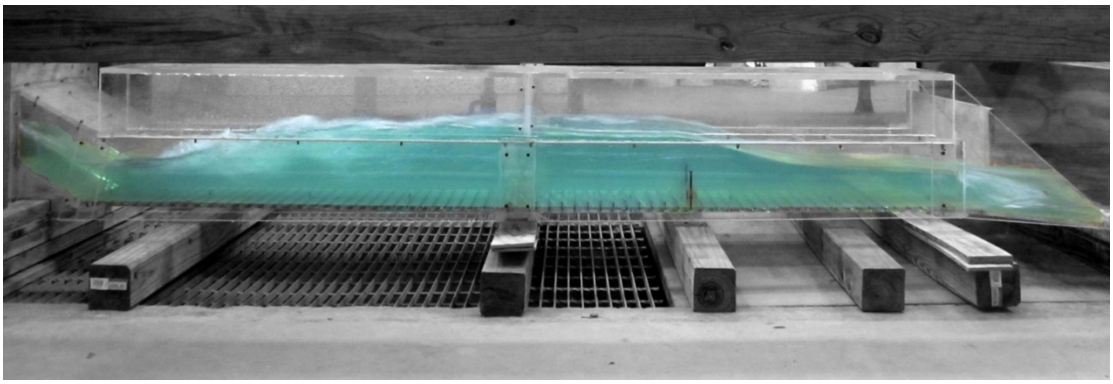

Figure A71. Experiment 27B

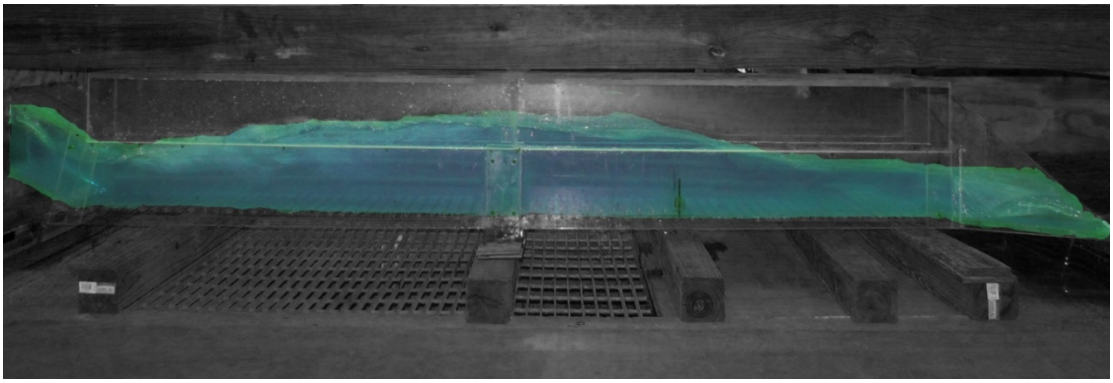

Figure A72. Experiment 27C

Table A27. Experiment 27 using Open Channel Condition with a 1.75 inch sill at 25 inches from the end of the culvert with 45 flat-faced friction blocks in front of the sill.

H.J.	Run	H	W_{temp}	Q	$V_{u/s}$	Y_s	Y_{toe}	Y_1	Y_2	$Y_{d/s}$	Fr1	V_1	V_2	$V_{d/s}$	L	X	ΔE	THL	E_2/E_1
Y	27A	0.8d	57.0	0.9893	2.473	2.63	2.38	2.38	6.50	2.75	2.2572	5.3833 P-tube	2.8934 P-tube	5.01159 P-tube	13.00	54.00	1.13	2.109801	0.888
Y	27B	1.0d	57.1	1.3355	2.671	3.00	3.50	3.50	7.38	3.25	1.8103	5.61747 P-tube	3.49799 P-tube	5.44280 P-tube	13.00	52.50	0.57	2.159348	0.935
Y	27C	1.2d	57.2	1.7094	2.849	3.88	4.00	4.38	8.25	3.75	1.6479	5.78688 P-tube	3.8486 P-tube	5.84230 P-tube	14.00	52.25	0.40	2.202360	0.956

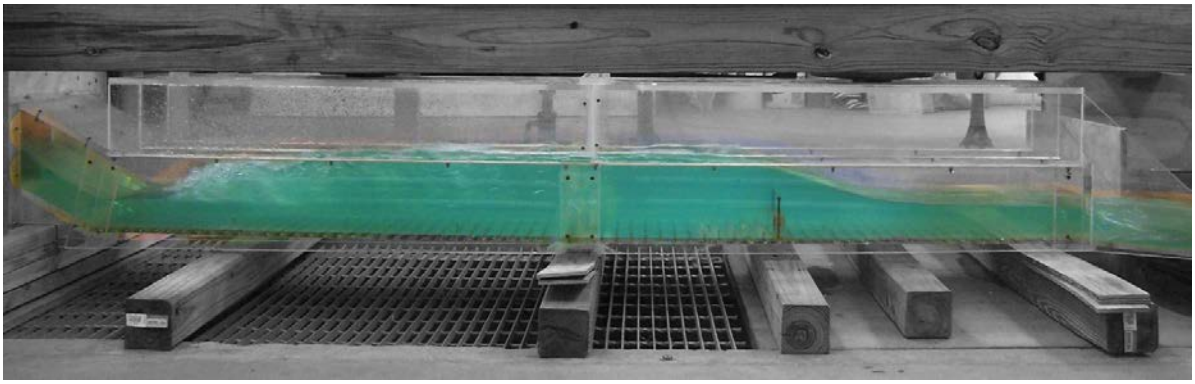

Figure A73. Experiment 28A

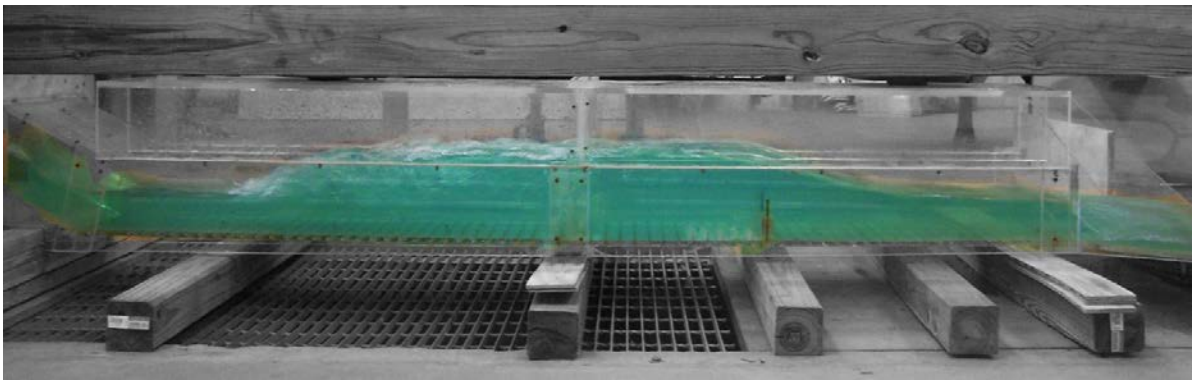

Figure A74. Experiment 28B

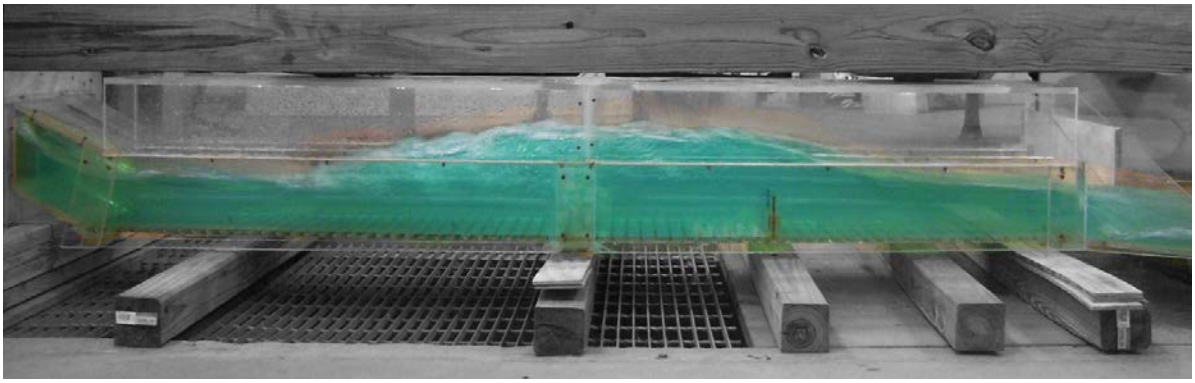

Figure A75. Experiment 28C

Table A28. Experiment 28 using Open Channel Condition with a 1.75 inch sill at 25 inches from the end of the culvert with 15 curved-face friction blocks in front of the sill.

H.J.	Run	H	W_{temp}	Q	$V_{u/s}$	Y_s	Y_{toe}	Y_1	Y_2	$Y_{d/s}$	Fr1	V_1	V_2	$V_{d/s}$	L	X	ΔE	THL	E_2/E_1
Y	28A	0.8d	57.7	0.9893	2.500	2.50	2.38	2.38	6.50	2.75	2.2572	5.2623 P-tube	2.4075 P-tube	5.0754 P-tube	10.00	51.50	1.13	2.014655	0.866
Y	28B	1.0d	58.0	1.3325	2.700	2.88	3.38	3.50	7.13	3.38	1.7588	5.32316 P-tube	3.10808 P-tube	5.44279 P-tube	13.00	44.00	0.48	2.058392	0.946
Y	28C	1.2d	58.6	1.7047	2.800	4.00	3.85	3.88	8.25	2.88	1.8231	5.73097 P-tube	2.89345 P-tube	5.89712 P-tube	13.50	39.00	0.65	2.900865	0.937

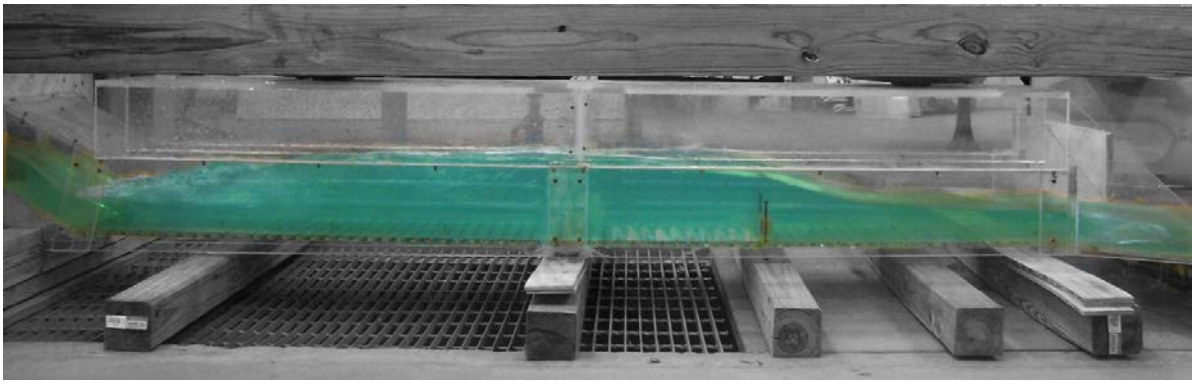

Figure A76. Experiment 29A

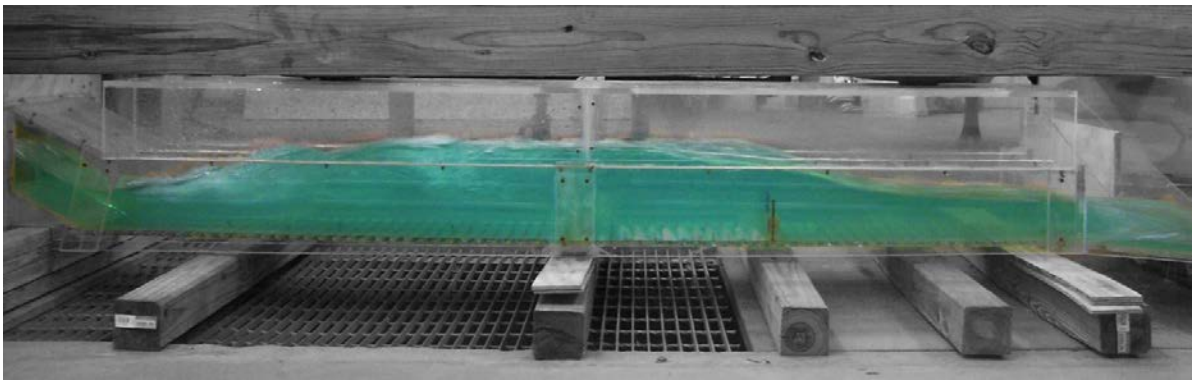

Figure A77. Experiment 29B

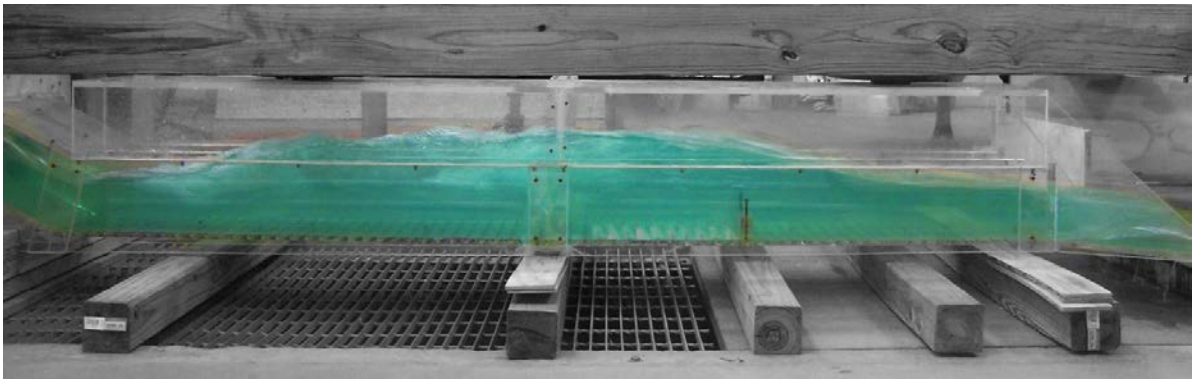

Figure A78. Experiment 29C

Table A29. Experiment 29 using Open Channel Condition with a 1.75 inch sill at 25 inches from the end of the culvert with 30 curved-face friction blocks in front of the sill.

H.J.	Run	H	W_{temp}	Q	$V_{u/s}$	Y_s	Y_{toe}	Y_1	Y_2	$Y_{d/s}$	Fr1	V_1	V_2	$V_{d/s}$	L	X	ΔE	THL	E_2/E_1
Y	29A	0.8d	59.1	0.9973	2.500	2.38	2.50	2.50	6.50	2.75	2.1633	5.01159 P-tube	2.53715 P-tube	4.94692 P-tube	10.00	56.00	0.98	2.254593	0.882
Y	29B	1.0d	59.7	1.3084	2.700	2.88	3.25	3.25	7.50	3.38	1.9536	5.55986 P-tube	2.89344 P-tube	5.32316 P-tube	12.00	53.00	0.79	-0.321621	0.917
Y	29C	1.2d	59.8	1.7140	2.800	4.13	4.00	4.13	8.38	4.13	1.7530	5.78688 P-tube	3.10805 P-tube	5.95147 P-tube	12.00	49.00	0.55	1.530870	0.947

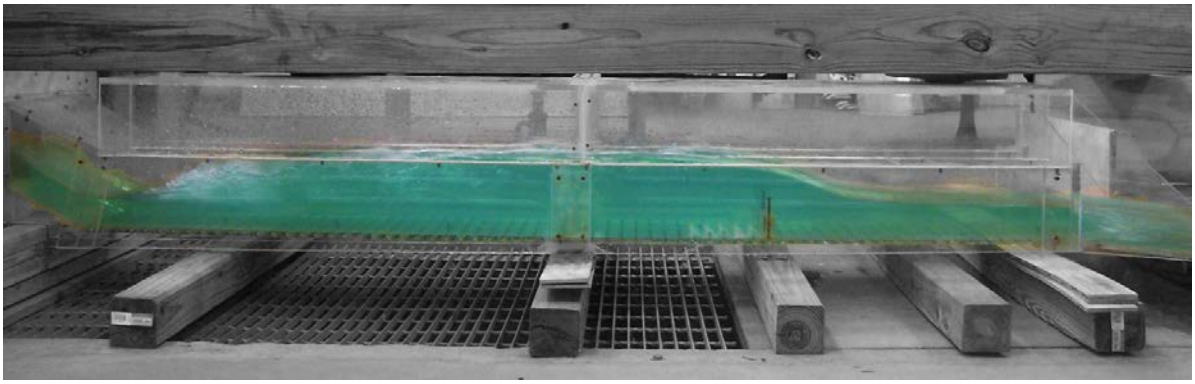

Figure A79. Experiment 30A

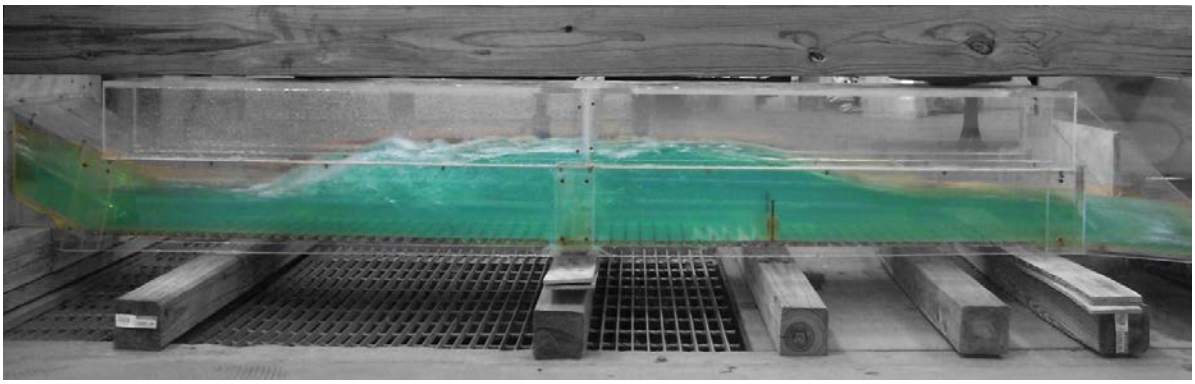

Figure A80. Experiment 30B

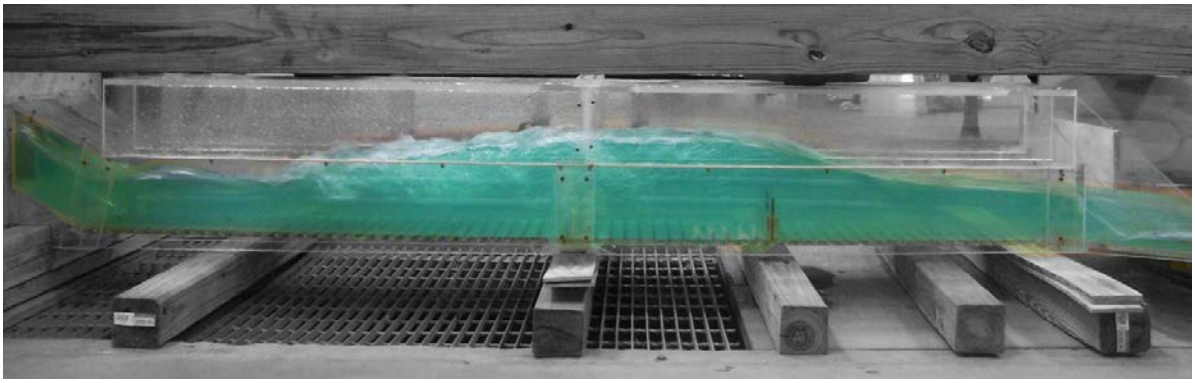

Figure A81. Experiment 30C

Table A30. Experiment 30 using Open Channel Condition with a 1.75 inch sill at 25 inches from the end of the culvert with 15 C-shaped friction blocks in front of the sill.

H.J.	Run	H	W_{temp}	Q	$V_{u/s}$	Y_s	Y_{toe}	Y_1	Y_2	$Y_{d/s}$	Fr1	V_1	V_2	$V_{d/s}$	L	X	ΔE	THL	E_2/E_1
Y	30A	0.8d	59.6	0.9933	2.500	2.63	2.38	2.50	6.63	2.75	2.2006	5.4723 P-tube	2.4075 P-tube	5.01159 P-tube	14.00	53.00	1.06	2.134590	0.876
Y	30B	1.0d	59.9	1.3175	2.700	3.00	3.80	3.50	7.38	3.25	1.8103	5.9515 P-tube	2.7799 P-tube	5.3533 P-tube	13.00	44.25	0.57	2.368418	0.939
Y	30C	1.2d	60.2	1.7071	2.800	4.50	3.88	4.00	8.25	4.00	1.7771	6.2161 P-tube	2.66158 P-tube	5.8971 P-tube	10.00	41.50	0.58	1.780909	0.944

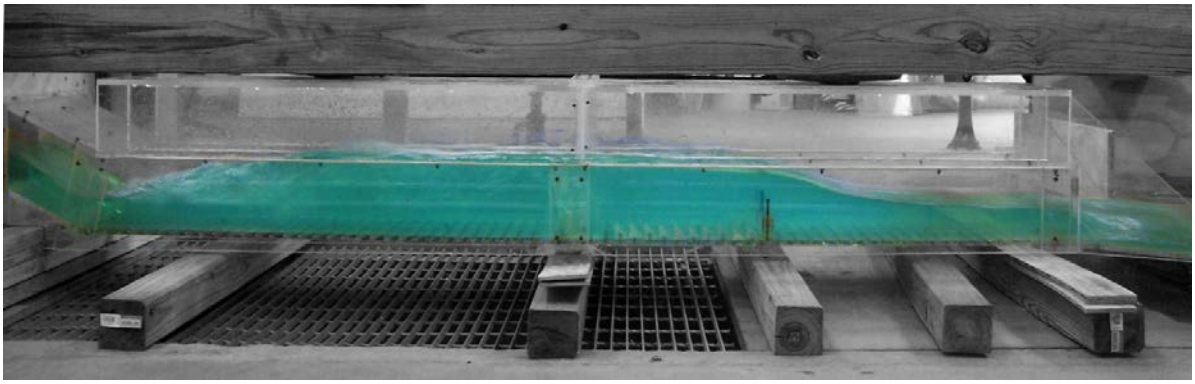

Figure A82. Experiment 31A

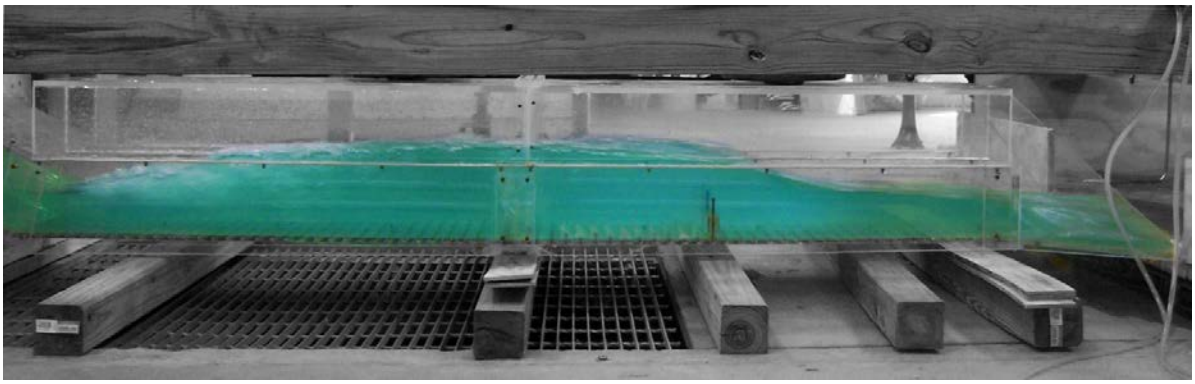

Figure A83. Experiment 31B

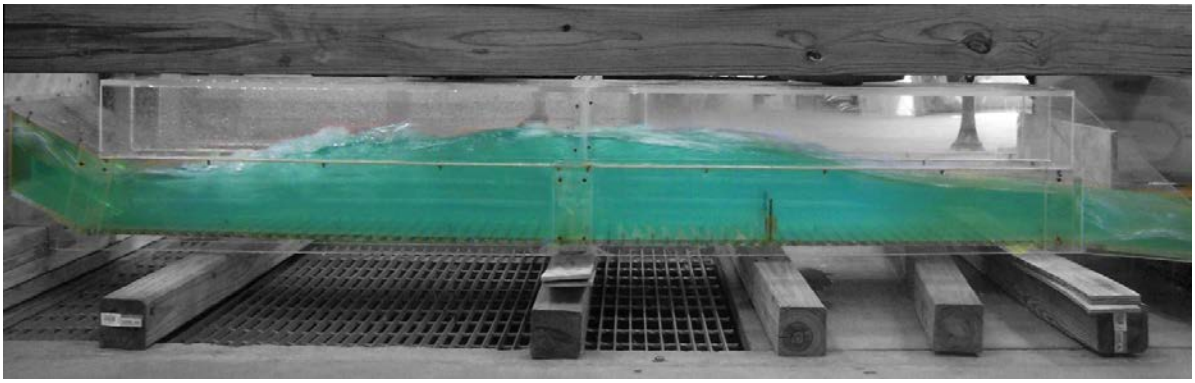

Figure A84. Experiment 31C

Table A31. Experiment 31 using Open Channel Condition with a 1.75 inch sill at 25 inches from the end of the culvert with 15 C-shaped friction blocks in front of the sill.

H.J.	Run	H	W_{temp}	Q	$V_{u/s}$	Y_s	Y_{toe}	Y_1	Y_2	$Y_{d/s}$	Fr1	V_1	V_2	$V_{d/s}$	L	X	ΔE	THL	E_2/E_1
Y	31A	0.8d	60.8	0.9937	2.500	2.63	2.50	2.50	6.50	2.88	2.1633	5.07543 P-tube	2.77992 P-tube	4.94690 P-tube	10.00	55.50	0.98	2.12463	0.882
Y	31B	1.0d	61.1	1.3175	2.700	3.00	3.38	4.00	7.50	3.25	1.6417	5.55986 P-tube	3.10803 P-tube	5.35330 P-tube	11.00	53.00	0.36	2.368418	0.962
Y	31C	1.2d	61.3	1.7302	2.800	4.00	3.88	5.00	8.50	4.25	1.5149	5.75899 P-tube	3.4047 P-tube	5.89712 P-tube	13.50	52.50	0.25	1.530865	0.977

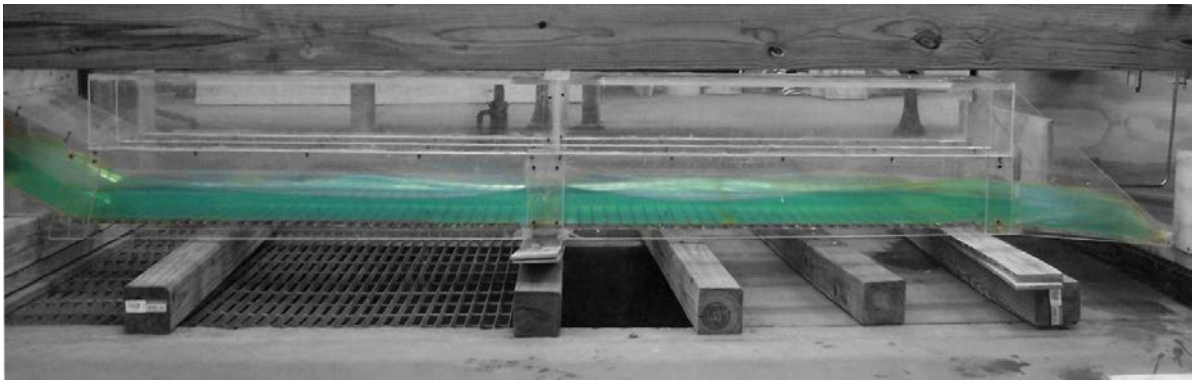

Figure A85. Experiment 32A

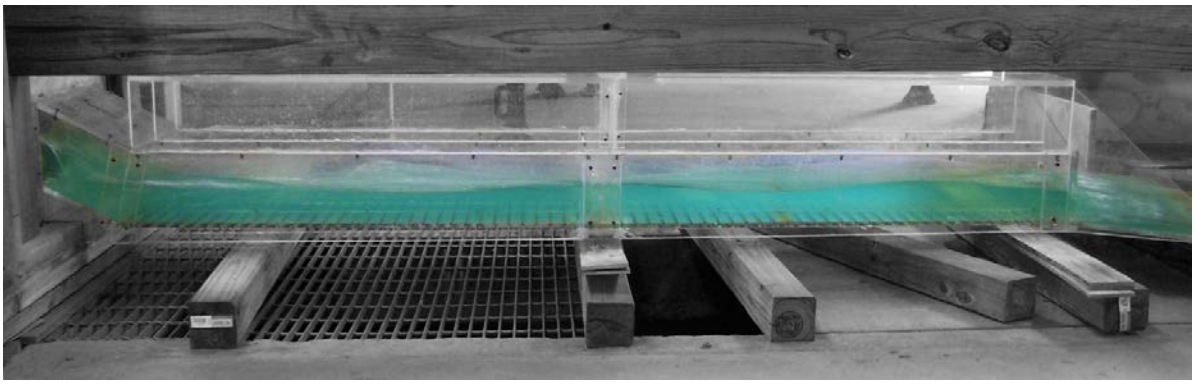

Figure A86. Experiment 32B

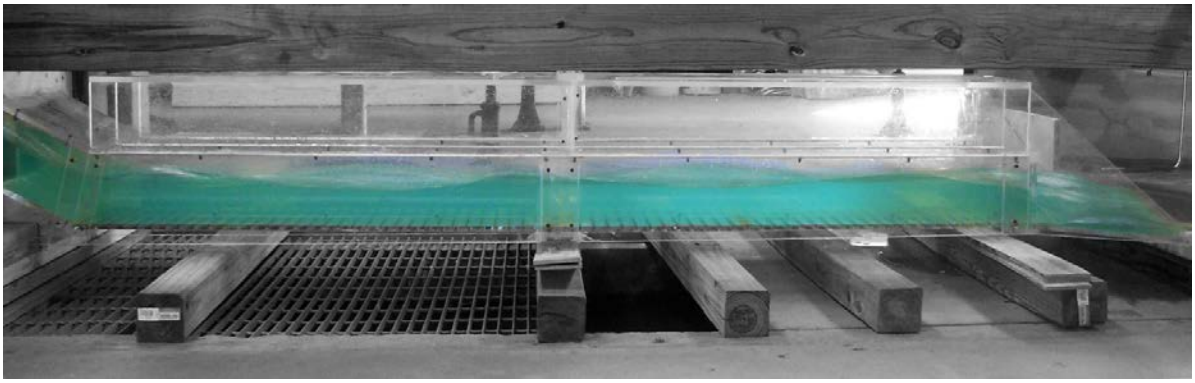

Figure A87. Experiment 32C

Table A32. Experiment 32 using Open Channel Condition with no sill in the culvert.

H.J.	Run	H	W_{temp}	Q	$V_{u/s}$	Y_s	Y_{toe}	Y_1	Y_2	$Y_{d/s}$	Fr1	V_1	V_2	$V_{d/s}$	L	X	ΔE	THL	E_2/E_1
N	32A	0.8d	53.4	0.9852	2.500	2.75	2.38	-	-	2.00	2.3118	5.8423 P-tube	- -	6.0587 P-tube	-	-	-	0.724625	-
N	32B	1.0d	53.3	1.3444	2.700	2.50	3.25	-	-	2.63	1.9969	5.8971 P-tube	- -	6.34429 P-tube	-	-	-	0.828382	-
N	32C	1.2d	53.6	1.7348	2.800	3.78	4.00	-	-	3.25	1.8412	6.03208 P-tube	- -	6.444998 P-tube	-	-	-	1.270870	-